



TECHNISCHE
UNIVERSITÄT
WIEN
Vienna University of Technology

MASTER'S THESIS

DEVELOPMENT OF AN ADVANCED BIOMECHANICAL
MODEL OF THE SHOULDER COMPLEX WITH A FOCUS ON
THE SCAPULOTHORACIC JOINT AND THE EVALUATION OF
THE EFFECTS OF AN ASSISTIVE SHOULDER EXOSKELETON.

Author:
AYECHU ABENDAÑO Ada

Supervisors:
GFÖHLER Margit
ANCILLAO Andrea

March 2023



Die approbierte gedruckte Originalversion dieser Diplomarbeit ist an der TU Wien Bibliothek verfügbar
The approved original version of this thesis is available in print at TU Wien Bibliothek.

Acknowledgments

First of all, I would like to express my sincere appreciation to the Technische Universität Wien for taking me in as ERASMUS student and to my home university, the University of Zaragoza for the received training in both technical aspects and human values.

To my direct supervisor in this project, Andrea Ancillao, thank you for your time, patience and dedication. I have learned a lot from your experience and advice on motion capture and on how to be open to new thoughts and ideas. I am pleased to have discovered this field in the biomedical engineering, which has made the experience challenging and very pleasant, opening my mind to new applications for my technical and engineering acquaintances.

I would also like to express my gratitude to my supervisor Margit Gföhler and to the entire Research Unit of Biomechanics and Rehabilitation Engineering at the TU Wien for the warm welcome in the group and the advise received.

To my family, specially to my parents and siblings, for their wholehearted support.

To my friends and class colleagues, for all the shared experiences all along these years.

Resumen

En los últimos años, se ha experimentado un crecimiento en popularidad de los exoesqueletos pasivos gracias al desarrollo de nuevas e innovadoras tecnologías permitiendo el diseño de dispositivos ligeros y efectivos basados en muelles y poleas para ejercer los pares de fuerza y fuerzas cuyo objeto final es reducir la carga sobre las articulaciones humanas.

Las aplicaciones típicas de estos dispositivos se dan en rehabilitación o en la industria para asistir a los trabajadores durante la realización de tareas pesadas o con riesgo para así prevenir la aparición de desórdenes musculoesqueléticos relacionados con las labores de trabajo. La confección de estos dispositivos tiene como aplicación su uso en un ambiente laboral, por lo que son diseñados para ser ligeros, compactos, manejables y cómodos para el usuario.

El objetivo de este trabajo es introducir un nuevo y detallado modelo biomecánico del complejo del hombro y evaluar los efectos de un exoesqueleto comercial ("Paexo" de Ottobock) en la cinemática del hombro con un enfoque particular en la articulación escapulotorácica, para asistir finalmente en el posterior diseño de un nuevo exoesqueleto para la extremidad superior.

Palabras clave

Modelado biomecánico, articulación escapulotorácica, captura de movimiento, sEMG, cinética escapular

Abstract

In the last years, wearable passive exoskeletons have experienced a growth in popularity thanks to the development of modern technologies allowing to design lightweight and effective devices that rely only on springs and cantilevers to exert torques and forces aimed to reduce the load on human joints.

Typical applications are in rehabilitation or in industry to assist workers during heavy and risky tasks and prevent them from suffering work-related musculoskeletal disorders. Devices meant to be used in working environment, are designed to be lightweight, compact, easy to use and not to cause discomfort to the user.

The aim of this work is to introduce a new detailed biomechanical model of the shoulder complex and to study the effects on shoulder kinematics of a commercial exoskeleton (“Paexo” by Ottobock) with a focus on the scapulothoracic joint, to further assess in the design of a new upper-limb exoskeleton.

Keywords

Biomechanical model, scapulothoracic joint, motion capture, sEMG, scapular kinetics

Abbreviations/Acronyms

- WMSDs: Work-related musculoskeletal disorders
- ST: scapulothoracic
- DoF: Degree of freedom
- STA: soft-tissue artifact
- EMG: electromiography
- sEMG: surface electromiography
- ISB: International Society of Biomechanics
- IK: Inverse kinematics
- ID: Inverse dynamics
- AD: Anterior Deltoid
- MD: Medium Deltoid
- PD: Posterior Deltoid
- ES: Erector Spinae
- MIVC: Maximum isovolumetric contraction
- SD: standard deviation

Contents

1	Introduction	7
1.1	Motivation	7
1.2	Objectives	7
1.2.1	Development of biomechanical model focused on the scapulothoracic joint	7
1.2.2	Design of a motion capture protocol	8
1.2.3	Conduction of EMG and Videometry measurements	8
1.2.4	Analysis of exoskeleton effects	9
2	Literature review	11
2.1	Biomechanical modeling of the shoulder complex	11
2.2	Scapula tracking methods	12
2.3	Previous studies on the performance of upper-limb exoskeletons	13
3	Methodology	15
3.1	Focus and tools	15
3.2	Participants	15
3.3	Schedule: research steps	16
3.4	Data Workflow	17
4	Model	19
4.1	Jointset and geometry	19
4.2	Muscleset	20
4.3	Markerset	22
5	Test protocol	27
5.1	Target and tasks	27
5.2	Motion Capture System set up	28
5.2.1	Environment	29
5.2.2	Markerset	30
5.3	sEMG set up	33
5.4	Trials	33
5.4.1	Calibration	33
5.4.2	Dynamic tasks	34
5.5	Subject query	37
6	Postprocess of experimental data	39
6.1	Postprocessing of motion data	39
6.2	sEMG data processing	40
6.2.1	High pass filtering	40
6.2.2	Rectification	40
6.2.3	Envelope extraction: low pass filtering	41

6.2.4	Normalization	41
7	Kinematics and Kinetics calculations	43
7.1	Virtual markers calculation	43
7.2	Model scaling	43
7.3	Kinematics calculation	44
7.4	Kinetics calculation	44
8	Model validation	47
8.1	Bilaterality	47
8.2	Validation with literature	47
9	Results	53
9.1	Inter-variability between subjects	53
9.2	Exoskeleton effects	57
9.2.1	Kinematics	57
9.2.2	Muscle activation	57
9.2.3	Weight effect	58
10	Conclusions and future perspectives	65
10.1	Discussion	65
10.2	Limitations	67
10.3	Conclusions	68
10.4	Future perspectives	69

List of Figures

1	Commercial upper-limb exoskeletons: a) Levitate AIRFRAME , b) SuitX ShoulderX , c) Ekso Bionics Eksovest , d) Hyundai H-VEX , e) Ottobock PAEXO and f) Conau MATE-XT	8
2	Scapula locator methodology for scapula tracking. [12]	12
3	(a) Scapular markers in initial static position and (b) scapular markers in 180° abduction position. All markers from initial static position were left intact. TSp, pointed marker that corresponds to actual TS bony landmark; AIp, pointed marker that corresponds to actual AI bony landmark [13]	13
4	Data workflow from acquisition till results	17
5	The four modeled functional coordinates of the ST joint by Seth et al. [10]	19
6	Shoulder marker cluster	22
7	Shoulder marker cluster, version 2.	23
8	Humerus marker cluster.	23
9	Frontal and rear views of the markerset on the musculoskeletal model.	24
10	Other views of the markerset on the musculoskeletal model.	24
11	Frontal and rear views of the musculoskeletal model.	25
12	Kestrel camera [32]	28
13	Example of calibration wand and L-frame from Qualysis [33]	28
14	Camera setup seen from Cortex software	29
15	Frontal and rear views of the markerset on a subject.	30
16	Frontal and rear views of the markerset on a subject with Paexo exoskeleton.	31
17	Positioning of sEMG sensors for the selected muscles: a) Anterior Deltoid, b) Medial Deltoid, c) Posterior Deltoid, d) Upper Trapezius, e) Latissimus Dorsi and f) Erector Spinae [36]	34
18	Example of static pose by one subject	35
19	Calibration motion for the right arm on Cortex	35
20	Scapular plane definition [37]	36
21	Elevation of the left arm in the scapular plane	36
22	Example of sEMG signal processing workflow conducted for Subject 4, Right Anterior Deltoid muscle during elevations in the scapular plane with the right arm.	42
23	ST joint kinematics comparison for right and left limb during repetitive right and left elevation-depression of the arm in the scapular plane. The curves represent the mean of the subjects and the cycles and the shaded area the +/- standard deviation (SD).	48
24	ST joint kinetics comparison for right and left limb during repetitive elevation-depression of the arm in the scapular plane. The curves represent the mean of the subjects and the cycles and the shaded area the +/- SD.	49
25	ST joint coordinates during elevation-depression motion in the scapular plane for the subjects, sides and cycles mean. The curves represent the mean of the subjects and the cycles and the shaded area the +/- SD.	50

26	ST joint coordinates during abduction-adduction motion reconstructed motion from measured bone-pin marker [10]	50
27	Scapulohumeral rhythm mean for the four different subjects. The curves represent the mean of each of the subjects for all the cycles and the shaded area the +/- SD.	51
28	Scapulohumeral rhythm different patterns obtained in the study from Bagg et al. [54]	52
29	Abduction, elevation and winging ST joint coordinates and scapulohumeral rhythm during elevation-depression motion in the scapular plane for the mean of each subject. The curves represent the mean of each subject for all the cycles and the shaded area the +/- SD.	54
30	ST joint normalized moments during elevation-depression motion in the scapular plane for the mean of each subject. The curves represent the mean of each subject for all the cycles and the shaded area the +/- SD.	55
31	ROM for the ST joint coordinates for each subject mean during elevation-depression motion in the scapular plane. The O represent the mean of each subject for all the cycles and the segment constituted by the X, the +/- SD.	56
32	Abduction, elevation and winging ST joint coordinates and scapulohumeral rhythm during elevation-depression motion in the scapular plane for the subjects mean with (blue) and without (red) an upper-limb exoskeleton. The curves represent the mean of the subjects for all the cycles and the shaded area the +/- SD.	59
33	ROM for the ST joint coordinates for the subjects mean with and without the exoskeleton during elevation-depression motion in the scapular plane. The O represent the mean of the subjects for all the cycles and the segment constituted by the X, the +/- SD.	60
34	sEMG subjects mean for the AD, MD and PD of the working side, along with the ES of the contralateral side, for the elevation-depression motion in the scapular plane with (blue) and without (red) exoskeleton. The curves represent the mean of the subjects for all the cycles and the shaded area the +/- SD.	61
35	Abduction, elevation and winging ST joint coordinates and scapulohumeral rhythm during elevation-depression motion in the scapular plane with a 2.5 kg weight for the subjects mean with (blue) and without (red) an upper-limb exoskeleton. The curves represent the mean of the subjects for all the cycles and the shaded area the +/- SD.	62
36	sEMG subjects mean for the AD, MD and PD of the working side, along with the ES of the contralateral side, for the elevation-depression motion in the scapular plane with a 2.5 kg weight, with (blue) and without (red) an exoskeleton. The curves represent the mean of the subjects for all the cycles and the shaded area the +/- SD.	63

List of Tables

1	Detailed schedule plan with the different research steps	16
2	Biomechanical model muscle parameters based on Seth et al. [26] and Hamner et al. [28].	21
3	Marker landmarks. R-prefix = marker on the right side; L-prefix = marker on the left side. * for only calibrating markers and ** virtual markers.	32

Annexes

- 1 Annex I. Subjects data
- 2 Annex II. Kinematics and kinetics report
- 3 Annex III. Raw EMG data

Chapter 1

Introduction

Work-related musculoskeletal disorders (WMSDs) remain the most prevalent occupational health problem, constituting 60% of the work-related health problems [1]. One of the most affected areas are the neck or upper limbs, as reported by the 42% of workers in Europe having suffered from muscular pains in these areas as a consequence of work activities [2]. This proportion even tends to grow with the workers age and also depends on gender. For instance, the percentage of workers reporting muscular pains in shoulders, neck and/or upper limbs along a 12 months study grew from 26% on under 25 years old male workers up to 52% on female workers older than 55 years old [1].

That highlights the need for solutions, which have been focused on the design of assistive devices to help reducing injuries and improve ergonomy.

1.1 Motivation

Precisely, there has been a growth in popularity for exoskeletons used to improve ergonomy and reduce the prevalence of WMSDs. Despite being the majority focused on the lower limbs, also upper-limb exoskeletons have experienced an increase in the market. These devices, as meant to be used in working environment, are designed to be lightweight, compact, easy to use and not to cause discomfort to the user.

Some of the most relevant and already commercialized models are summed up in Figure 1.

This master thesis is conducted under the guidelines of a bigger project in the Technische Universität Wien, whose goal is the design of an improved upper-limb exoskeleton. My role and work within this project focus on the preliminary study to evaluate the effects of a commercialized exoskeleton and help in the design of a new and improved exoskeleton by means of biomechanical modelling.

1.2 Objectives

In accordance to the presented project's goal and particular role of this thesis, the following objectives are pursued.

1.2.1 Development of biomechanical model focused on the scapulothoracic joint

The scapular motion constitutes one of the principal diagnostic indicators of shoulder pathology [3]. Because of this relevant role of scapular kinematics, the development of the biomechanical model focuses on the scapulothoracic (ST) joint, with the goal to represent realistically the shoulder complex and the scapula motion.

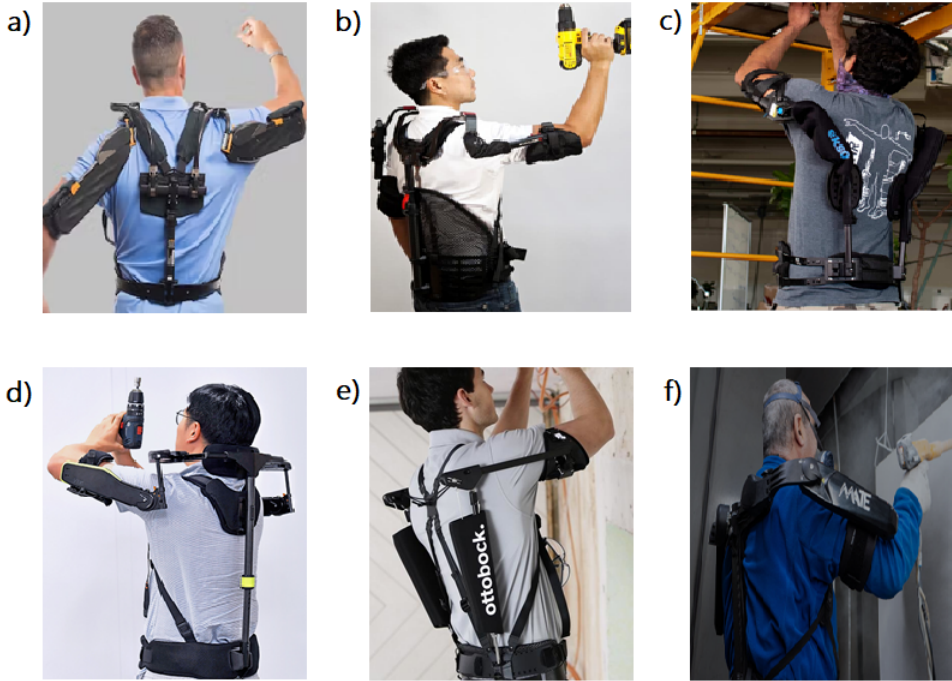


Figure 1: Commercial upper-limb exoskeletons: a) Levitate **AIRFRAME**, b) SuitX **ShoulderX**, c) Ekso Bionics **Eksovest**, d) Hyundai **H-VEX**, e) Ottobock **PAEXO** and f) Conau **MATE-XT**.

Additionally, some other requirements are pursued, such as bilaterality in order to reflect real working motion and effects on both limbs or the modelling of lower back muscles, given the possible side-effects affecting them because of the exoskeleton.

1.2.2 Design of a motion capture protocol

Another goal is to develop a methodology to track the scapula realistically and in a way that it is compatible with the exoskeleton use.

With these requirements, the creation of a motion capture protocol aims to be created. It pursues to minimize possible artifacts and improve as much as possible the data acquisition process.

Giving that one of main goals of the current project is the analysis of the effects of an upper-limb exoskeleton on the scapula kinetics and kinematics, the protocol should also include the guidelines to reach a reasonable repeatability and reproducibility of the test conditions for the different subjects under the different tasks.

1.2.3 Conduction of EMG and Videometry measurements

The exoskeleton tests aiming to study the effects of the exoskeleton would be done based on surface electromyography (sEMG) combined with motion capture obtained through videometry. These technologies would be used to reflect the effects on the muscular activity and in the kinematics, respectively and simultaneously. With respect to the kinematics, a special focus would be made on the scapular motion.

1.2.4 Analysis of exoskeleton effects

Lastly, the data recorded from the tests measurements along with the developed model would allow some calculation, whose analysis would be of interest to interpret the effects of the exoskeleton on the subjects. The analysis would be conducted on a commercialized exoskeleton, whose effects would be address from the scapular motion and muscular acitivity focus, given that most of the previous exo studies were not considering kinematics effects, but just muscular effects.

Being the topic and goals of the project already presented, the next chapters will address a literature review, the model and protocol design, the methodology followed to process the collected data, an analysis and finally, the extracted conclusions.

Chapter 2

Literature review

Before working on the set objectives, a literature review should be made. Firstly, to condense what has been done in this area of research, which were the directions and focus made by other studies, and most importantly, to identify the gaps in these studies that my work intends to fill.

2.1 Biomechanical modeling of the shoulder complex

The shoulder joint complex is composed of three synovial joints (glenohumeral, acromioclavicular, and sternoclavicular) along with the articulation between the ventral surface of the scapula and the dorsal thorax, referred to as the ST articulation. However, it is not a true joint in any sense of the term, although the relative motion of the scapula with respect to the thorax. These movements of the scapula on the thorax are a result from combined motions of the sternoclavicular and acromioclavicular joints and contribute to reach the full mobility of the shoulder complex.[4]

The real challenge when modelling the upper-limb consists in obtaining a complex model which shows realistic motion while minimizing the computational costs associated with higher complexity.

First models of the upper limb were considering just 4 rigid bodies (thorax, humerus, ulna and radius) constrained by 3 anatomical joints (glenohumeral joint, humeroulnar joint and radioulnar joint). In other words, the clavicle and scapula were considered stationary and as an integrated part of the thorax, so no relative motion between them was considered and muscles acting in the interphase neglected. [5][6]

Not considering the scapula motion represents a too restrictive limitation, given the relation of abnormal scapular motion to a number of shoulder pathologies. To correctly study how the exoskeleton may affect the shoulder, taking into account the role of the scapula is therefore essential

The ST joint, which had been neglected until then, was originally modeled by constraining the scapula to remain in contact with the rib cage of the thorax, represented itself as an ellipsoid. [7][8][5] This ensures the scapula to slide over the rib cage and it is achieved by enforcing the constraint points of the scapula to remain in contact with the defined ellipsoid all the time. However, this constraints can lead to inaccuracies in the model predictions and result in unrealistic positions. [9][10]

Lately, Seth et al. [10] developed a new biomechanical model of the shoulder complex, where the ST joint captures the scapular kinematics without kinematic surface constraints. This model showed promising results, as it showed realistic motion when compared to a healthy subject's experimental bone-pin data for three different shoulder tasks.

Considering the different contributions made on the biomechanical modelling for the upper limb, there is still some gap for future improvement in some prospects. First of all, most of the analyzed models do not include bilaterality and therefore are not adequate to evaluate the effects on both limbs simultaneously for bilateral or unilateral tasks, with the possible effects on some tasks on the non working side for this last case. Additionally, most

of them do not incorporate the pelvis and therefore the lower back muscles, whose side effects are really interesting to address when analyzing the exoskeleton performance, given the possible overload there. Finally, although the last approach on modelling the ST joint by Seth et al. [10] seems result into realistic scapular motion, the modelling has been based on healthy subjects.

2.2 Scapula tracking methods

To record the three-dimensional motion of a rigid body, it is necessary to effectively describe its 6 degrees of freedom (DoF). Ideally, each rigid body, each bone in this case, should be having three anatomical traceable landmarks during the complete motion period. Although the scapula presents three palpable bony landmarks, accurate tracking through these surface markers is not possible.[5].

Tracking the scapula has become a real challenge in motion capture for the upper limb, because of the great soft tissue artifact (STA). This artifact is due to the non-negligible motion of the scapula bone with respect to the covering skin, where markers are placed. This leads to a displacement between the marker and the corresponding anatomical landmark, that can be even larger than 2 cm [11], and therefore result into wrong and unrealistic scapula tracking.

Although scapula tracking is not very documented yet, there are some methods being considered. For instance, in the study from Shaheen et al.[12], a scapula locator (see Figure 2) is used and the results proved to be accurate. However, this method is based on quasi-static positions, in which the locator needs to be readjusted. Therefore, it is not really applicable for dynamic tests. Moreover, this method is not compatible with the use of an exoskeleton and therefore not useful for the evaluation of the exoskeleton effects on the scapular motion.

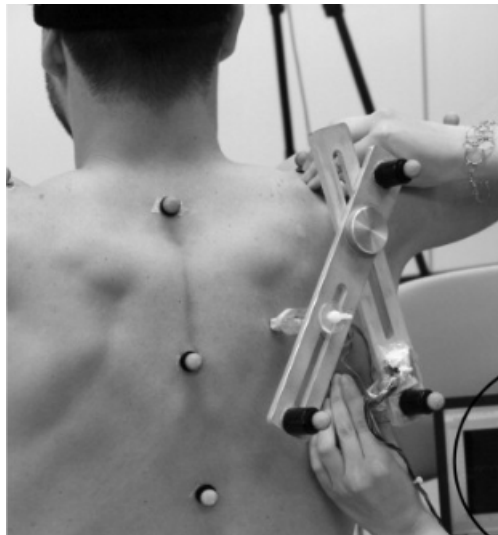


Figure 2: Scapula locator methodology for scapula tracking. [12]

Other study propose the reconstruction of the scapula markers based on the definition of a non-deformable solid by 3 markers through local optimisation and the posterior recalculation applied to the rest of the scapula markers with respect to this defined solid movement trough the motion capture period. They then compared the recalculated positions of the markers with the actual bony landmarks in the abducted arm [13]. Figure 3 also helps to illustrate the great STA happening in the scapula during the arm motion.

However, this study also have some limitations. It makes use of a significant number of scapula surface markers, and because of the lack of space would not be useful for scapula tracking while wearing an upper-limb exoskeleton. Moreover, it works under the hypothesis of non-deformable solid for surface markers placed on the

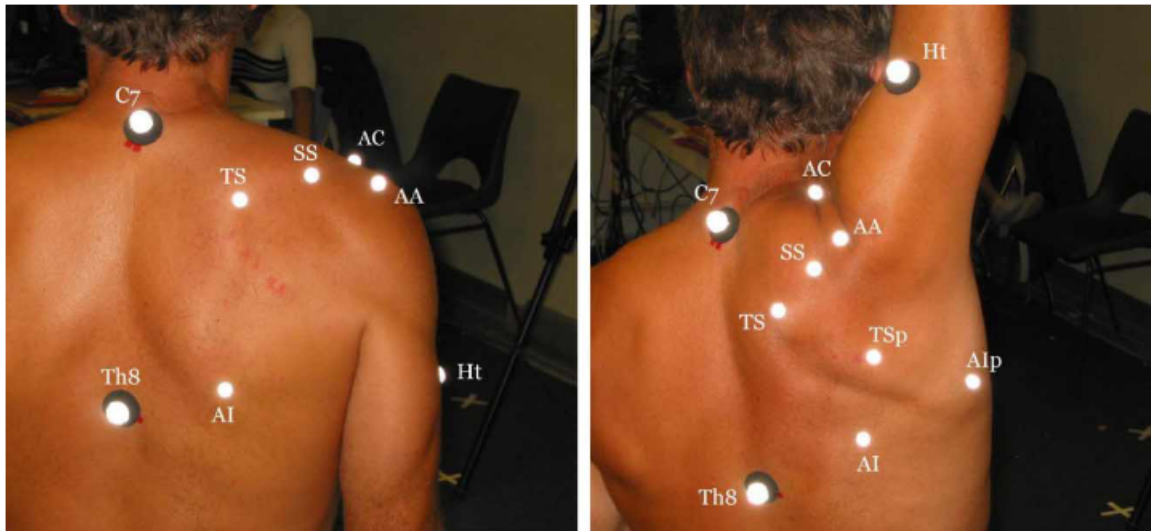


Figure 3: (a) Scapular markers in initial static position and (b) scapular markers in 180° abduction position. All markers from initial static position were left intact. TSp, pointed marker that corresponds to actual TS bony landmark; AIp, pointed marker that corresponds to actual AI bony landmark [13]

acromioclavicular joint, which itself is not free from STA. So, even though local optimisation is conducted to minimize that error, this method is still affected by STA.

Despite showing good results and a solid methodology, these approaches leave still a big room for improvement. The future prospects to address would be then to minimize even further the STA and to compatibilize the scapula tracking system used for the tasks with and without the exoskeleton, so the data are comparable.

2.3 Previous studies on the performance of upper-limb exoskeletons

Several studies have been conducted in order to test the capacity of some of the commercial exoskeletons presented previously to reduce shoulder injury risk [14][15][16][17][18][19][20]. Although in some of the aforementioned studies additional perspectives were addressed on the performance of the exoskeletons, in all of them, the effects were assessed mainly in terms of perceived discomfort, shoulder muscle activity, and task performance.

Indeed, in most of them, the evaluation of the exoskeleton effects is qualitative, as it is based on subjective questionnaires. For example, subjective measures are taken from the participants perception of discomfort and effort while wearing the exoskeleton. [14][17]

Consequently, and emphasizing again the importance of the scapular motion in shoulder injuries diagnosis, a path for improvement in this particular area would include the possible effects of the exoskeleton on the scapular kinematics.

Chapter 3

Methodology

With the objectives in mind and the main focus to develop the model and exploit it to analyze the effects of an upper-limb exoskeleton, it is important to establish clearly the methodology followed in terms of tools and workflow.

3.1 Focus and tools

To achieve the different goals determined in the introduction, some Software and Hardware systems are needed:

- Opensim software: use for the development of the biomechanical model and for solving inverse kinematics and dynamics with the motion experimental data.
- Optoelectronic motion capture system consisting of 8 Kestrel cameras and hardware by Motion Analysis and Cortex software.
- sEMG Delsys hardware consisting of EMG wearable sensors and a base to connect to the computer
- Paexo Exoskeleton from Ottobock, available at the rehabilitation laboratory from the Institute of Engineering of the TU Wien.
- Matlab calculation software: employed to process the data, calculate the virtual markers and plot results from Opensim calculations.

3.2 Participants

Four healthy subjects were taken as subjects for this preliminary study, being 3 male students (26 ± 2 yrs old, 183 ± 8.66 cm, 89.33 ± 16.29 kg) and 1 female student (23 yrs, 168 cm, 62 kg) with no previous shoulder injuries and all right side dominant.

3.3 Schedule: research steps

With respect to the research steps, the schedule plan followed is illustrated in Table 1 below.

SCHEDULE PLAN						
Research step	Oct	Nov	Dec	Jan	Feb	Mar
1.Literature review	█					
2.Model		█	█			
3.Protocol design			█			
4.Tests			█	█	█	
5.Data processing				█	█	█
6.Calculations				█	█	█
7.Results and analysis						█

Table 1: Detailed schedule plan with the different research steps

3.4 Data Workflow

Lastly, given that the terminology for data processing encompasses several substeps, the data workflow is detailed in the chart below (Figure 4).

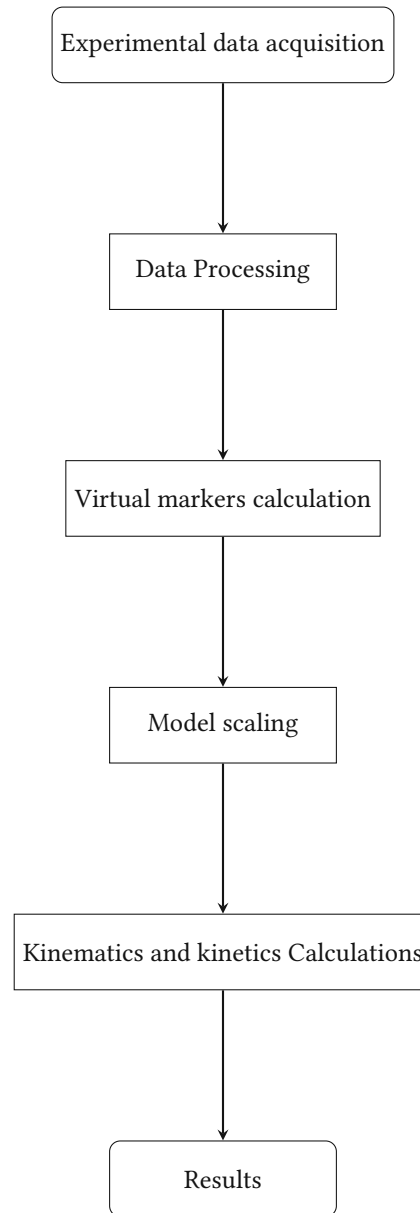


Figure 4: Data workflow from acquisition till results

Chapter 4

Model

After the careful consideration of the previous upper-limb models created by other authors and the need for improvement, an updated biomechanical model is developed in this project with the aim to obtain relevant kinematic and dynamic information for the design of the exoskeleton. The new updates included are mentioned in the next sections considering modelling from the jointset, muscleset and markerset points of view.

4.1 Jointset and geometry

Given the importance of the scapular motion and the different representations of the ST joint in literature, the one developed by Seth et al. [10] is taken as the starting point. The reason behind is the fact that this is the only study up to date whose results show a realistic motion of the scapula with respect to the thorax without excessive computational cost. The implemented joint permits the translation and rotation of the scapula on the surface of the thorax rib cage, modelled as an ellipsoid. Additionally, the coordinates of the joint comprise uniquely the functional kinematics of the scapula, easier to interpret. These 4 position coordinates are: abduction, elevation, upward rotation and winging, as represented in Figure 5.

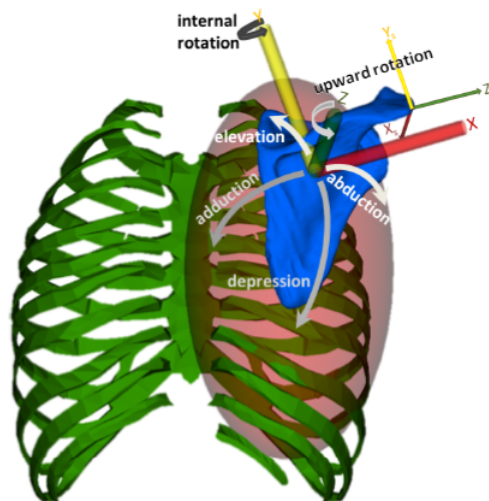


Figure 5: The four modeled functional coordinates of the ST joint by Seth et al. [10]

Although motion typically is represented as independent coordinates along three orthogonal axes that represent three-dimensional motion allowing 3 independent rotations and 3 independent translations (that is, 6 DoF), in this case, the selected coordinates are dependant but are chosen as a functional representation of the joint.

Abduction and elevation locate the scapula with respect to the thorax, similarly as longitude and latitude on a globe. Upward rotation represents the rotation of the scapula about the normal to the ellipsoid surface, in other terms, orients the scapula on the thoracic surface. Finally, winging or the internal rotation, rotates the scapula about a longitudinal axis in the plane of the scapula that enables the medial border and the inferior angle to raise off the thoracic surface. Although the 4 coordinates are modelled as rotations and express in degrees, the first two coordinates include both translation and rotation of the scapula with respect to the ellipsoid representing the thorax, as are based on both rotational matrix and translational vectors. [10]

The rest of the joints of the upper limb are modelled as follow. The sternoclavicular joint theoretically is represented as a ball joint enabling protraction-retraction, elevation-depression and axial rotation of the clavicle. However, given the intrinsic inaccuracy in axial rotation measurements, just the first two rotations mentioned are modeled, resulting in a universal or Hooke's joint [21]. Then, the acromioclavicular joint is modeled as a ball joint, by means of the definition of a point constraint, allowing 3 rotational DoF and denying the translational DoF. The glenohumeral joint is modeled as a ball-socket joint allowing rotation on the elevation plane, elevation, and internal rotation. [10] Additionally, the radioulnar joint is included to allow pronation-supination, as well as the wrist joint, including in this case wrist flexion-extension and deviation coordinates. [6]

Given that the original model was unilateral, bilaterality is introduced as an important update in terms of joints and muscular modelling. Considering that the geometry data employed [10] represented just one side, the other side geometry was mirrored by the assumption of symmetry. The convenient transformations were applied to obtain the symmetric geometry by means of the Software for data visualization "Paraview" [22].

Additionally, the geometry of the pelvis is included and the lumbar motion, between the pelvis and the thorax, is modeled as a ball-and-socket joint with 3 DoF: lumbar extension-flexion, bending and rotation. [23]

Finally, the skull and jaw are included for aesthetic reasons, keeping them welded to the torso for simplicity.

4.2 Muscleset

Opensim software, other than calculate the kinematics and kinetics of the motion capture trials, offers a greater toolset that includes also the estimation of muscle activation, as computed through Static Optimization or Computed Muscle Control.

To estimate as good as possible the muscles activation, the set of muscles should be represented adequately to reality. Although the analysis and sEMG measurements are conducted in a few number of muscles, the upper-limb model should consider a greater set of muscles in order to correctly determine the activation of each muscle and not overestimate the activation of some muscles because of the omission of the agonist muscles involved in the movements.

Although several muscle models can be employed, a good balance between realistic fiber length and computational viability with no errors should be achieved. The models published by Thelen [24] and Millard et al. [25] are used for this purpose, contributing to reliability without an excessive computational cost.

Regarding the different muscle characterization curves and other needed parameters to define each muscle modelling, the muscle parameters defined in [26], which are adapted from [27] are taken for the upper limb muscles. Additionally, lower back muscles are added, in this case Erector Spinae both for left and right sides, whose parameters have been extracted from Hamner's model [28]. This information is condensed in Table 2.

Finally, considering the muscles paths, the origin and insertion of each muscle are reviewed, and corrected if necessary, following the guidelines of the *Complete Anatomy* 3D anatomy platform [29].

Muscle	Group	Max isometric force	Optimal fiber length	Tendon slack length	Pennation angle
Trapezius	Scapula superior	1043	0.1127	0.027	0
	Scapula middle	470.4	0.0832	0.032	0
	Scapula inferior	414.4	0.1264	0.035	0
	Clavicle	201.6	0.1116	0.027	0
Serratus anterior	Superior	387.3	0.0945	0.000	0
	Middle	508	0.1538	0.012	0
	Inferior	430	0.1587	0.000	0
Rhomboides	Superior	200.2	0.0986	0.015	0
	Inferior	407.4	0.1152	0.028	0
Levator scapulae		280	0.1578	0.019	0
Coracobrachialis		648.2	0.0683	0.104	0
Deltoideus	Anterior	707.7	0.0940	0.088	5
	Middle	2597.8	0.0748	0.064	5
	Posterior	1324.4	0.0949	0.076	5
Latissimus Dorsi	Superior	201.6	0.2109	0.081	0
	Middle	315	0.2656	0.095	0
	Inferior	270.2	0.3062	0.062	0
Pectoralis Major	Clavicle	408.8	0.1087	0.014	0
	Thorax middle	683.2	0.1500	0.026	0
	Thorax inferior	571.2	0.1830	0.043	0
Teres Major		851.2	0.1410	0.006	0
Infraspinatus	Superior	967.4	0.0698	0.050	0
	Inferior	1037.4	0.0677	0.084	0
Pectoralis minor		429.8	0.1183	0.032	0
Teres minor		695.8	0.0550	0.051	0
Subscapularis	Superior	540.4	0.0676	0.059	5
	Middle	609	0.0744	0.055	5
	Inferior	854	0.0721	0.059	0
Supraspinatus	Anterior	543.2	0.0554	0.031	0
	Posterior	326.2	0.0591	0.025	0
Triceps long		1580.6	0.0969	0.241	10
Biceps	Long	485.8	0.1412	0.257	0
	Brevis	693	0.1264	0.212	0
Erector Spinae		2500	0.1200	0.029	0

Table 2: Biomechanical model muscle parameters based on Seth et al. [26] and Hamner et al. [28].

4.3 Markerset

Once jointset and muscleset have been addressed, the markerset employed is explained in this section. To generate the appropriate markerset for the specific motion analysis of interest, it is relevant to follow some indications.

In first place and considering the part of the body of interest, as well as the movements to follow, the body segments must be selected. To accurately detect the motion of each of the bodies, 3 markers should be placed in each of them, and the convenient links between them created.

According to the International Society of Biomechanics (ISB), consistent naming has been used all over the model for the markers. Markers are placed on the corresponding bony landmarks following ISB recommendations [30][31] for the body segments on the upper-limb and the pelvis, explained with further detail in Chapter 5.

In addition to this recommended markerset, marker clusters are included on the most relevant body segments to track in the current project. Precisely, for segments in which STA is highly relevant, additional marker clusters allow better segment tracking and could help minimize the artifacts.

This is the case of the scapula, whose tracking implies a high degree of difficulty given the non-negligible STA occurring, as explained before. To reduce this phenomenon from occurring, a cluster with 3 markers is attached to the acromion of the scapula, named shoulder cluster. Similarly to Senk et al. [13] the shoulder cluster is used as a non-deformable rigid body to reconstruct the scapular motion.

However, instead of using 3 surface markers to create a non-deformable solid to reconstruct the position, the use of the shoulder cluster illustrated in Figure 6, permits minimize the STA, as it replaces the 3 skin markers, all experimenting STA, for just the effect of the STA on the acromion. Indeed, there is no need for local optimisation as the distance in between the markers on the cluster is not going to change taking into account that they actually belong to the same rigid body.



Figure 6: Shoulder marker cluster

Although the STA was reduced with the use of the shoulder cluster above (Figure 6), some other artifacts appear in the preliminary collected data, as a consequence of the contact of the cluster sticks with the shoulder during the elevation of the arm. This interference causes wiggling and wobbling on the markers of the cluster and leads to noisy motion capture data, which results into inaccurate scapula motion. An improved version of this shoulder cluster was then implemented, which avoids contact interferences while doing arm elevations (Figure 7).



Figure 7: Shoulder marker cluster, version 2.

Finally, a humerus cluster is added to improve the arm tracking, as illustrated in Figure 8. Given the addition of sEMG sensors for the deltoids in the same humerus area, their position should be placed according to the space left by the sEMG sensors. The positioning of the sEMG sensors in this case is a priority because it must record the data from the targeted muscle and avoid cross-talk with the adjacent muscles.



Figure 8: Humerus marker cluster.

Further and more detailed indications of the correct positioning of the markers is further explained in the Motion Capture Protocol, explained in this document in Chapter 5. The following images sum up the markerset positioning on the model (Figures 9,10).

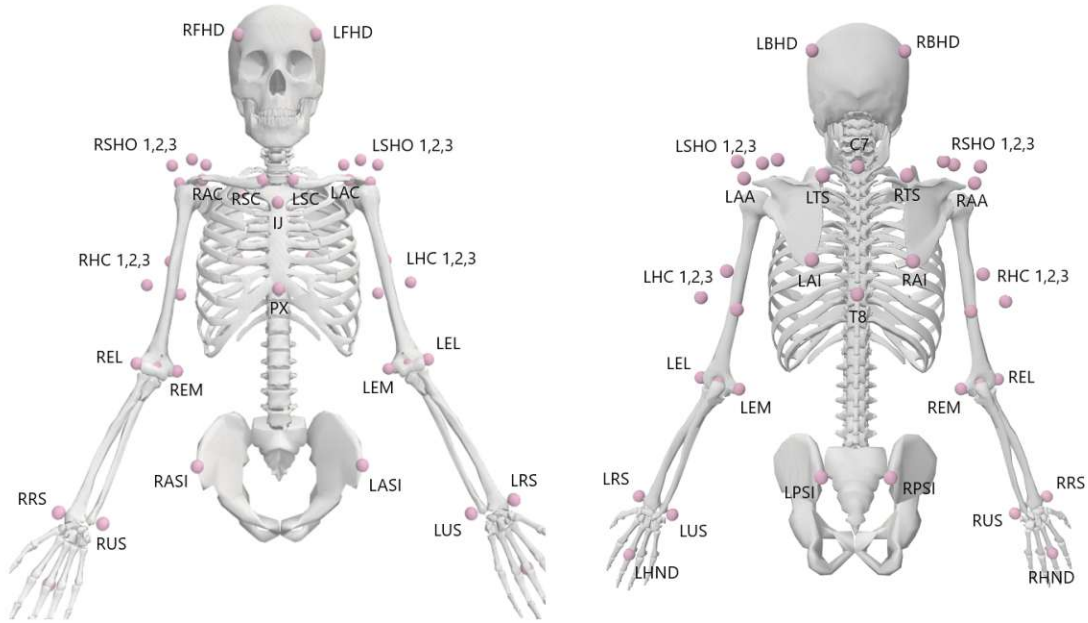


Figure 9: Frontal and rear views of the markerset on the musculoskeletal model.

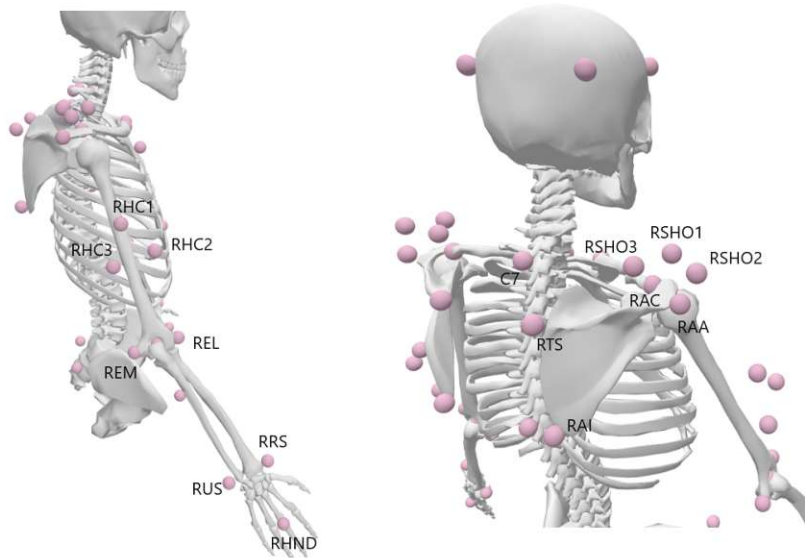


Figure 10: Other views of the markerset on the musculoskeletal model.

Finally, the complete model with its muscleset and markerset is plotted in Figure 11.

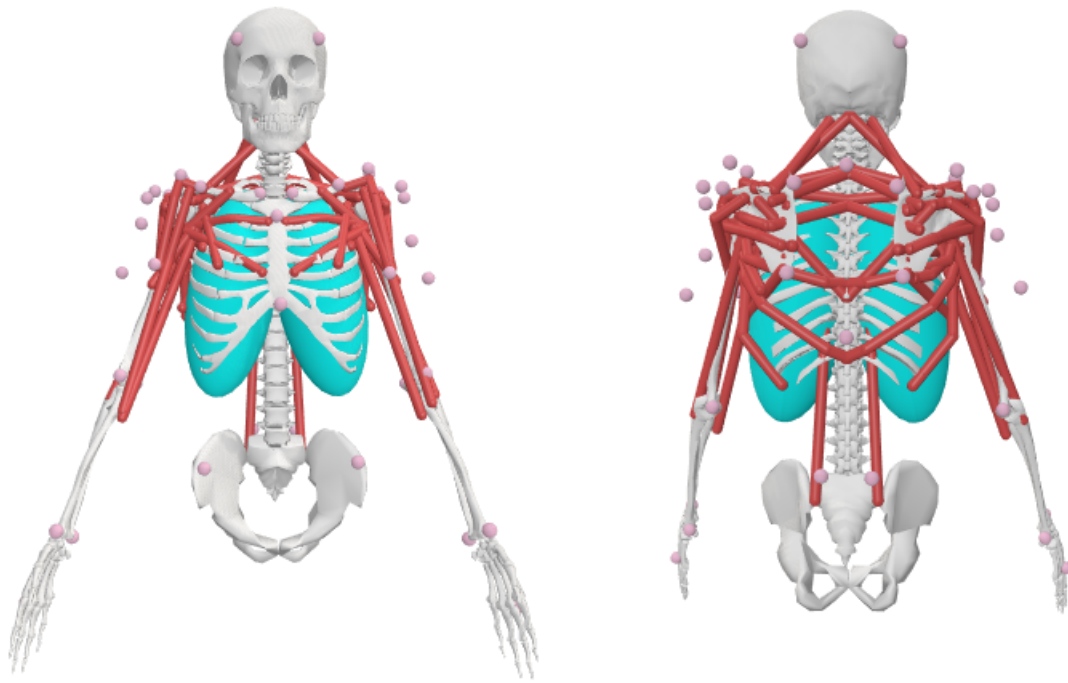


Figure 11: Frontal and rear views of the musculoskeletal model.

Chapter 5

Test protocol

To track and model the three-dimensional motion and muscular activity of the shoulder complex and upper limbs, a non-invasive motion capture protocol is written hereunder.

An optoelectronic system with passive markers is exploited along with a sEMG system. Both of them are synchronized to facilitate the analysis of the output data. The measurements are meant to drive the developed biomechanical musculoskeletal model for the upper body.

This protocol is being written to contribute with a measurements guide to ensure good data collection for further analysis within the objectives of a greater project consisting in the design of a passive exoskeleton for the upper limb.

5.1 Target and tasks

Healthy shoulder of workers whose occupation requires shoulder postures and exposure to several physical factors are the target of analysis for these measurements. The motivation behind lays in the fact that the working conditions they are exposed to can lead to shoulder WMSDs.

The main objective of upper-limb exoskeletons is to decrease the incidence of these injuries, which can be reflected in the upper limb kinematics and muscular activity. To investigate the effect of the exoskeleton, the shoulder motion is tested in two conditions: (i) with and (ii) without the exoskeleton.

With the aim to cover the great range of different movements executed by the target group of study in their work environment, the following variables are to be considered in the tests:

- **Arms working height:** posture with a flexion or abduction greater than 60° from the rest pose need to be considered, as they are a risk of WMSDs. Also postures with arms in underhead movement need to be studied as they may lead to discomfort when wearing the exoskeleton.
- **Tool mass:** interesting to establish the relation of muscle effort and torque required for different tools.
- **Task time:** consideration of muscle fatigue and possible appearance of discomfort in the case of the exoskeleton
- **ROM:** different amplitude of movements. Could be used to determine possible movements restrictions originated by the use of the exoskeleton.

In addition to these variables of analysis, the trial is designed to reproduce at the same time tasks that are naturally conducted in the selected working environments (automotive chain and food processing industries among others), such as painting, welding, drilling and other overhead tasks as well as heavy load lifting tasks.

Note: although the protocol is designed to be used in studies with real workers under activities resembling the real working conditions, this thesis just constitutes a preliminary study. As a consequence, the tests are conducted on available subjects, mainly students, and the tasks are simplified as further explained.

5.2 Motion Capture System set up

The motion analysis system used for the tests is composed by the following items:

- 8 Kestrel Cameras, 100 Hz capture frequency (Figure 12)
- Black box hub: permits the synchronization and connection of the cameras with each other and to the power supply
- Set of optical markers
- Calibration kit: L-frame and wand from Qualysis (Figure 13)
- Cortex capture and analysis Software



Figure 12: Kestrel camera [32]



Figure 13: Example of calibration wand and L-frame from Qualysis [33]

The set up of this system is focused on the environment conditioning and markerset positioning.

5.2.1 Environment

To make the capture and posterior analysis as accurate as possible, the following recommendations are followed.

- Use of a small volume of capture
- Volume of capture as free as possible of reflecting objects
- Use of clean or new markers
- Configuration of cameras such that they are focused on the segment of interest: the shoulder
- Use of marker cluster in the points of most importance to track the motion of the scapula and the humerus
- Marker labels should followed the consistent naming defined in the model
- Marker trajectories must be consistent and free of gaps along the recording: each marker should be captured at least by 2 of the cameras during the whole test trials. This ensures that position triangulation is possible and markers positions are not lost during the trial.

Prior to any motion recording, it is of high importance to check if the volume of capture is free from reflects, removing or covering them as much as possible by replacing the reflecting objects or changing the cameras diaphragm opening. To avoid cameras reflecting each other, they should be masked in each of the cameras capture space. Masking of other reflecting objects should be avoided because that also implies the reduction of the field of view of the markers for the cameras.

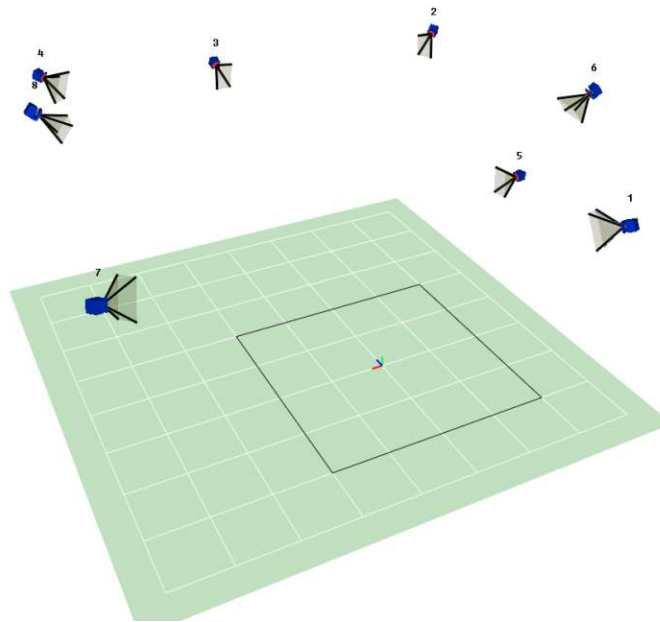


Figure 14: Camera setup seen from Cortex software

Once the volumen of capture as been set up following the indications, a calibration procedure is conducted. This procedure consists of an initial static calibration and a dynamic calibration afterwards. The initial calibration is done using a L frame with 4 markers (origin and two axes, the third one will result from the vectorial product of these two) to establish the ground system of reference in the capture environment. Then, a wand is used for the dynamic calibration, whose movement the tester should insist on the area of interest for the trials, in this case, the area in which the subject's shoulder is going to be. Figure 13 shows the different calibration tools.

Note: if the calibration is correct according to the volume of capture and it can be ensured that the cameras position and orientation are going to remain constant along all the trials, calibration will no longer be needed and the system could be considered calibrated for all the different captures afterwards. However, it is recommended to recalibrate when possible as reflections may appear because of the different room lighting conditions.

5.2.2 Markerset

The placement of the markers is of high relevance and should be set up in order to avoid as much as possible some artifacts as the STA, overlapping between markers or high relative motion of linked markers belonging to the same body segment.

The identified bony landmarks where to place them are resumed in the Table 3, which correspond to the ones of the model, in terms of placement and naming. Additionally, Figures 15 and 16 illustrate the positioning on a subject with and without exoskeleton.

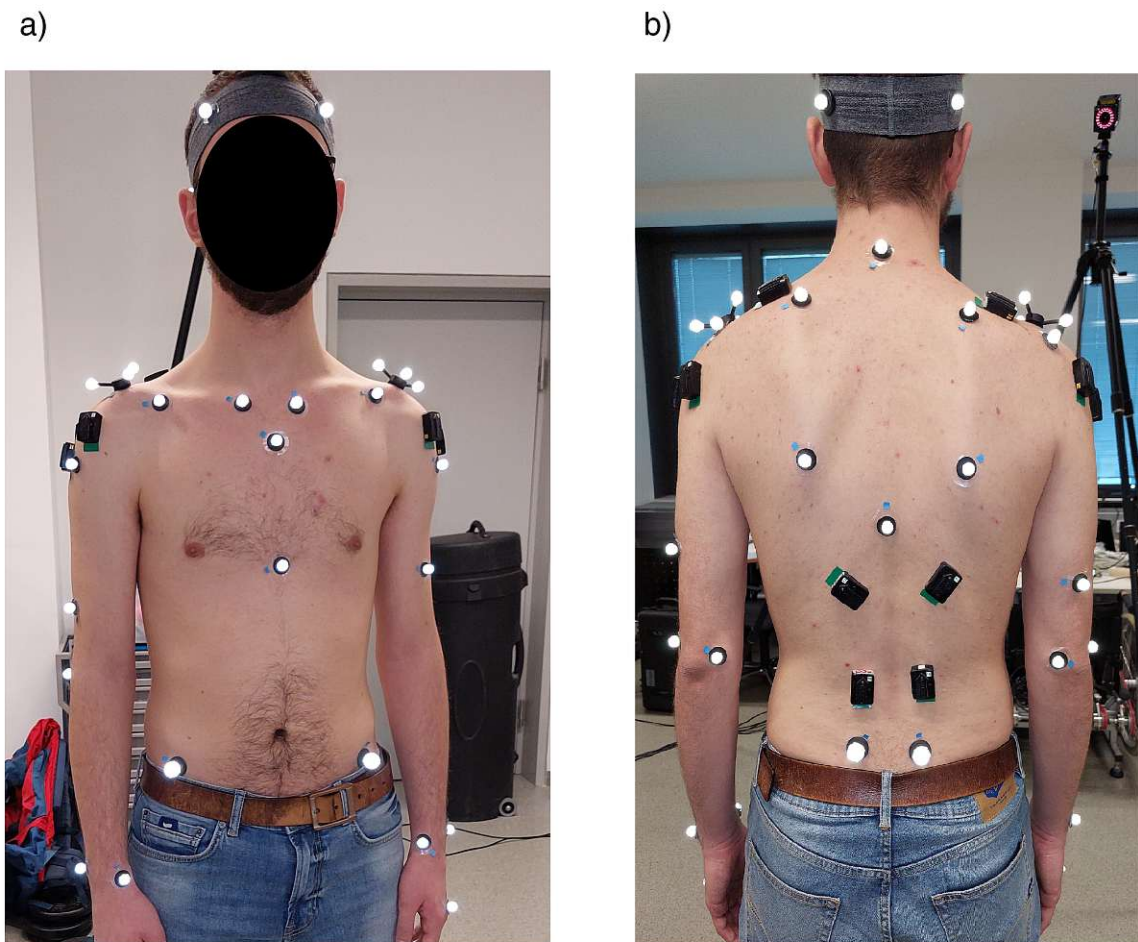


Figure 15: Frontal and rear views of the markerset on a subject.

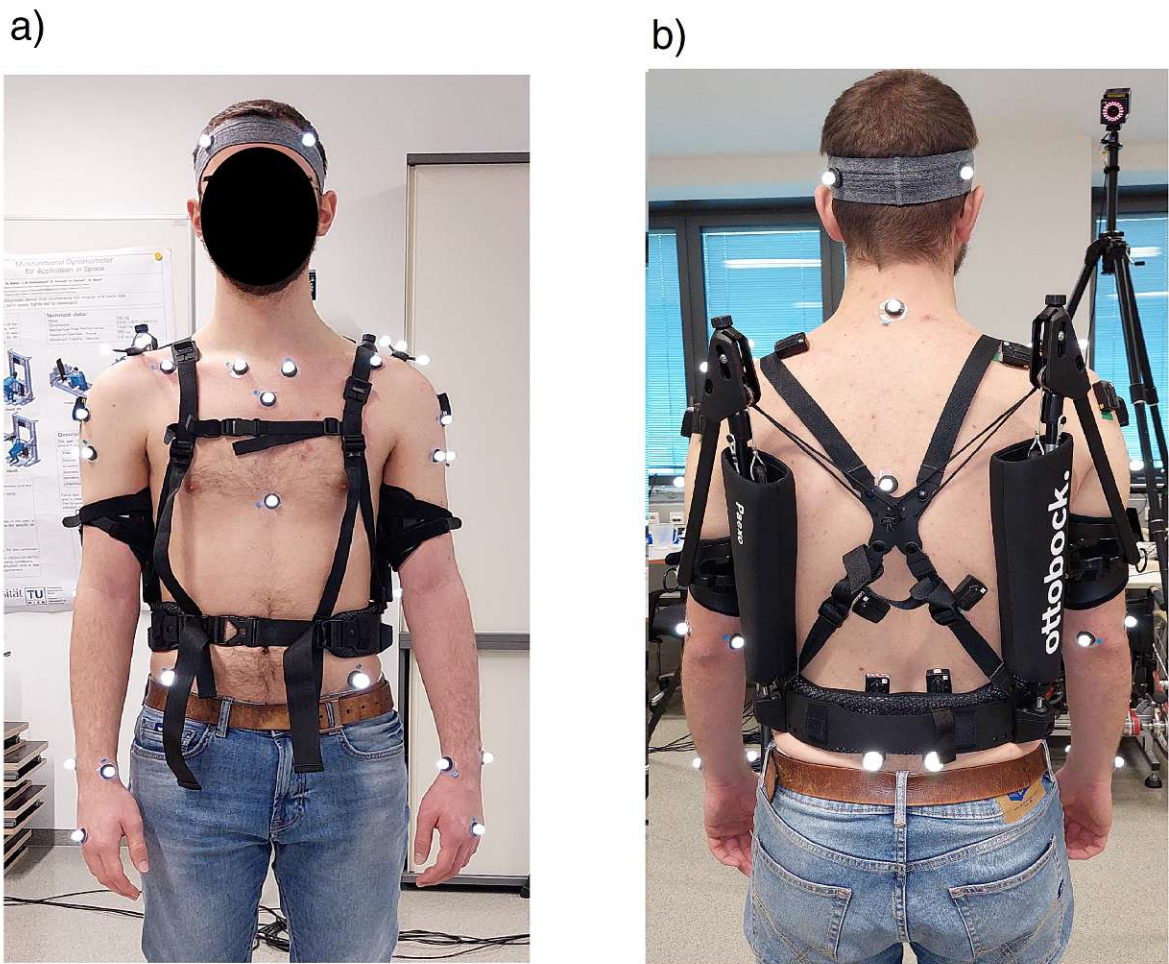


Figure 16: Frontal and rear views of the markerset on a subject with Paexo exoskeleton.

It is relevant to notice that the markers for the scapula are removed when the exo is worn, given that the straps will cover them or make them detach. However, this is not a problem, given that scapula markers are just used to scale the model, which does not need to be redone when the exo is worn, given that the subject is the same.

Additionally, scapula markers are not recommended to be used to track the movement, given the great STA produced by the great relative motion of the scapula under the skin. In their behalf, the shoulder cluster attached to the acromion would try to track this motion.

District	Marker	Landmark
Head	RFHD	Eminentia frontalis
	LFHD	
	RBHD	Eminentia occipitalis
	LBHD	
Thorax	C7	Processus Spinosus of the 7th cervical vertebra
	T8	Processus Pinosus of the 8th thoracic vertebra
	IJ	Deepest point of the Incisura Jugularis
	PX	Processus Xiphoideus, most caudal point on the sternum
Clavicle	RSC	Most ventral point on the sternoclavicular joint
	LSC	
	RAC	Most dorsal point on the acromioclavicular joint
	LAC	
Scapula	RTS	Trigonum Spinae Scapulae (root of the spine)*
	LTS	
	RAI	Angulus Inferior, most caudal point of the scapula *
	LAI	
	RAA	Angulus Acromialis (acromial angle), most laterodorsal point of the scapula *
	LAA	
RSHO1,2,3	Technical cluster on the acromion	
LSHO1,2,3		
Humerus	RGH	Glenohumeral rotation center**
	LGH	
	REL	Most caudal point on lateral epicondyle
	LEL	
	REM	Most caudal point on medial epicondyle
	LEM	
	REC	Elbow rotation center**
	LEC	
RHC1,2,3	Technical cluster on the humerus	
LCH1,2,3		
Forearm	RRS	Most caudal–lateral point on the radial styloid
	LRS	
	RUS	Most caudal–medial point on the ulnar styloid
	LUS	
Hand	RHND	Third metacarpal bone, in proximity of the phalangeal joint
	LHND	
Pelvis	RASI	Anterior superior iliac spine
	LASI	
	RPSI	Posterior superior iliac spine
	LPSI	

Table 3: Marker landmarks. R-prefix = marker on the right side; L-prefix = marker on the left side. * for only calibrating markers and ** virtual markers.

5.3 sEMG set up

The sEMG system consists of Delsys Trigno wearable EMG sensors, together with the Delsys Trigno base. This protocol section includes the positioning of these sensors and the synchronization of the EMG system with the motion capture system.

According to other authors [15][14][18][34][20][19], the main agonists and antagonists muscles involved in shoulder movements as well as some of the lower back are selected in order to compare the muscle activation among the different exercises and the effects of the use of a commercial exoskeleton. Additionally, a focus is made on the Deltoid muscles, given that they constitute the prime mover of shoulder abduction. [35]

Selected muscles for sEMG:

- Anterior Deltoid (Deltoideus Clavicularis): the main agonist muscle active during overhead work [34]
- Medial Deltoid (Deltoideus Acromialis)
- Posterior Deltoid (Deltoideus scapularis): co-contraction of antagonist muscles
- Upper trapezius (Trapezius Descendens): other agonist muscle
- Latissimus dorsi: effect on low and middle back
- Erector Spinae: effect on low back

The pictures from Hermens et al. [36] grouped together in Figure 17 indicate where the sEMG sensors should be placed. However, it is advisable that the tester itself tries to perceive the muscles on each of the subjects, in order to be as accurate as possible with the sensors positioning and avoid cross-talk with other muscles activation signals.

Although camera acquisition is done at 100 Hz frequency while EMG sampling frequency is around 2000 Hz, synchronization of both signals is easily attained. Precisely, it is achieved by means of Trigno Delsys base and Cortex software. The Delsys EMG base should be connected to the PC where Cortex software is going to be used. Afterwards, it is necessary to detach the sensors from the base and connect them to the PC by means of Trigno Control Utility software tool. Once the sensors are recognized, Cortex can be opened and the Delsys device connected. Then the software automatically recognizes the connected sensors and is allowed to collect the data simultaneously with the data from motion capture markers.

5.4 Trials

The trials to be recorded are divided into 2 main groups: calibration and dynamic tasks. To ensure an adequate test practice, all the trials should be executed within the limits of comfort of the subject, with the subject standing, and separately recorded for both shoulders.

5.4.1 Calibration

The purpose of this section is to get the necessary data to scale the model in terms of the anthropometry of each subject, as well as to facilitate the calculation of virtual markers. The procedure is described afterwards.

1. A static trial is conducted, where the subject stands still in a natural pose for 5 seconds approximately. Taking pictures of the subject at this point would facilitate further scaling. (Figure 18)
2. Shoulder rotation calibration. The subject performs small oscillations and circumduction of the arm. This should be done separately for each of the arms and the scapula should move as less as possible during the movement. (Figure 19)

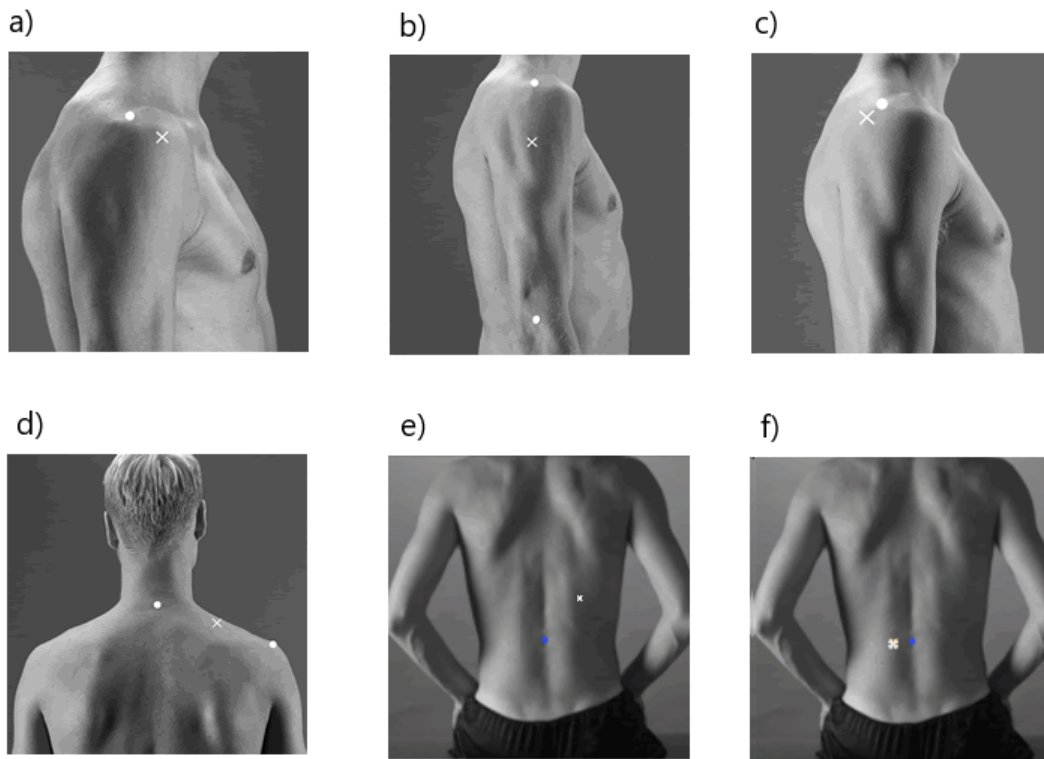


Figure 17: Positioning of sEMG sensors for the selected muscles: a) Anterior Deltoid, b) Medial Deltoid, c) Posterior Deltoid, d) Upper Trapezius, e) Latissimus Dorsi and f) Erector Spinae [36]

Then the output data is processed in Cortex and exported as .trc files to a Matlab implemented code that calculates the center of rotation of the glenohumeral and elbow joints with the shoulder rotation calibration data and incorporates them as virtual markers to the data from the static trial. Finally, the static trial data with the added virtual markers is used for scaling the model in OpenSim.

5.4.2 Dynamic tasks

This sections' aim is to collect data to analyze the muscle activity and kinematics of the subjects as a result of simulated work tasks that other works have defined to be physical risk factors in the development of shoulder WMDs. In addition, this tasks are to be performed with and without a commercial exoskeleton in order to compare the efficiency of it. The considered exercises are the following:

1. Right arm elevation in the scapular plane
2. Left arm elevation in the scapular plane
3. Right arm elevation in the scapular plane with extra weight on the hand
4. Left arm elevation in the scapular plane with extra weight on the hand

Where the scapular plane is defined to be approximately 30 to 40° anterior to the frontal plane, as defined by Hall et al. [37] and illustrated in Figure 20.

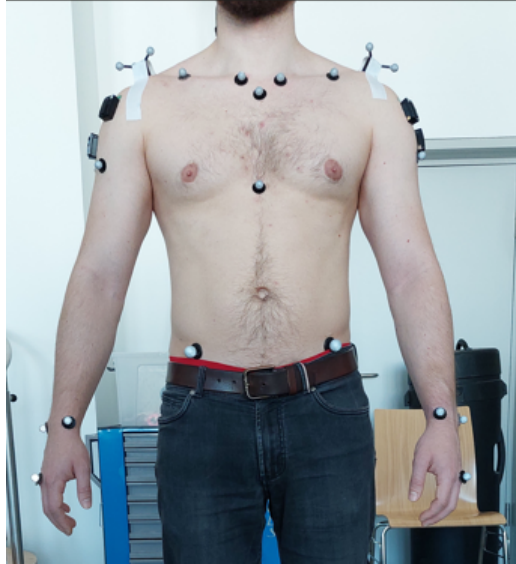


Figure 18: Example of static pose by one subject

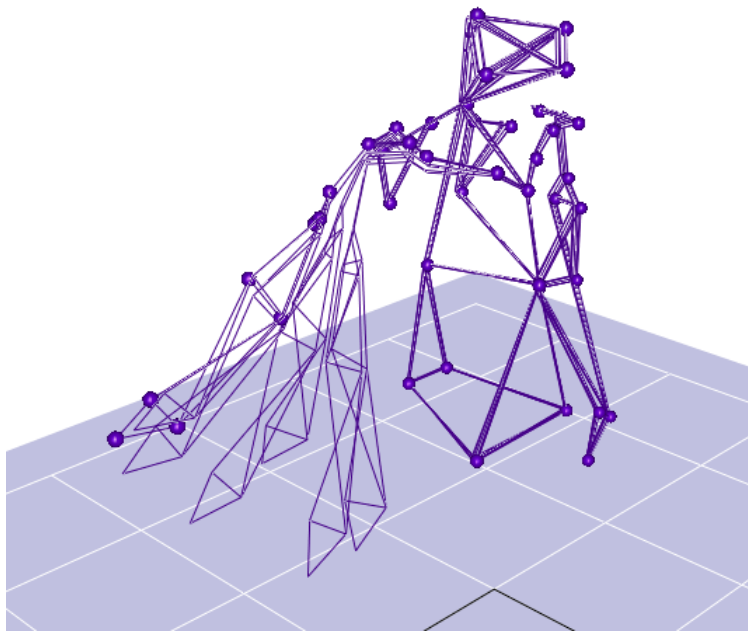


Figure 19: Calibration motion for the right arm on Cortex

All these dynamic tasks would be conducted for each subject under two conditions: (i) without and (ii) with an upper-limb exoskeleton.

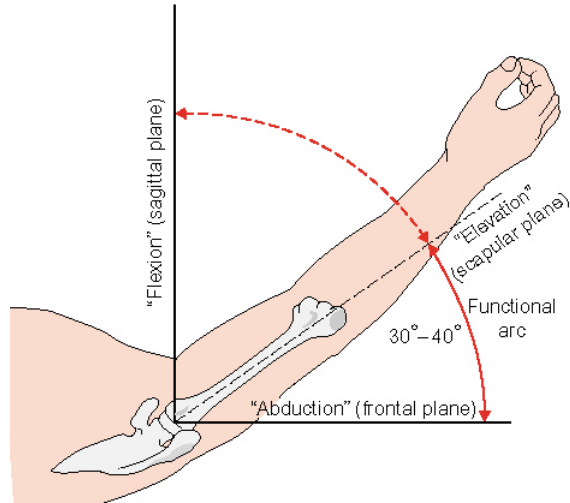


Figure 20: Scapular plane definition [37]

Figure 21 shows the elevation of the left arm in the scapular plane conducted by a subject under the no exoskeleton condition.



Figure 21: Elevation of the left arm in the scapular plane

5.5 Subject query

In addition to the collected data, other information should be collected from the subjects that may be helpful to interpret the results regarding subjects variability or aspects including other study variables. The following aspects are collected from each of the subjects.

- Name
- Subject number
- Height (cm)
- Weight (kg)
- Age (years)
- Gender
- Dominant side
- Profession, working tasks and working time (daily and in total)
- Previous shoulder injury (Y/N)

Chapter 6

Postprocess of experimental data

Although the protocol is designed to improve test reproducibility and to obtain clean data without artifacts or noise, there is still some post process that needs to be done on the motion capture and sEMG data.

6.1 Postprocessing of motion data

Even though the camera setup is intended to cover correctly the subject during the different tests and tasks, the subject clothing or other objects such as the EMG sensors can occlude at some point some of the markers. The protocol developed and followed in the tests is intended to avoid as much as possible this from occurring, but if some marker is not detected at a punctual instant, then interpolation may be a solution as a postprocess tool. In addition, other than losing a marker, in full contraction movements, two markers can be superposed for some of the cameras, and this is something to correct too in the post process.

The postprocess of the motion capture data is done using the Software Cortex, and conducted following some steps:

- **Rectify unnamed:** all unidentified markers are being rectified over all frames. This is useful as it rectifies the markers that have not been recognized as markers from the template and bring together separated segments of data belonging to the same unnamed markers.
- **Correct markers overlapped tracking:** that is, wherever cameras change the positioning of one marker for another because they got close in the trials. Exchange tool in Cortex is used to exchange the 3d positions of the selected markers over the selected frames.
- **Clean artifact peaks:** in some cases noise appears provoking sudden changes on the markers positioning. If these changes in the coordinates do not match reality, then this kind of noise should be cleaned. In this case the selected frame where the noisy peak appears can be cut out from the marker data.
- **Identify the tracked unnamed markers:** with the template where each marker belongs to a bony landmark.
- **Apply interpolation:** to fill the gaps of information in the 3d position graphs for markers that have not been completely tracked or were cut out because of noisy flickering by means of a cubic spline.
- **Smoothen data:** with Butterworth filter 5 point moving average to the selected markers in the selected frame

6.2 sEMG data processing

Surface EMG (sEMG) signals were recorded from 3 upper limb and 1 lower back muscles for both sides in this preliminary study. These include: the Anterior Deltoid (AD_L, AD_R), Medial Deltoid (MD_L, MD_R), Posterior Deltoid (PD_L, PD_R) and Erector Spinae (ES_L, ES_R). The sample rate was set at 2000 Hz. Although in the protocol, more muscles were defined to measure, they were simplified to this group, given the availability of a smaller number of sensors.

There are challenges of EMG signal processing including removal of systematic noise, identification of EMG unrelated to the activity itself, overcoming signal variability, the presence of artifacts... [38] In order to clean the data and facilitate the later analysis and interpretation, some filters and treatments are conducted on the data.

The collected sEMG signals were filtered by a 20 Hz high pass Butterworth filter, then rectified, then filtered by a 6 Hz low pass Butterworth filter to extract the enveloped and finally normalized.

6.2.1 High pass filtering

The application of high pass filtering in the processing of sEMG signals has as main goal reducing the baseline noise and suppressing the movement artifact while avoiding or minimizing the distortion of the EMG signal in the low-frequency.

The low-frequency noise which is aimed to eliminate in this first processing step is caused by several sources:

- **Extrinsic noise sources:** such as the power line noise and the cable motion artifact. Their presence can be totally eliminated with the selection of the appropriate equipment and technology.
- **Intrinsic noise sources:** the two intrinsic noise sources originate in the electronics of the amplification system (thermal noise) and at the skin-electrode interface (electro-chemical noise) [39]

According to De Luca et al. [39], the balance between noise filtering and no signal distortion at low-frequencies is obtained setting the high pass corner frequency at 20 Hz. Additionally, following Reaz et al. recommendations [40], notch-filtering is avoided. As a consequence, a high pass 4th order Butterworth filter with a corner frequency of 20 Hz is employed to reduce the last two mentioned sources of noise in the sEMG signals.

6.2.2 Rectification

Because of the later interpretation and analysis of the sEMG signals, rectification of these signals is preferred, given that the analysis focuses on the amplitude of the signal, which represents the level of activation of the muscle.

While half-wave rectification neglects the negative values, full-wave rectification takes the absolute value of each data point that is used. Usually for rectification, full-wave rectification is preferred [40]. In this post-process workflow, rectification is made by means of full-wave rectification.

6.2.3 Envelope extraction: low pass filtering

Because of the interest to analyze the amplitude of the sEMG signal, obtaining the sEMG envelope leads to a smoother signal amplitude profile, which could result helpful to highlight the changes on amplitude and relate them to the muscular activity.

One of the employed techniques of sEMG envelope estimation is performing a low-pass filter to the rectified version of the signal, at cutoff frequencies that vary approximately in the range 2–20 Hz for general applications [41].

An important consideration should be made before. As isometric voluntary contractions are sustained in time, the EMG signal progressively slows down and spectral components of the signal shift toward lower frequencies. In other words, muscular fatigue manifests in the signal power shift towards the low-frequency area. As a consequence, the lowpass filter may lose its effectiveness. [42][43]

However, in the current study, the sEMG measurements were done under tasks performed in short periods of time, so the fatigue effect is not expected and a low-pass filter is applied to the rectified signal. Similarly to McManus et al. [44], a low pass 4th order Butterworth filter with a cut frequency of 6 Hz was applied.

6.2.4 Normalization

Generally, the method followed for normalization uses maximal voluntary isometric contractions (MVICs) as the reference level to compare muscle activity levels and activation patterns between muscles, tasks and individuals, considering that the maximum neural activation is achieved in all muscles and individuals tested.[45][46]

In order to generate the MVIC, some tests are used. However there is not an agreement or consensus on the optimal test for each muscle, resulting in a considerable number of different reference tests for each muscles. [46]

Given the lack of consensus and the number of MVIC tests to be conducted in each subject for each of the studied muscles, normalization is done by a simplified method, using the maximum level of activation for each muscle and subject during all the recorded trials.

To sum up the sEMG processing workflow, Figure 22 illustrates an example for the results from each workflow step for the right anterior deltoid of subject 4 during elevations in the scapular plane with the right arm.

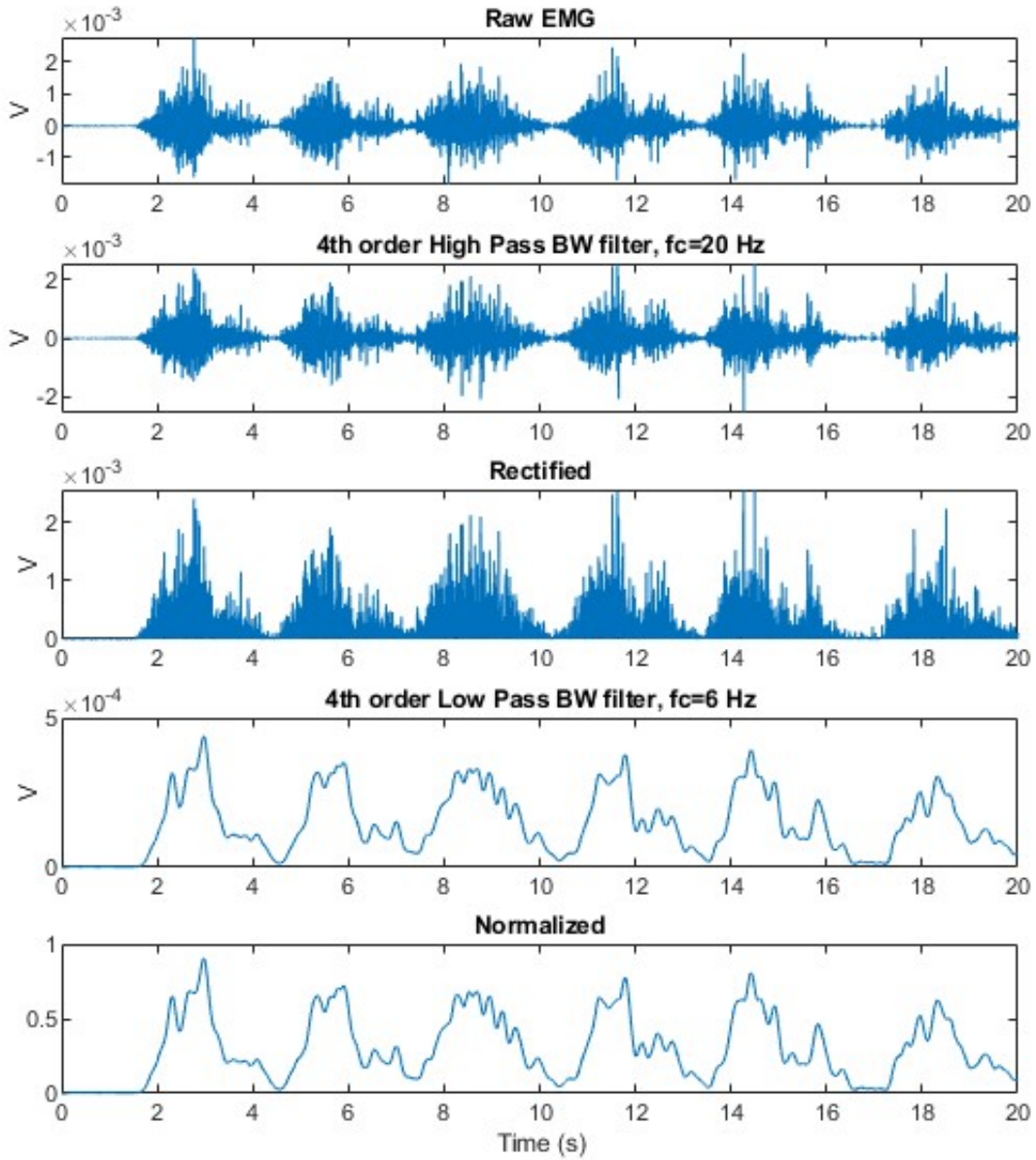


Figure 22: Example of sEMG signal processing workflow conducted for Subject 4, Right Anterior Deltoid muscle during elevations in the scapular plane with the right arm.

Chapter 7

Kinematics and Kinetics calculations

Once the biomechanical model is developed and the experimental data processed, the model can be further exploited in order to obtain information on the kinematics and kinetics from the different trials and subjects.

7.1 Virtual markers calculation

Prior to scale the model, some virtual markers are calculated to improve this further scaling. Precisely, the glenohumeral rotation center and elbow joint center are calculated.

The estimation of the joints center of rotation can be done by regression or by means of functional tasks. In this case, the functional task method is selected, and these movements defined in the protocol as calibration tasks.

In this calibration procedure, the subject performs the functional movements that would be then used to estimate the functional joint centers at the shoulders and elbows, and once calculated, they are appended to the subject static trial data for further model scaling.

While the estimation of the elbow joint center (REC and LEC for right and left sides) is simple and consists in calculating the medial point in between the bony landmarks for the most caudal points on the lateral and medial epicondyles of the humerus (REL,REM for the right side and LEL and LEM for the left) for every instant, the estimation for the glenohumeral rotation center is more complex.

Because of the nature of the glenohumeral joint, the relative motion between the scapula and the humerus can be decomposed into a rotation about and a translation along a single axis. This axis, which generally varies in position and orientation instantaneously, is called a helical axis of motion, or screw axis.[47] Calculating the helical axis means determining its orientation and its position, based on the recorded motion of the joint, which is done following the method and code developed by Ancillao [48]. The virtual markers for the glenohumeral joint are the RGH and LGH for the right and left sides and are defined as the pseudo-intersection of the consecutive helical axes associated to the motion.

7.2 Model scaling

Model scaling is a really complex process but highly necessary, given that all the following calculations realized with the scaled model for each subject depend on the model scaling and repositioning of the markers. It is conducted in OpenSim software, using the original model as base and with the recorded static trials in which the calculated virtual markers have been appended as input.

Firstly, mass distribution of the original model is preserved and the weight of the scaled model is estimated as a percentage from the subject total body weight, given that the model does not account for all the body but just

the upper-limb, thorax and pelvis. The percentage used is extracted from the study of segment weight percentages conducted by de Leva et al. [49]. Precisely, as the model does not include the lower limbs, it corresponds to the 59.26 % of the total body weight. The subject weight is included in the subject query from the protocol.

In order to simplify the scaling process, the same scale factor is used for each body segment. Scaling is obtained by matching the model markers to the experimental ones in the static pose. This is done by means of error minimization, and weights for each marker are assigned and used to determine how strongly the algorithm should try to match them. [50]

To correctly scale the model and obtain the minimum error between the static trial markers positions and the scaled model markers, some guidelines are followed:

- Markers that are reliably attached to the correct bony landmarks, as well as the virtual markers calculated for the rotation centers are fixed to avoid the software to move them when scaling. This should be done on those markers whose bony landmark is easy to identify, as for example: IJ, C7, RSC and LSC.
- Assign high weight to trustfully located markers, while the clusters are given low values or even disabled as they are not stucked to bony landmarks.

To validate scaling, the optimization should be checked as optimization failure is a clear sign of incorrect scaling. It is also necessary to check the marker error and the joint angles, which we can be compared with the pictures taken from the subject. [50]

7.3 Kinematics calculation

With the scaled model for each subject, Opensim is used to calculate the kinematics for the position coordinates defined in the model for the different tasks from which the motion and muscular activity were captured.

It is done by means of Inverse Kinematics (IK), with the so named tool in OpenSim. IK consists in the calculation of the values for the different generalized coordinates from the model that best match the experimental markers from the motion data for each time step. The difference between the model markers and experimental markers is seek to be minimized as much as possible through a weighted least squares method. [51]

Similarly to the scaling procedure, weights should be assigned for each model marker, depending on how strong the match with the experimental markers is aimed. However, for the IK calculation, on the contrary to scaling, high weights should be assigned for the clusters and low for the bony landmarks, were a greater STA or muscle movement is expected. For example, to scale, high weights are given for the scapula markers in order to place it correctly but when kinematics are calculated, the scapula markers that are not included in the shoulder cluster are disabled because of the highly relevant STA. Additionally, with the use of the exoskeleton, those markers can not be tracked as the exoskeleton straps occlude them.

Although in some body segments, if no enough tracking markers or a marker cluster is used, then the anatomical markers should be weighted also heavily, to ensure that the body segment is correctly tracked in the motion. But, always those in which STA is not really relevant during motion, such as IJ or C7.

7.4 Kinetics calculation

The next step would be the kinetics calculation, which, given the kinematics calculated from the IK, are calculated by means of Inverse Dynamics (ID). ID technique employs kinematics and external forces to calculate torques and forces acting on the joints for the particular studied motion. To determine these internal forces and moments, the equations of motion for the system are solved with external forces, mass properties and accelerations calculated by the double differentiation of the kinematics results. [52]

Given that noise is amplified by differentiation and to calculate the accelerations the kinematics data is differentiated twice, it is highly recommended to filter the kinematics data. [52]

Then, with respect to the external forces, in the trials where the subject was wearing the exoskeleton or holding an extra weight on the hand, external force data should be considered. In the case of the trials conducted without the exoskeleton and with the weight, the external forces are easily applied as the weight of the mass on the hand applied as a punctual mass. However, the external forces applied by the exoskeleton are not easily deduced and would require future force measurements. As a consequence, kinetics would only be calculated for the trials in which the subjects were not wearing the exoskeleton.

Chapter 8

Model validation

Before analyzing the results, a validation of the model is done. First, in terms of bilaterality and then, some parameters are compared with other studies from literature. For validation, the tasks without weight and the exoskeleton are used, as comparable data exists in literature for these cases.

8.1 Bilaterality

Given that the original model included just the geometry, jointset and muscleset for the right side and the left side was added afterwards, it is considered necessary to first validate the left side and see if both sides work analogously. The comparison between the right and left sides is illustrated below in terms of kinematics and kinetics.

The curves for the kinematics of the different ST joint coordinates defined in the model and calculated by IK are plotted against the cycle percentage in Figure 23. In red and blue are shown the subjects and cycles mean for the right and left scapula respectively, where the cycle represents the elevation and depression of the respective arm (right or left) in the scapular plane.

Similar results are obtained for right and left sides, despite a noticeable standard deviation, for the four defined coordinates.

The results coincide not only in kinematics but also in kinetics, showing in this case similar moments for the ST joint in the same scapular planes of motion for which kinematics were analyzed before (see Figure 24). Notice that the moments resulting from the kinetics are normalized to weight, given that if not the subjects mean can not be calculated, as kinetics depend directly on the subjects mass.

8.2 Validation with literature

Regarding the validation with literature, having implemented the ST joint based on the model of Seth [10] the calculated ST joint coordinates kinematics are plotted and compared with the ST joint coordinates reconstructed motion from the measured bone-pin markers used in the reference study.

In Figure 25 the curves for the ST joint coordinates are plotted for the mean of the subjects and cycles during elevation-depression task in the scapular plane, while in Figure 26 the coordinates are plotted for an abduction-adduction task, in other words, an elevation-depression in the frontal plane.

The obtained curves are similar to the ones of the reference study, although some differences can be observed. First of all, the scapular motion in both cases is dominated by scapula upward rotation and abduction.

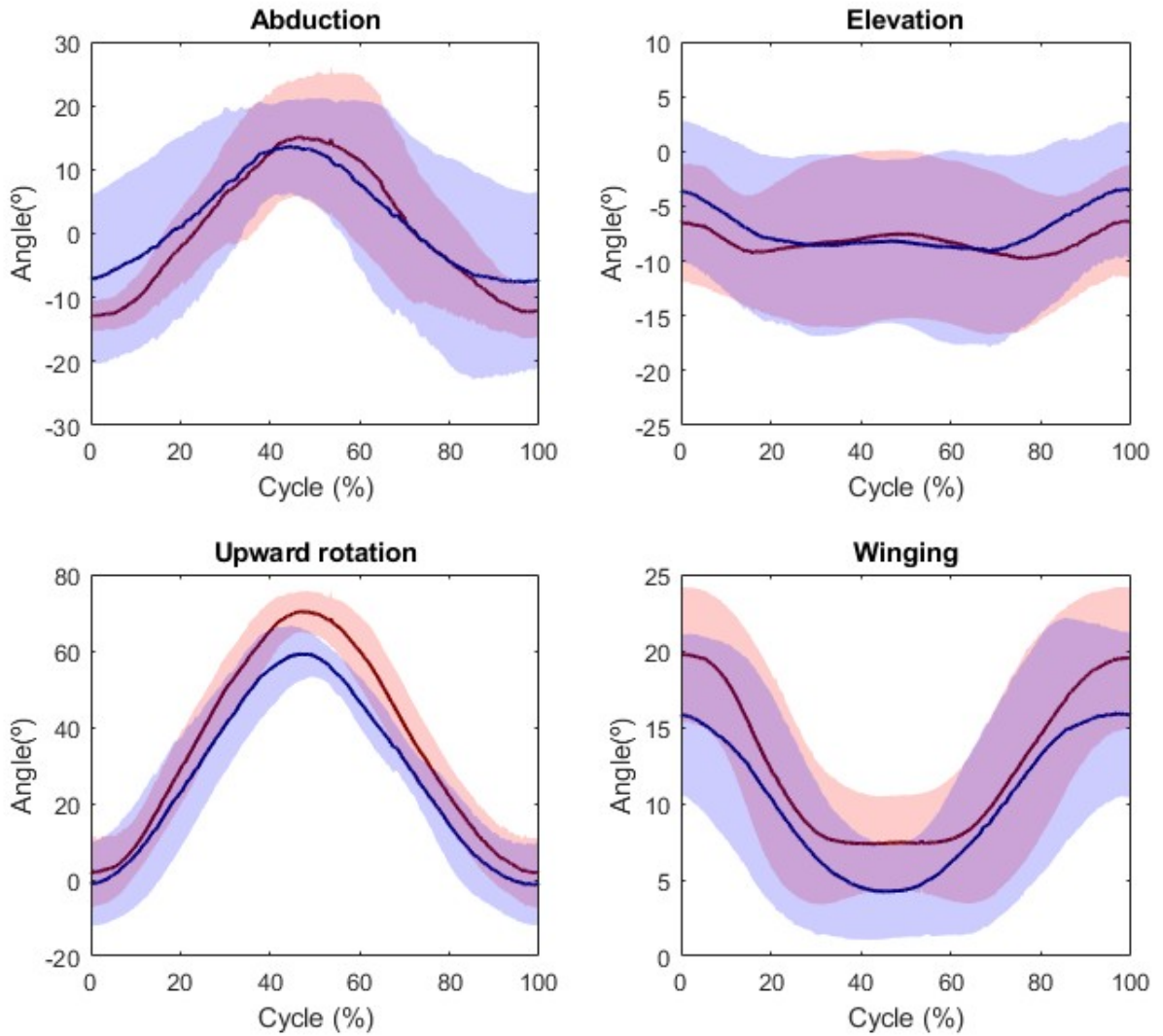


Figure 23: ST joint kinematics comparison for right and left limb during repetitive right and left elevation-depression of the arm in the scapular plane. The curves represent the mean of the subjects and the cycles and the shaded area the +/- standard deviation (SD).

On the contrary, the curves do not start and end in the same angles as in the reference, although this can be explained by the differences on the defined initial configuration of the scapula in the model and the different static pose of the models. Despite this, the curves seem to follow the same patterns as in the reference although starting in different angles.

Moreover, the amplitude of the curves seems greater than the observed in the reference for the different joint coordinates. This could be explained by the fact that the plane of motion is not exactly the same, as in the reference the elevation is done in the frontal plane, while in this study trials the elevation is conducted in the scapular plane, 30° anterior to the frontal plane.

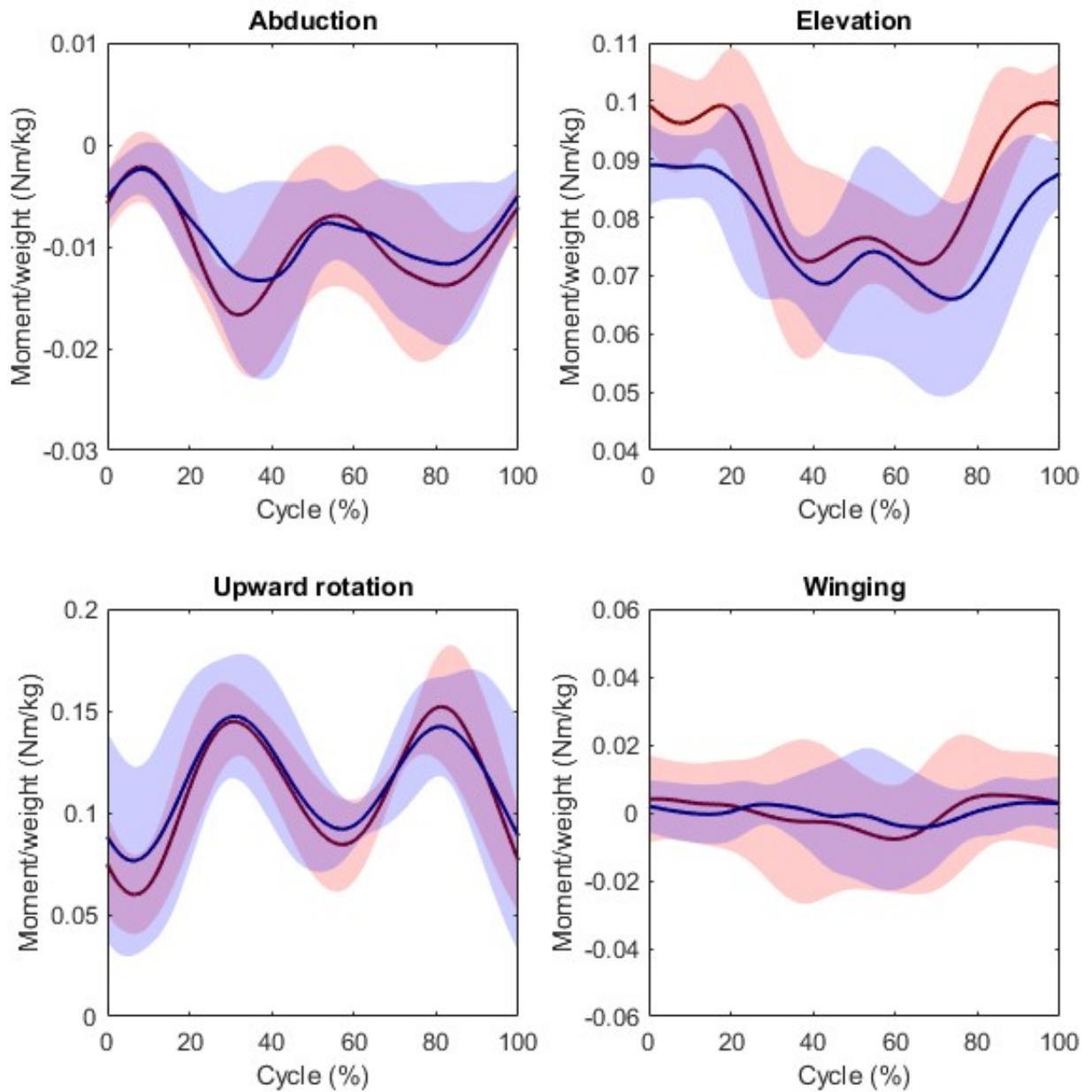


Figure 24: ST joint kinetics comparison for right and left limb during repetitive elevation-depression of the arm in the scapular plane. The curves represent the mean of the subjects and the cycles and the shaded area the +/- SD.

Additionally, in the literature reference, the results from the bone-pin experiments are plotted, while some error was obtained when comparing these results to the results obtained from the inverse kinematics calculated on the model. [10]. These differences should be considered, as maybe some further improvements could be done in the ST joint, as the range of motion of the scapula seems to exceed a little bit the reference values from literature. [53]

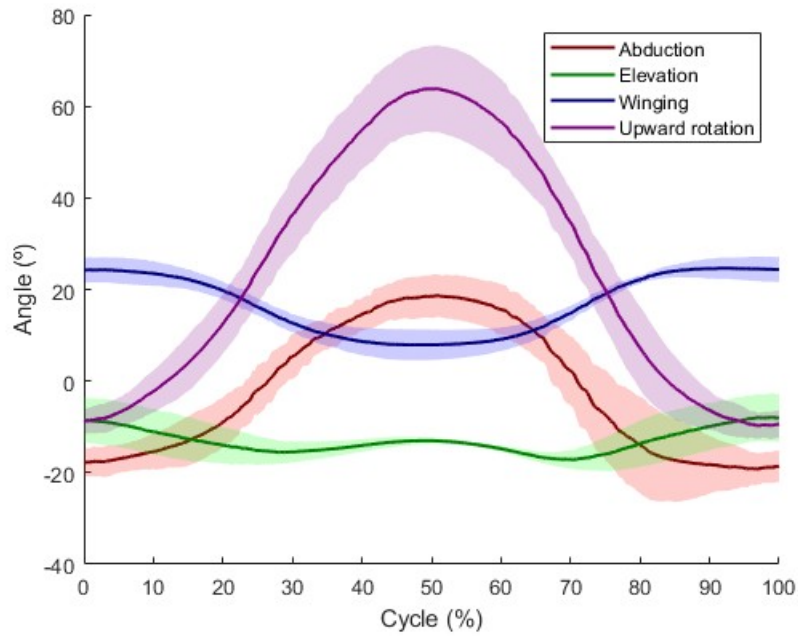


Figure 25: ST joint coordinates during elevation-depression motion in the scapular plane for the subjects, sides and cycles mean. The curves represent the mean of the subjects and the cycles and the shaded area the +/- SD.

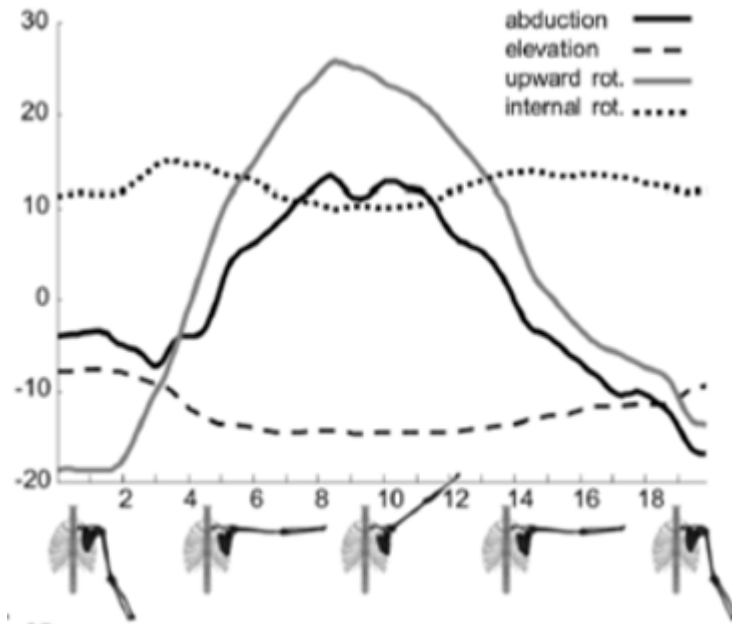


Figure 26: ST joint coordinates during abduction-adduction motion reconstructed motion from measured bone-pin marker [10]

Nevertheless, from a general point of view, the model representation of the shoulder complex, and more precisely of the ST joint, seems to be reasonably adequate to reality.

Finally, another parameter discussed by other authors with respect to the scapula motion, such as the scapulohumeral rhythm analyzed by Bagg [54], is compared. The scapulohumeral rhythm in this case reflects the contribution of the scapula when elevating the arm in the scapular plane, as it corresponds to the scapular upward rotation in terms of shoulder elevation. In Figure 27 the rhythms calculated for the mean of the cycles for each of the subjects are plotted, which are comparable to the different patterns observed in the author's study, represented in Figure 28.

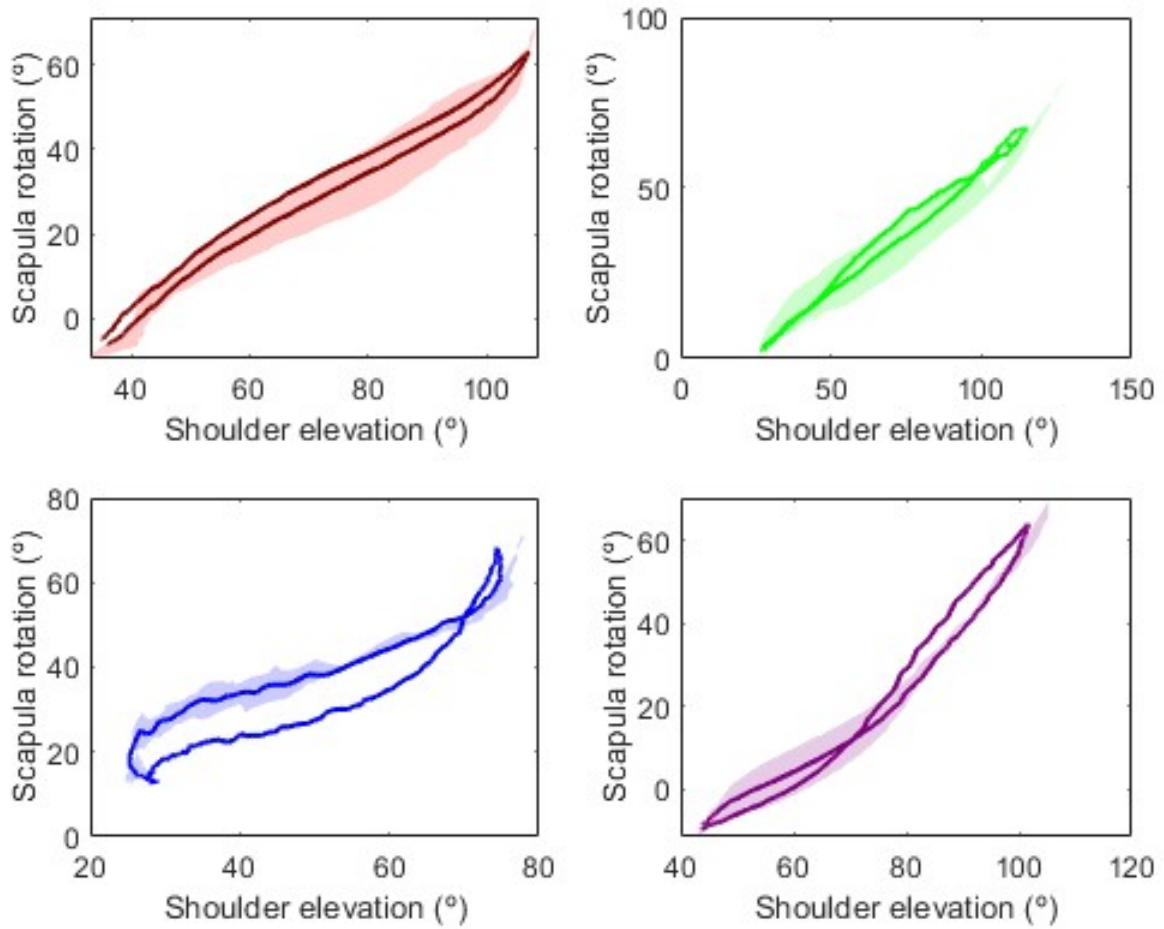


Figure 27: Scapulohumeral rhythm mean for the four different subjects. The curves represent the mean of each of the subjects for all the cycles and the shaded area the +/- SD.

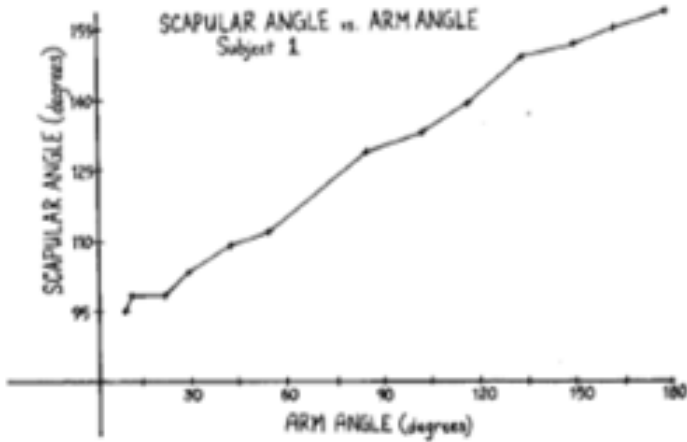
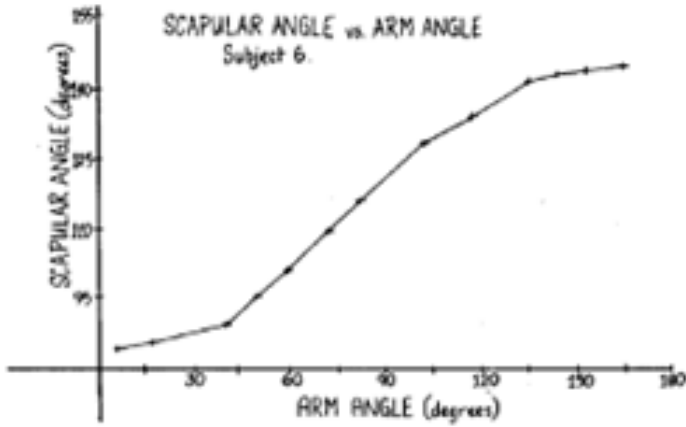
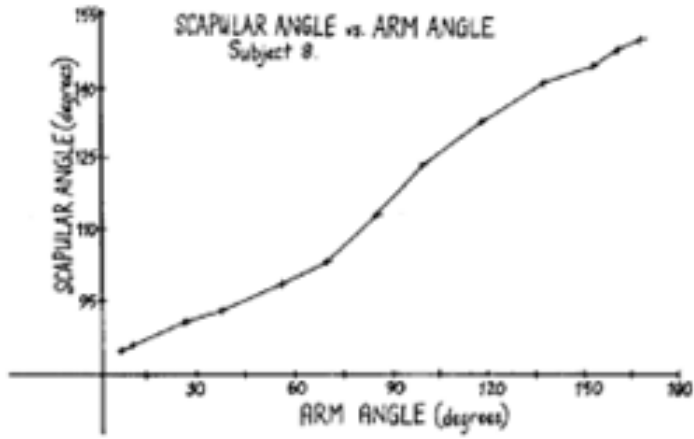


Figure 28: Scapulohumeral rhythm different patterns obtained in the study from Bagg et al. [54]

Chapter 9

Results

Once validation is discussed, results from the tests can be analyzed. First of all, subjects variability is studied and afterwards, the effects of the commercialized exoskeleton on the scapular motion are evaluated.

9.1 Inter-variability between subjects

In Figure 29, the kinematics represented show the mean for each of the subjects for three different ST joint coordinates along the cycle and the scapulohumeral rhythm, which includes implicitly the fourth coordinate, during an elevation-depression movement in the scapular plane. When comparing the kinematics between the different subjects, the scapula motion seems similar for most of them in the global trend but differ slightly on the measured angles.

One observable difference is the greater amplitude of the scapular motion for Subject number 4, whose results for scapula abduction and winging show a greater range of motion when compared to the rest of the subjects.

To further assess the possible differences in between the subjects, kinetics were calculated applying ID to the filtered kinematics for each subject. Then, the means were calculated for each subject and plotted in Figure 30. In order to make a reasonable comparison, the obtained moments for the different ST joint coordinates were normalized in terms of the respective subject's weight, given that the moments are calculated considering the weight of the arm of the subject. Under the supposition of uniform mass distribution, the normalization is done with the total subject weight.

From the normalized to weight moments, the curves are similar for the different subjects, despite the observed cycle shift in between them.

Finally, the different ROM for all the subjects and scapular kinematics are represented in Figure 31. The standard deviation obtained for each of the subjects is small, showing a great repeatability in the tests for each of the subjects. However, again the results show differences in between the subjects, showing Subjects 1 and 2 similar results in between them, but differing noticeably from the other subjects. Subject 4 shows the greater amplitude of scapular motion for every coordinate, as expected from Figure 29, and on the contrary, Subject 3 shows the most limited motion.

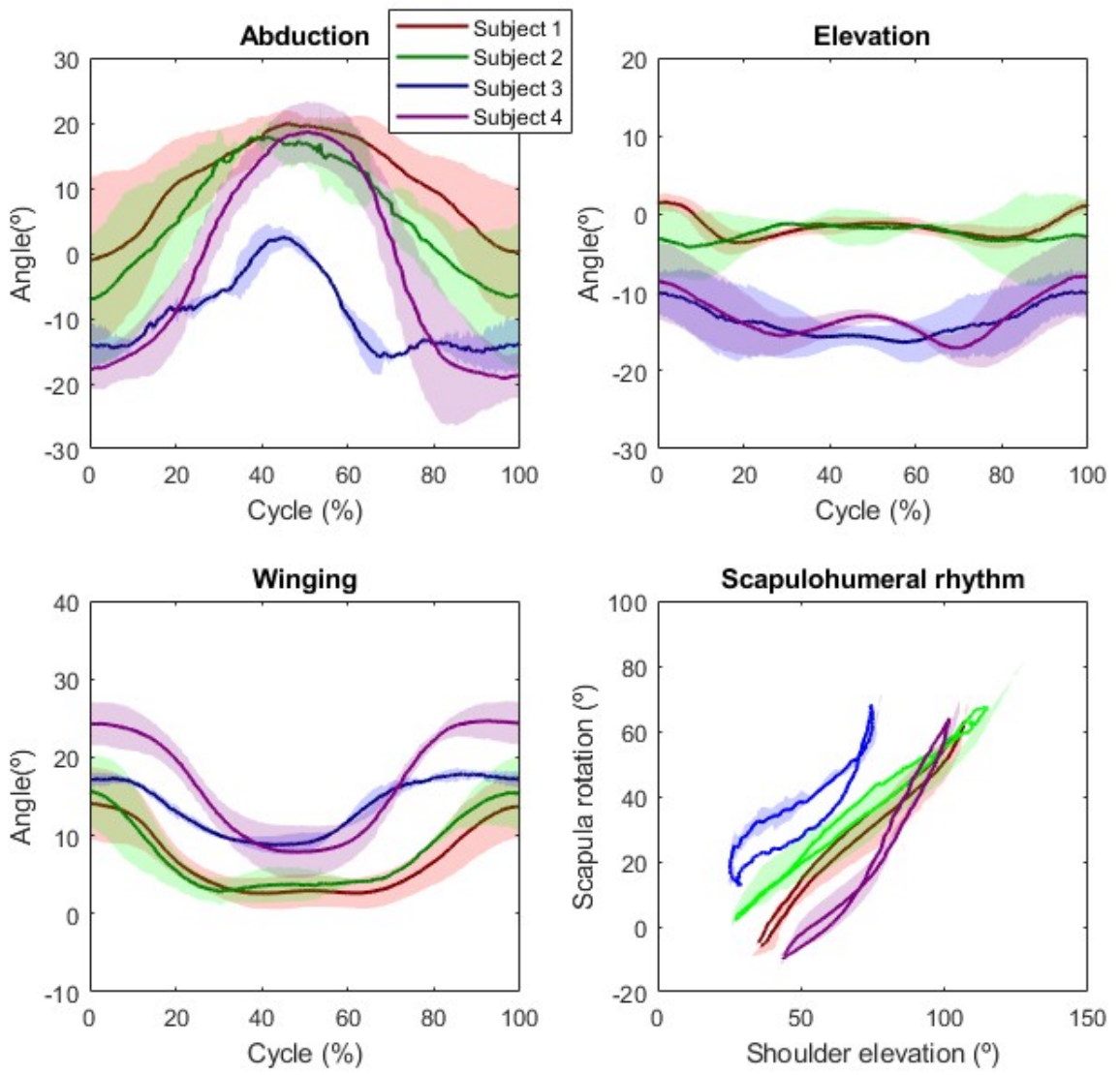


Figure 29: Abduction, elevation and winging ST joint coordinates and scapulohumeral rhythm during elevation-depression motion in the scapular plane for the mean of each subject. The curves represent the mean of each subject for all the cycles and the shaded area the +/- SD.

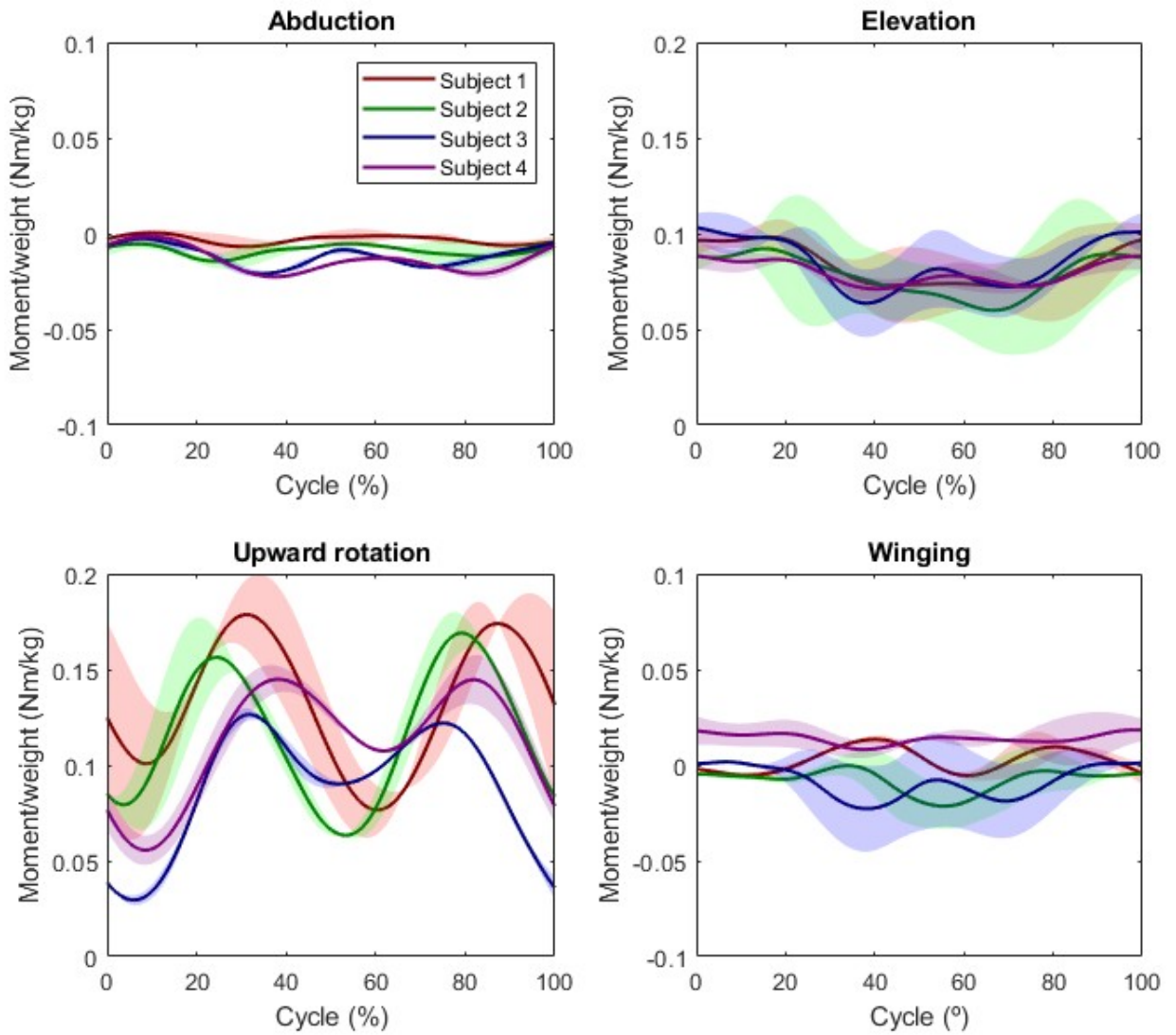


Figure 30: ST joint normalized moments during elevation-depression motion in the scapular plane for the mean of each subject. The curves represent the mean of each subject for all the cycles and the shaded area the +/- SD.

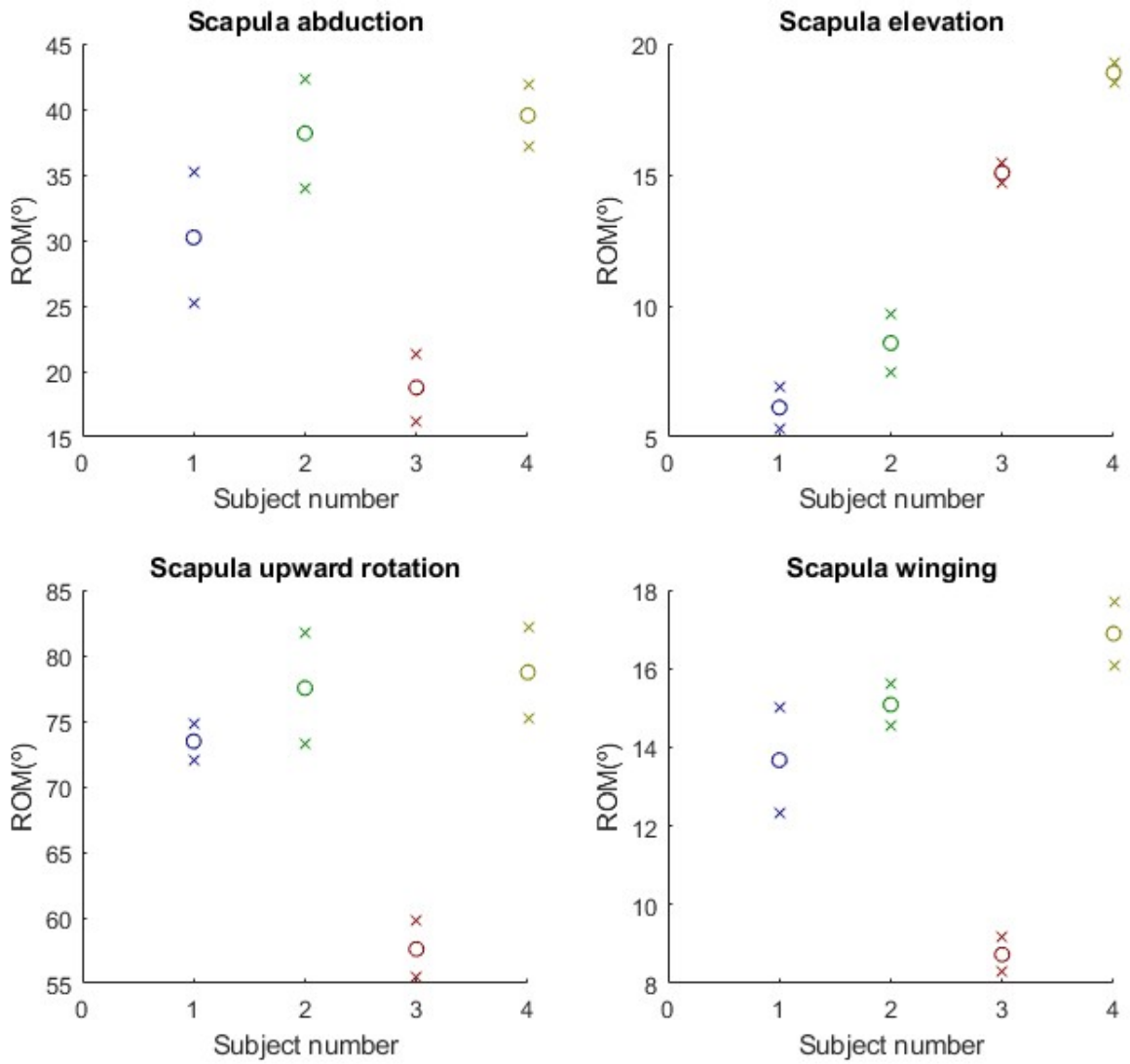


Figure 31: ROM for the ST joint coordinates for each subject mean during elevation-depression motion in the scapular plane. The O represent the mean of each subject for all the cycles and the segment constituted by the X, the +/- SD.

9.2 Exoskeleton effects

With the subject variability in mind, in order to analyze the effects of the Paexo exoskeleton, the mean of the subjects is taken for the scapular kinematics and muscular activity for the test configurations with and without exoskeleton.

9.2.1 Kinematics

Similarly to Figure 29, the motion of the scapula related to three of the ST joint coordinates is analyzed, as well as the scapulohumeral rhythm (see Figure 32).

At first sight, the global trend comparison plotted seems to be similar for the tasks with (blue) and without (red) the exoskeleton. However, if it is observed with a greater detail, the exoskeleton curves suggest a decrease in the scapular abduction and an increase in the scapular elevation with respect to the curves without the exoskeleton.

Focusing now on the ROM for the subjects mean (Figure 33), no differences are suggested for the tasks with and without the exo. Additionally, the great standard deviation because of the subjects variability is strongly reflected here.

9.2.2 Muscle activation

In terms of muscular activity, the mean for the subjects normalized sEMG under the same tasks is computed and plotted in Figure 34. Precisely, the muscular activity for the deltoids from the working side and the contralateral lower back muscle, the ES, are represented. This muscle selection was based on the level of activation of the muscles, so just the most implied or working muscles for the movements are analyzed.

Theoretically, from the deltoids, the anterior portion is more active in the upwards movement of the arm, the posterior portion acts more in extension and downwards movements and the largest middle portion allows abduction of the arm and its activation is similar in both directions.[35]

Apparently, the plotted curves show a similar activation trend along the cycle and do not suggest a reduction of muscular activity in shoulder-involved muscles as the deltoids, neither on the contralateral lower back muscles. The most active muscle from the elevation-depression motion in the scapular plane is the AD, as expected, followed by the MD and finally by the PD together with the ES.

With a higher level of detail, some differences could be noticed in the deltoids. In first place, a slightly decrease in the anterior and MDs slope during the elevation (approximately 0-50% of the cycle) with the exoskeleton with respect to the curve without it can be noticed.

Additionally, a greater activation of the deltoids at the half of the cycle when wearing the exoskeleton is seen as a peak in the graph.

Finally, another difference could be the greater activation of the medial and PDs (more implied in the downward movements) in the depression movement (approx. 50.100% of the cycle).

9.2.3 Weight effect

To further study the effects of the exoskeleton, the same tasks with a 2.5 kg weight plate on the hand were conducted by the subjects and once again, kinematics and muscular activity discussed.

Similarly to the kinematics from the tasks without weight, the exoskeleton curves show similar trends to the curves without the exoskeleton (Figure 35). On the contrary, differences observed in the comparison with weight are not as clear.

Looking into the muscular activity in Figure 36, similarly to the case without the weight, the curves patterns are similar with and without the exoskeleton, generally speaking. But, there are some observable differences if the relationship between the curves for the exoskeleton and without it are compared for the weighted and unweighted trials.

Firstly, there is not a decrease on the AD and MD in the elevation of the arm, corresponding to the first half of the cycle, as the one presented in the unweighted tests.

With respect to the half of the cycle, similarly to the unweighted exercises, a peak is manifested for the PD and MD when wearing the exoskeleton. In this case, the peak seen in the curve for the PD with the exoskeleton is even more noticeable.

The difference on the descent of the arm is not as clear but the activation increases slightly with the exoskeleton to compensate the lifting forces. Finally, considering the lower back, the resulted activation of the ES is greater than in the tasks without weight.

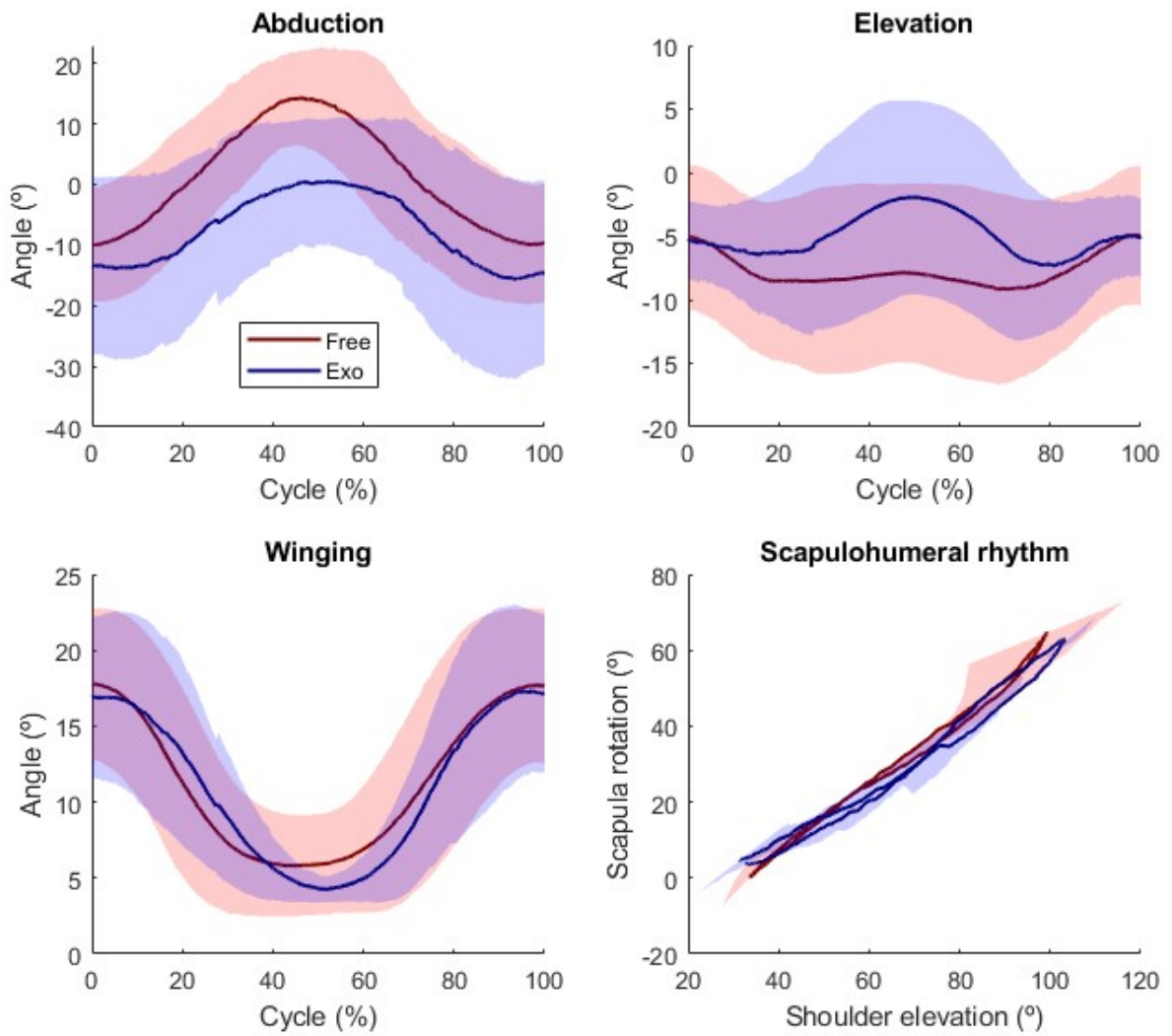


Figure 32: Abduction, elevation and winging ST joint coordinates and scapulohumeral rhythm during elevation-depression motion in the scapular plane for the subjects mean with (blue) and without (red) an upper-limb exoskeleton. The curves represent the mean of the subjects for all the cycles and the shaded area the +/- SD.

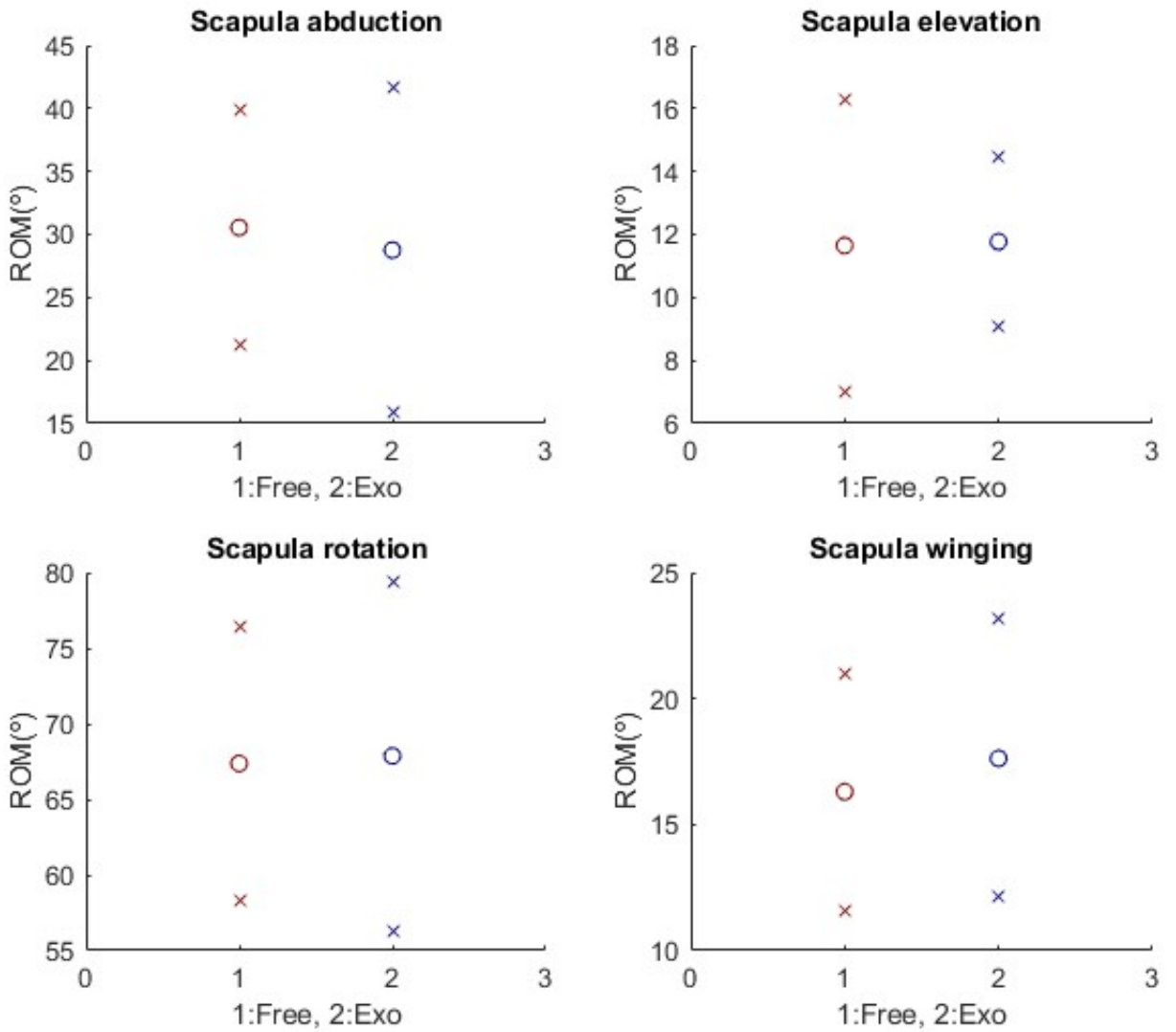


Figure 33: ROM for the ST joint coordinates for the subjects mean with and without the exoskeleton during elevation-depression motion in the scapular plane. The O represent the mean of the subjects for all the cycles and the segment constituted by the X, the +/- SD.

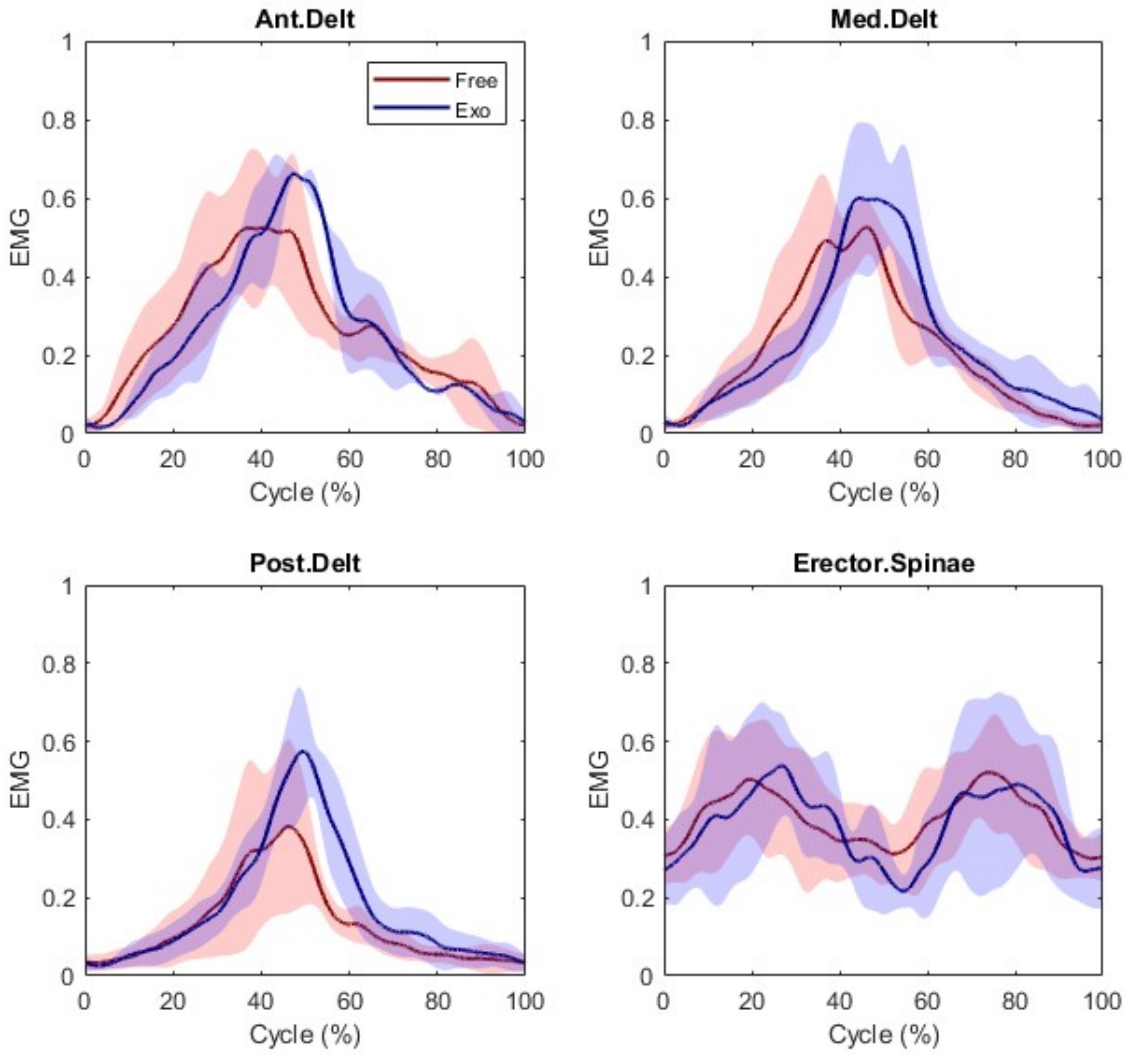


Figure 34: sEMG subjects mean for the AD, MD and PD of the working side, along with the ES of the contralateral side, for the elevation-depression motion in the scapular plane with (blue) and without (red) exoskeleton. The curves represent the mean of the subjects for all the cycles and the shaded area the +/- SD.

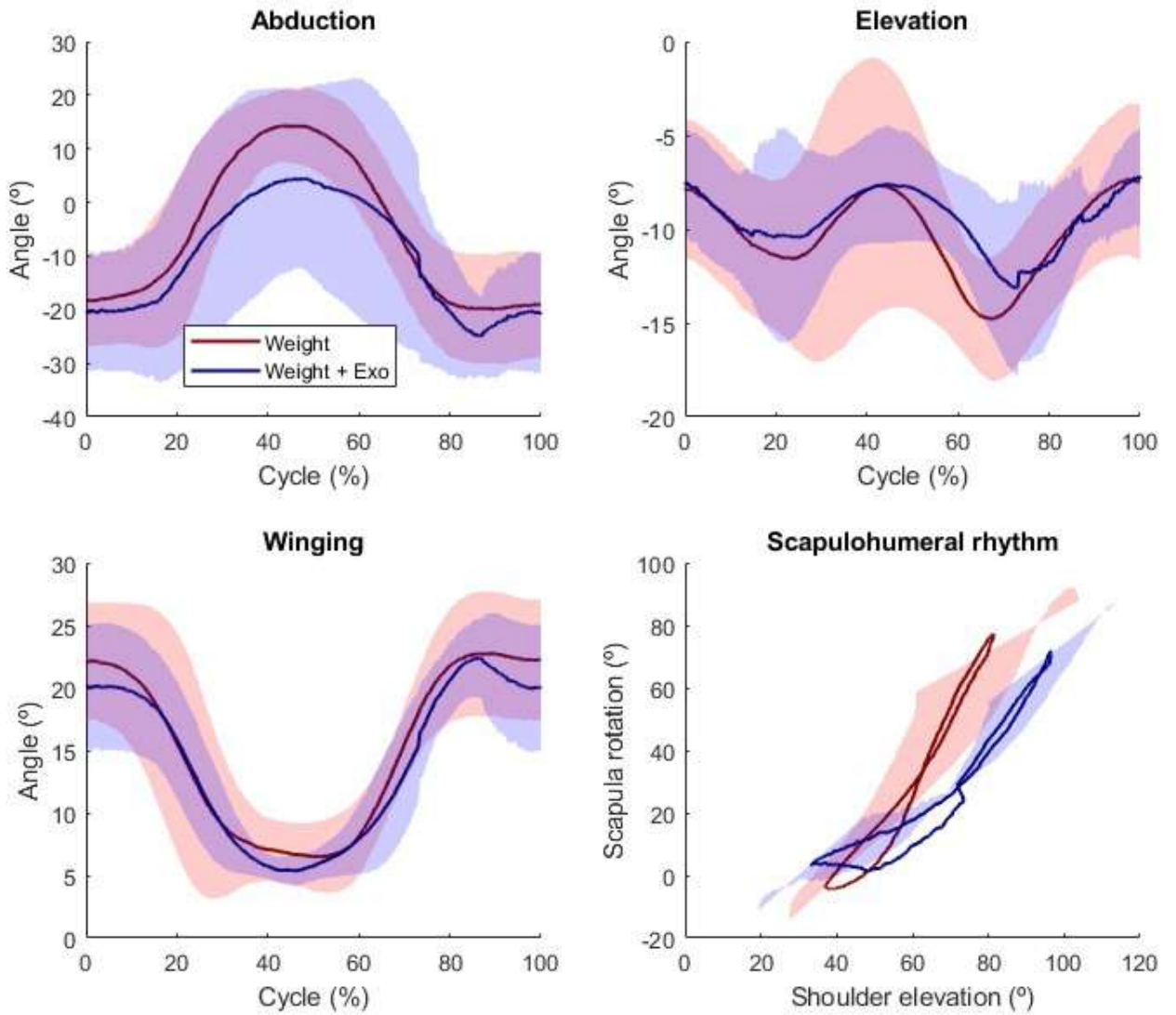


Figure 35: Abduction, elevation and winging ST joint coordinates and scapulothoracic rhythm during elevation-depression motion in the scapular plane with a 2.5 kg weight for the subjects mean with (blue) and without (red) an upper-limb exoskeleton. The curves represent the mean of the subjects for all the cycles and the shaded area the +/- SD.

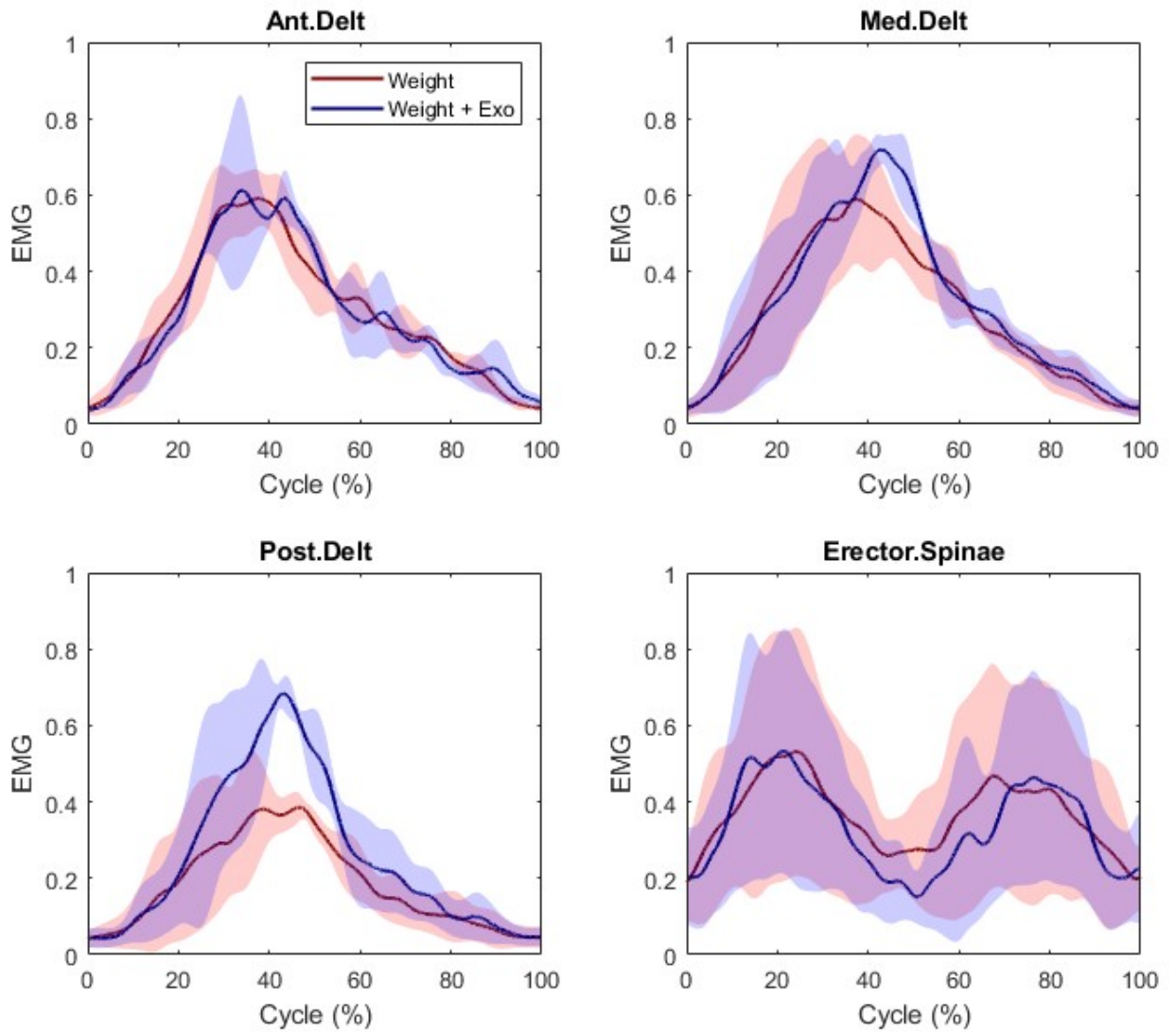


Figure 36: sEMG subjects mean for the AD, MD and PD of the working side, along with the ES of the contralateral side, for the elevation-depression motion in the scapular plane with a 2.5 kg weight, with (blue) and without (red) an exoskeleton. The curves represent the mean of the subjects for all the cycles and the shaded area the +/- SD.

Chapter 10

Conclusions and future perspectives

Looking back to the beginning of the study, the development of a complex biomechanical model focused on the scapulothoracic joint resulted as challenging as expected, but some hypothesis and achievements were extracted. It was also possible to work on the motion capture protocol, to conduct the adequate tests with an exoskeleton and to analyze the effects of its use.

In this chapter, the discussion of the obtained results and their comparison with literature is synthesized, along with the limitations, the summed conclusions and the drawing of future research needs.

10.1 Discussion

Although comparisons with other studies are not straight forward because of the lack of consensus for the testing procedure and the different upper-limb exoskeletons employed, some analogies and contrasts can be seen.

Many shoulder models are related in the literature [55][5]. In general terms, simple models considered the scapula fixed to the thorax frame while more complex models allow the scapula to glide over the thorax, represented as an ellipsoid. The current model considers the scapulothoracic joint, and therefore it belongs to the second category of shoulder models. As a result, it shows a more physiologic and realistic motion of the scapula than previous models [9][10]. However, although the kinematics obtained in this preliminary study by simplified scaling seem reasonable, some studies suggest that given the complexity of the scapulothoracic joint, scaling of this kind of models to individuals is not trivial and could result in inaccurate kinematics [56][55] given that the thorax and scapula scaling affect to the relative motion in between them and therefore to the scapula kinematics.

Regarding subjects variability and taking into account the plots represented for the bilaterality validation, where the subjects mean was represented (Figures 23 and 24), a non-negligible subject variability is expected, given the considerable standard deviation obtained and represented in these figures.

Precisely, some differences are observed in the kinematic scapula curves plotted in Figure 29 for each of the subjects. This can be due to the different initial pose or configuration of the scapula for each subject at the beginning of the trial.

However, subject 4 shows a greater amplitude of movements with respect to the rest of the subjects, which can not be explained by the different initial position. This difference can be due to several reasons regarding the subjects physique differential variables as the subjects mobility, strength, limbs length...Or, on the contrary, it could be a sign of poor test reproducibility. However, as the study has so far included a number of four subjects, the sample size is too small to determine the reasons of this variability or the possible lack of test reproducibility.

Similar results for the subjects were obtained for the scapula kinetics plotted in 30, where just the shifts differ between the subjects curves. Nevertheless, these shifts could be explained by the different velocities under which

each subject performed the movements. Precisely, if Figure 29 is analyzed in detail, the slope of the curves change in between the subjects. As a result, when differentiating the motion to obtain velocities and accelerations, the moments resulting from these accelerations are affected by the slope of the kinematic curves.

To end up with inter-variability between subjects, the ROM for all the subjects and scapular kinematics in Figure 31 show a great repeatability in the tests for each of the subjects, because of the small standard deviation. However, differences are again observed between the subjects. To summarize, some subjects inter-variability is observed from the kinematics and kinetics points of view, but as the sample size is not big enough, further conclusions could not be made yet about the variability's possible origins.

Comparing with literature, large variation was also observed in other studies. For example, differences among the subjects of the study conducted by Hyun et al. [15] were seen and related to different muscular operating strategies and arm kinematics between the individuals.

With respect to the exoskeleton effects on the shoulder motion, this preliminary study introduces as novelty the study of the scapular motion, which can not be compared with other studies yet. However, some studies do mention the effects on the general shoulder motion. For example, one study suggested that wearing PAEXO does not degrade task performance, though it does modify shoulder movement [34]. Another, pointed out that the Paexo was not limiting the ROM [16], although this suggestion was based on the users perception and not on objective measurements. On the contrary, a study conducted with other exoskeleton, the Eksovest, suggested that wearing it reduced maximum voluntary shoulder ROM [57].

Although the differences are not very clear given the high standard deviation, no strong conclusions can be made but some hypothesis extracted from the effects of the exoskeleton in this study. For instance, the motion restriction on the abduction direction could be compensated by a greater motion in the elevation direction. In contrast, the exoskeleton may not be affecting the scapular winging or the scapulohumeral rhythm (see Figure 29).

On the contrary, from the study of Figure 33 a hypothesis of no motion restriction with the exoskeleton could be extracted.

Comparing muscular activity, most of the studies conducted with the different upper-limb commercialized exoskeletons agree in the significant reduction of deltoid muscles or shoulder effort caused by the exoskeleton. [20][18][16][19][15][58]. This is not as clearly suggested in the results of the preliminary study, but it can be explained by the different tasks conducted in the trials. While these studies focus on overhead tasks, this preliminary study tested elevations in the scapular plane, but overhead positions were not maintained. Regarding the side-effects on the lower back muscles, some studies agreed on the non existing overload on the lower back as the current study [18][16][19] and some others suggested an increase on the lower back load. [15][58]

With a higher level of detail, some differences were noticed from the use of the exoskeleton in the muscles activity in this study. According to literature, AD and MD experiences a slight decrease of activation during the elevation, which could be explained by the external forces exerted by the exoskeleton, which tries to compensate the arm weight by lifting it.

Surprisingly, a greater activation of the deltoids at the half of the cycle when wearing the exoskeleton was seen. Taking into account the apparent similarity of ROM obtained with and without the exoskeleton (Figure 33), this could suggest that the subjects needed to make an extra effort to reach the same top position while elevating the arm as without the exo because of some mobility restriction.

Another small difference was seen in the greater activation of the MD and PD in the depression movement. The hypothesis extracted from here would be the need of a greater effort to make the arm descent because of the lifting forces exerted by the exoskeleton in the upwards direction when comparing to the curves without the exoskeleton.

Up to this point, although the sEMG signals may suggest effects on the muscular activity caused by the exoskeleton, it is necessary to emphasize again the small number of participants in the current study and its value as a preliminary study yet, which results may help in the reasoning of variables or development of study hypothesis for a greater study.

Moreover, the muscular activity was obtained by means of sEMG sensors, which only measure the surface muscular activity. Furthermore, the sEMG sensors are close to each other, which may result in cross-talk in between them, also likely to happen with other muscles.[44]

Finally, the results from the weighted tasks suggest some changes with respect to the hypotheses extracted without weight. However, given that the experimental protocol was designed simultaneously as the first tests were conducted, this weighted tasks were just considered for the last two subjects. Consequently, being the sample size smaller in this case, the conclusions would not be so reliable but could be useful to establish possible weight effects and hints for further studies.

Comparing to the effects caused by the use of the exoskeleton in the kinematics, the outcome is not so clear in the tasks with weight, which could suggest that the exoskeleton is not changing the scapular kinematics in this case. However, from the different scapulohumeral rhythms, it can be suggested that with the exoskeleton the contribution to the elevation in terms of scapula upward rotation is decreased for the tasks with weight.

The reduction of the exoskeleton effect is also seen in the muscular activity when adding weight, not decreasing the deltoids activity in the elevation as much as in the unweighted cases. This could be explained again by the fact that in the case without weight, the exoskeleton was compensating the arms' weight but maybe when adding extra weight the exoskeleton performance is not enough for the selected level of pretension.

The activation of the posterior and medium deltoid were greater in this case in the half of the cycle, which similarly to before, may be due to a restriction of movement leading to an extra effort made by the subjects. On the contrary, their activation at the depression does not differ as much as before, maybe because the added weight is helping the arm to descent and the exoskeleton is not compensating enough the weight of the arm with the weight.

Finlly, there is not a suggestion of a lower back overload when wearing the exoskeleton in any of the cases, as no difference was observed in the ES activation in any of the cases.

Taking into account that the exoskeleton function consists in compensating the arms weight so the worker does not need that much effort to work with the arms elevated over the head and that the level of compensation it is not changed for the tasks with and without weight, the smaller effect of the exoskeleton in the weighted trials could be explained by the lack of pretension to compensate not only the arm's weight but the extra added weight.

This variability when adding an extra weight was also observed in the study by Huysamen et al. [14], where the significant reductions on muscular activity by the exoskeleton were observed just for the tests conducted with an extra weight. In the current study, the results suggest the opposite as the results were not that different when adding the weight, but this contraposition of both studies can be explained by the different pretension levels configured in the different exoskeletons. However, they both suggest the importance of the tool or extra weight as a variable of study.

To summarize, the exoskeleton may be producing some changes in the scapular kinematics and muscular activity as shown for this sample size. Additionnally, the tests conducted with weight resulted into different results, which may indicate the importance of the weight to be considered a study variable in a greater future study.

10.2 Limitations

Before extracting the study conclusions, some limitations related to the study itself should be pointed out.

- **STA:** Although the motion capture protocol and the markerset definition aimed to minimize the STA from occuring, the solutions adopted achieved to further reduce the artifacts from happening but did not eliminate it. For example, although the shoulder cluster is used to track the scapula without the STA occurring in other the scapula tracking methods, where all the markers were placed directly on the scapula bony landmarks, there is still a STA happening where it is placed, that is, on the acromion.
- **Use of sEMG:** sEMG is only suitable for measuring superficial muscles activity. That does not ensure the correct muscle identification and increases the possibility of cross-talk between signals because of the signal contamination from surrounding muscles activation.[44]

- **Simplified scaling:** given the complexity of scaling the model to each of the subjects, some simplifications in this step were taken. For instance, scale factors for each body segment were not used and scaling was merely based in the repositioning of the markers according to the subject. This solution was adopted because the use of scale factors implies taking a lot of measurements on each of the subjects, which increases the tests duration, and implies complex calculations and transformations, given that in most of the body segments, the systems of reference are chosen to facilitate the coordinates definition and do not correspond to the axes defined by the bony landmarks. As a consequence, the axes of the scaling factors do not correspond to the axes formed by the bony landmarks.
- **Test environment:** although cameras and environment calibration was thoughtfully conducted in each of the trials to avoid possible external reflexes causing artifacts and noise in the recorded motion, as the motion capture lab is shared for other projects, the camera set up may have slightly change in between the different subjects tests. Consequently, a good test reproducibility may have been hindered.
- **Sample size:** the tests were conducted on just four participants, a too small sample size. As a consequence, strong conclusions can not be made from this study, but some hints on how to proceed next or some suggestions can be extracted for a complete study.

10.3 Conclusions

Taking into account the limitations, conclusions strictly speaking can not be extracted from this preliminary study, but the following effects could be suggested and expected to happen when enlarging the sample size.

- **Improved biomechanical model of the shoulder complex:** the introduced updates to the previous upper limb models refine the shoulder representation and allow a more realistic motion. Despite the great standard deviation, the model is validated in terms of bilaterality and scapular kinematics. Nevertheless, a greater than expected scapula motion could happen in some planes, so scapula tracking or the scapulothoracic joint should be rechecked with a greater sample size.
- **Subjects variability:** it was observable and lead to a great standard deviation. This could suggest differences on the physique conditions of the subjects in terms of mobility or a poor test reproducibility, so more subjects would be needed to address this matter. Additionally, using simplified scaling may not be sufficient and a more complex scaling improve it. For instance, if the subject has a extraordinary wide thorax, the simplified scaling may not be accurate to represent the relative motion between the scapula and the thorax, resulting in overestimated relative motion.
- **Paexo exoskeleton may modify the scapula kinematics:** although it did not seem to modify the range of motion of the scapulothoracic joint, the exoskeleton did seem to change the scapula motion pattern decreasing the scapular abduction while enlarging the elevation.
- **Paexo exoskeleton may modify muscular activity:** even though the effects did not seem to be really big, the sEMG signals may indicate the decrease in the deltoids activity while elevating the arm, an increase in the top position and while decreasing the arm, and not apparent side-effects on the lower back as effects of wearing the exoskeleton.
- **Tool weight may be useful as a study variable:** adding weight could show different results as in this preliminary study in terms of scapula kinematics and muscular activity. Therefore, it would be interesting to keep it as a study variable

10.4 Future perspectives

To conclude, some prospects in which to continue the current study and address in the future are highlighted.

Firstly, regarding the biomechanical model, more complex and detailed scaling should be address in order to avoid inaccuracy in the calculation of the kinematics.

Additionally, it would be important to consider improvements or other alternatives for the scapula tracking to reduce even more the STA.

Concerning data acquisition, a greater sample size consideration will strongly benefit the discussion of the Paexo effects and also determine if there is a need of improving the test reproducibility through a more strict protocol.

With respect to the exoskeleton study, in order to analyze also the kinetics and not just the kinematics, taking exoskeleton force measurements and adding them to the model would help estimating the effects on the kinetics.

Additionally, the model could be further exploited as a predictive tool for the exoskeleton effects by introducing different exoskeleton curves in order to help in the future design.

Going even further, the model could be employed to predict the muscles activation, which could be really interesting to model the muscular activity, as the placement of the sEMG sensors is limited when using the exoskeleton and not as reliable as deep muscle activation measurements.

Bibliography

- [1] Jan De Kok et al. *Work-related musculoskeletal disorders: prevalence, costs and demographics in the EU*. European Agency for Safety and Health at Work, 2019. DOI: [10.2802/66947](https://doi.org/10.2802/66947). URL: <http://europa.eu>.
- [2] Eurofound et al. “Working conditions in a global perspective”. In: *International Labour Organization* (2019). URL: <https://op.europa.eu/en/publication-detail/-/publication/19767879-917b-11e9-9369-01aa75ed71a1/language-en>.
- [3] F. Struyf et al. “Scapular positioning and movement in unimpaired shoulders, shoulder impingement syndrome, and glenohumeral instability”. In: *Scandinavian Journal of Medicine Science in Sports* 21 (3 June 2011), pp. 352–358. ISSN: 1600-0838. DOI: [10.1111/J.1600-0838.2010.01274.X](https://doi.org/10.1111/J.1600-0838.2010.01274.X).
- [4] NB Reese and WD Bandy. *Joint range of motion and muscle length testing*. 2016.
- [5] Jorge Ambrósio et al. “Multibody biomechanical models of the upper limb”. In: *Procedia IUTAM* 2 (Jan. 2011), pp. 4–17. ISSN: 2210-9838. DOI: [10.1016/J.PIUTAM.2011.04.002](https://doi.org/10.1016/J.PIUTAM.2011.04.002).
- [6] Katherine R. Saul et al. “Benchmarking of dynamic simulation predictions in two software platforms using an upper limb musculoskeletal model”. In: *Comput Methods Biomech Biomed Engin* 18 (13 Oct. 2015), pp. 1445–1458. ISSN: 14768259. DOI: [10.1080/10255842.2014.916698](https://doi.org/10.1080/10255842.2014.916698).
- [7] F. C.T. Van der Helm. “Analysis of the kinematic and dynamic behavior of the shoulder mechanism”. In: *Journal of Biomechanics* 27 (5 May 1994), pp. 527–550. ISSN: 0021-9290. DOI: [10.1016/0021-9290\(94\)90064-7](https://doi.org/10.1016/0021-9290(94)90064-7).
- [8] Clark R Dickerson, Don B Chaffin, and Richard E Hughes. “Computer Methods in Biomechanics and Biomedical Engineering A mathematical musculoskeletal shoulder model for proactive ergonomic analysis A mathematical musculoskeletal shoulder model for proactive ergonomic analysis”. In: *Computer Methods in Biomechanics and Biomedical Engineering* 10 (6 2007). ISSN: 1476-8259. DOI: [10.1080/10255840701592727](https://doi.org/10.1080/10255840701592727). URL: <https://www.tandfonline.com/action/journalInformation?journalCode=gcmb20>.
- [9] Bart Bolsterlee, Dirkjan H E J Veeger, and Edward K Chadwick. “Clinical applications of musculoskeletal modelling for the shoulder and upper limb”. In: *Med Biol Eng Comput* 51 (2013), pp. 953–963. DOI: [10.1007/s11517-013-1099-5](https://doi.org/10.1007/s11517-013-1099-5).
- [10] Ajay Seth et al. “A Biomechanical Model of the Scapulothoracic Joint to Accurately Capture Scapular Kinematics during Shoulder Movements”. In: *PLoS One* 11 (1 2016). DOI: [10.1371/journal.pone.0141028](https://doi.org/10.1371/journal.pone.0141028).
- [11] L. Chèze, B. J. Fregly, and J. Dimnet. “A solidification procedure to facilitate kinematic analyses based on video system data”. In: *Journal of Biomechanics* 28 (7 July 1995), pp. 879–884. ISSN: 0021-9290. DOI: [10.1016/0021-9290\(95\)95278-D](https://doi.org/10.1016/0021-9290(95)95278-D).
- [12] A. F. Shaheen, C. M. Alexander, and A. M.J. Bull. “Tracking the scapula using the scapula locator with and without feedback from pressure-sensors: A comparative study”. In: *Journal of Biomechanics* 44 (8 May 2011), pp. 1633–1636. ISSN: 0021-9290. DOI: [10.1016/J.JBIOMECH.2011.02.139](https://doi.org/10.1016/J.JBIOMECH.2011.02.139).
- [13] Miroslav Šenk, Laurence Chèze, and Miroslav Šenk. “Computer Methods in Biomechanics and Biomedical Engineering A new method for motion capture of the scapula using an optoelectronic tracking device: a feasibility study A new method for motion capture of the scapula using an optoelectronic tracking device: a feasibility study”. In: *Computer Methods in Biomechanics and Biomedical Engineering* 13 (3 2009), pp. 397–401. ISSN: 1476-8259. DOI: [10.1080/10255840903263945](https://doi.org/10.1080/10255840903263945).

- [14] Kirsten Huysamen et al. “Evaluation of a passive exoskeleton for static upper limb activities”. In: *Applied Ergonomics* 70 (July 2018), pp. 148–155. ISSN: 18729126. DOI: [10.1016/J.APERGO.2018.02.009](https://doi.org/10.1016/J.APERGO.2018.02.009).
- [15] Dong Jin Hyun et al. “A light-weight passive upper arm assistive exoskeleton based on multi-linkage spring-energy dissipation mechanism for overhead tasks”. In: *Robotics and Autonomous Systems* 122 (Dec. 2019). ISSN: 09218890. DOI: [10.1016/J.ROBOT.2019.103309](https://doi.org/10.1016/J.ROBOT.2019.103309).
- [16] Claudia Latella et al. “Analysis of Human Whole-Body Joint Torques During Overhead Work With a Passive Exoskeleton”. In: *IEEE TRANSACTIONS ON HUMAN-MACHINE SYSTEMS* 52 (5 2022), pp. 1060–1068. DOI: [10.1109/THMS.2021.3128892](https://doi.org/10.1109/THMS.2021.3128892).
- [17] Eric B. Weston et al. “A physiological and biomechanical investigation of three passive upper-extremity exoskeletons during simulated overhead work”. In: *Ergonomics* 65 (1 2021), pp. 105–117. ISSN: 13665847. DOI: [10.1080/00140139.2021.1963490](https://doi.org/10.1080/00140139.2021.1963490).
- [18] Logan Van Engelhoven et al. “Experimental Evaluation of a Shoulder-Support Exoskeleton for Overhead Work: Influences of Peak Torque Amplitude, Task, and Tool Mass Experimental Evaluation of a Shoulder-Support Exoskeleton for Overhead Work: Influences of Peak Torque Amplitude, Task, and Tool Mass”. In: *IIEE Transactions on Occupational Ergonomics and Human Factors* 7 (2019), pp. 250–263. ISSN: 2472-5846. DOI: [10.1080/24725838.2019.1637799](https://doi.org/10.1080/24725838.2019.1637799).
- [19] Sunwook Kim et al. “Assessing the influence of a passive, upper extremity exoskeletal vest for tasks requiring arm elevation: Part I – “Expected” effects on discomfort, shoulder muscle activity, and work task performance”. In: *Applied Ergonomics* 70 (July 2018), pp. 315–322. ISSN: 18729126. DOI: [10.1016/J.APERGO.2018.02.025](https://doi.org/10.1016/J.APERGO.2018.02.025).
- [20] Jason C. Gillette, Shekoofe Saadat, and Terry Butler. “Electromyography-based fatigue assessment of an upper body exoskeleton during automotive assembly”. In: *Wearable Technologies* 3 (2022), e23. ISSN: 2631-7176. DOI: [10.1017/WTC.2022.20](https://doi.org/10.1017/WTC.2022.20).
- [21] *Universal Joint Theory*. URL: https://doc.comsol.com/5.5/doc/com.comsol.help.mbd/mbd_ug_theory.4.14.html#1538417.
- [22] *ParaView - Open-source, multi-platform data analysis and visualization application*. URL: <https://www.paraview.org/>.
- [23] Frank C. Anderson and Marcus G. Pandy. “A Dynamic Optimization Solution for Vertical Jumping in Three Dimensions”. In: *Comput Methods Biomech Biomed Engin* . 2 (3 1999), pp. 201–231. ISSN: 10255842. DOI: [10.1080/10255849908907988](https://doi.org/10.1080/10255849908907988). URL: <https://www.tandfonline.com/doi/abs/10.1080/10255849908907988>.
- [24] Darryl G. Thelen. “Adjustment of muscle mechanics model parameters to simulate dynamic contractions in older adults”. In: *Journal of biomechanical engineering* 125 (1 Feb. 2003), pp. 70–77. ISSN: 0148-0731. DOI: [10.1115/1.1531112](https://doi.org/10.1115/1.1531112).
- [25] Matthew Millard et al. “Flexing Computational Muscle: Modeling and Simulation of Musculotendon Dynamics”. In: *Journal of Biomechanical Engineering* 135 (2 2013), p. 0210051. ISSN: 01480731. DOI: [10.1115/1.4023390](https://doi.org/10.1115/1.4023390).
- [26] Ajay Seth et al. “Muscle Contributions to Upper-Extremity Movement and Work From a Musculoskeletal Model of the Human Shoulder”. In: (2019). DOI: [10.3389/fnbot.2019.00090](https://doi.org/10.3389/fnbot.2019.00090).
- [27] Mary D. Klein Breteler, Cornelis W. Spoor, and Frans C.T. Van Der Helm. “Measuring muscle and joint geometry parameters of a shoulder for modeling purposes”. In: *Journal of Biomechanics* 32 (11 Nov. 1999), pp. 1191–1197. ISSN: 0021-9290. DOI: [10.1016/S0021-9290\(99\)00122-0](https://doi.org/10.1016/S0021-9290(99)00122-0).
- [28] Samuel R. Hamner, Ajay Seth, and Scott L. Delp. “Muscle contributions to propulsion and support during running”. In: *Journal of Biomechanics* 43 (14 Oct. 2010), pp. 2709–2716. ISSN: 00219290. DOI: [10.1016/J.JBIOMECH.2010.06.025](https://doi.org/10.1016/J.JBIOMECH.2010.06.025).
- [29] El Sevier. “3D 4 Medical from El Sevier”. In: (2023). URL: <https://3d4medical.com/>.
- [30] Ge Wu et al. “ISB recommendation on definitions of joint coordinate system of various joints for the reporting of human joint motion—part I: ankle, hip, and spine”. In: *Journal of Biomechanics* 35 (4 Apr. 2002), pp. 543–548. ISSN: 0021-9290. DOI: [10.1016/S0021-9290\(01\)00222-6](https://doi.org/10.1016/S0021-9290(01)00222-6).

- [31] Ge Wu et al. “ISB recommendation on definitions of joint coordinate systems of various joints for the reporting of human joint motion-Part II: shoulder, elbow, wrist and hand”. In: *Journal of Biomechanics* 38 (2005), pp. 981–992. DOI: [10.1016/j.jbiomech.2004.05.042](https://doi.org/10.1016/j.jbiomech.2004.05.042).
- [32] “Kestrel 2200 - Motion Analysis”. In: (). URL: <https://motionanalysis.com/cameras/kestrel-2200/>.
- [33] “Calibration kits | Product categories | Qualisys”. In: (). URL: <https://www.qualisys.com/accessories/calibration-kits/>.
- [34] Pauline Maurice et al. “Objective and Subjective Effects of a Passive Exoskeleton on Overhead Work”. In: *IEEE Transactions on Neural Systems and Rehabilitation Engineering* 28 (1 Jan. 2020), pp. 152–164. ISSN: 15580210. DOI: [10.1109/TNSRE.2019.2945368](https://doi.org/10.1109/TNSRE.2019.2945368).
- [35] Thomas Moser et al. “The deltoid, a forgotten muscle of the shoulder”. In: *Skeletal Radiology* 42 (10 Oct. 2013), pp. 1361–1375. ISSN: 03642348. DOI: [10.1007/S00256-013-1667-7/FIGURES/25](https://doi.org/10.1007/S00256-013-1667-7/FIGURES/25).
- [36] Hermie (Hermanus Jacobus) Hermens and Bart. Freriks. *The state of the art on sensors and sensor placement procedures for surface electromyography: a proposal for sensor placement procedures*. Ed. by Hermie J. Hermens and Bart Freriks. Vol. SENIAM 5. Roessingh Research and Development, 1997. ISBN: 90-75452-09-8. URL: <http://seniam.org/>.
- [37] Carrie M. Hall and Lori Thein Brody. *Therapeutic Exercise: Moving Toward Function*. Ed. by Lippincott Williams Wilkins. 2nd ed. 2.
- [38] Gui Yin et al. “Processing Surface EMG Signals for Exoskeleton Motion Control”. In: *Frontiers in Neurorobotics* 14 (July 2020). DOI: [10.3389/fnbot.2020.00040](https://doi.org/10.3389/fnbot.2020.00040). URL: www.frontiersin.org.
- [39] Carlo J De Luca et al. “Filtering the surface EMG signal: Movement artifact and baseline noise contamination”. In: *Journal of Biomechanics* (43 2010), pp. 1573–1579. DOI: [10.1016/j.jbiomech.2010.01.027](https://doi.org/10.1016/j.jbiomech.2010.01.027). URL: www.elsevier.com/locate/jbiomech.
- [40] M B I Raez, M S Hussain, and F Mohd-Yasin. “Techniques of EMG signal analysis: detection, processing, classification and applications”. In: *Biol. Proced. Online* 8 (1 2006), pp. 11–35. DOI: [10.1251/bpo115](https://doi.org/10.1251/bpo115).
- [41] Simone Ranaldi et al. “The Influence of the sEMG Amplitude Estimation Technique on the EMG–Force Relationship”. In: *Sensors* 22 (11 June 2022). ISSN: 14248220. DOI: [10.3390/S22113972](https://doi.org/10.3390/S22113972).
- [42] T. D’Alessio and S. Conforto. “Extraction of the envelope from surface EMG signals”. In: *IEEE Engineering in Medicine and Biology Magazine* 20 (6 2001), pp. 55–61. ISSN: 07395175. DOI: [10.1109/51.982276](https://doi.org/10.1109/51.982276).
- [43] Miriam González-Izal et al. “Electromyographic models to assess muscle fatigue”. In: *Journal of Electromyography and Kinesiology* 22 (4 Aug. 2012), pp. 501–512. ISSN: 10506411. DOI: [10.1016/J.JELEKIN.2012.02.019](https://doi.org/10.1016/J.JELEKIN.2012.02.019).
- [44] Lara McManus, Giuseppe De Vito, and Madeleine M. Lowery. “Analysis and Biophysics of Surface EMG for Physiotherapists and Kinesiologists: Toward a Common Language With Rehabilitation Engineers”. In: *Frontiers in Neurology* 11 (Oct. 2020). ISSN: 16642295. DOI: [10.3389/FNEUR.2020.576729](https://doi.org/10.3389/FNEUR.2020.576729).
- [45] Francisco J. Vera-Garcia, Janice M. Moreside, and Stuart M. McGill. “MVC techniques to normalize trunk muscle EMG in healthy women”. In: *Journal of Electromyography and Kinesiology* 20 (1 Feb. 2010), pp. 10–16. ISSN: 10506411. DOI: [10.1016/J.JELEKIN.2009.03.010](https://doi.org/10.1016/J.JELEKIN.2009.03.010).
- [46] Mark Halaki and Karen Gi. *Normalization of EMG Signals: To Normalize or Not to Normalize and What to Normalize to?* InTech, Oct. 2012. DOI: [10.5772/49957](https://doi.org/10.5772/49957).
- [47] A. Kettler et al. “Finite helical axes of motion are a useful tool to describe the three-dimensional in vitro kinematics of the intact, injured and stabilised spine”. In: *European Spine Journal* 13 (6 Oct. 2004), p. 553. ISSN: 09406719. DOI: [10.1007/S00586-004-0710-8](https://doi.org/10.1007/S00586-004-0710-8).
- [48] Andrea Ancillao. “The helical axis of anatomical joints: calculation methods, literature review, and software implementation”. In: *Medical and Biological Engineering and Computing* 60 (7 July 2022), pp. 1815–1825. ISSN: 17410444. DOI: [10.1007/S11517-022-02576-2/TABLES/1](https://doi.org/10.1007/S11517-022-02576-2/TABLES/1).
- [49] Paolo De Leva. “Adjustments to Zatsiorsky-Seluyanov’s Segment Inertia Parameters.” In: *Journal of Biomechanics* 29 (9 1996), pp. 1223–1230.

- [50] “How Scaling Works - OpenSim Documentation”. In: (). URL: <https://simtk-confluence.stanford.edu:8443/display/OpenSim/How+Scaling+Works>.
- [51] “How Inverse Kinematics Works - OpenSim Documentation”. In: (). URL: <https://simtk-confluence.stanford.edu:8443/display/OpenSim/How+Inverse+Kinematics+Works>.
- [52] “How Inverse Dynamics Works - OpenSim Documentation”. In: (). URL: <https://simtk-confluence.stanford.edu:8443/display/OpenSim/How+Inverse+Dynamics+Works>.
- [53] M. Schenkman and V. Rugo De Cartaya. “Kinesiology of the shoulder complex”. In: *Journal of Orthopaedic and Sports Physical Therapy* 8 (9 1987), pp. 438–450. ISSN: 01906011. DOI: [10.2519/JOSPT.1987.8.9.438](https://doi.org/10.2519/JOSPT.1987.8.9.438).
- [54] S. Bagg and W. Forrest. “A Biomechanical Analysis of Scapular Rotation during Arm Abduction in the Scapular Plane”. In: *American Journal of Physical Medicine Rehabilitation* (1988).
- [55] Sonia Duprey et al. “Kinematic models of the upper limb joints for multibody kinematics optimisation: An overview”. In: *Journal of Biomechanics* 62 (Sept. 2017), pp. 87–94. ISSN: 0021-9290. DOI: [10.1016/J.JBIOMECH.2016.12.005](https://doi.org/10.1016/j.jbiomech.2016.12.005).
- [56] Joe A.I. Prinold and Anthony M.J. Bull. “Scaling and kinematics optimisation of the scapula and thorax in upper limb musculoskeletal models”. In: *Journal of Biomechanics* 47 (11 Aug. 2014), pp. 2813–2819. ISSN: 18732380. DOI: [10.1016/J.JBIOMECH.2014.05.015](https://doi.org/10.1016/j.jbiomech.2014.05.015).
- [57] Sunwook Kim et al. “Assessing the influence of a passive, upper extremity exoskeletal vest for tasks requiring arm elevation: Part II – “Unexpected” effects on shoulder motion, balance, and spine loading”. In: *Applied Ergonomics* 70 (July 2018), pp. 323–330. ISSN: 18729126. DOI: [10.1016/J.APERGO.2018.02.024](https://doi.org/10.1016/j.apergo.2018.02.024).
- [58] Ilaria Pacifico et al. “An experimental evaluation of the proto-mate: A novel ergonomic upper-limb exoskeleton to reduce workers’ physical strain”. In: *IEEE Robotics and Automation Magazine* 27 (1 Mar. 2020), pp. 54–65. ISSN: 1558223X. DOI: [10.1109/MRA.2019.2954105](https://doi.org/10.1109/MRA.2019.2954105).

Annex I. Subjects data



Die approbierte gedruckte Originalversion dieser Diplomarbeit ist an der TU Wien Bibliothek verfügbar
The approved original version of this thesis is available in print at TU Wien Bibliothek.

Subjects query data

Subject name	Georgios	Tommaso	Hannah	Johannes
Subject n.	1	2	3	4
Height (cm)	188	188	168	173
Weight (kg)	108	82	62	78
Age (yrs)	28	24	23	26
Gender	Male	Male	Female	Male
Dominant side	Right	Right	Right	Right
Profession	PhD student	Student	Student	Student
Previous shoulder injury	No	No	No	No
Session date	2022.12.07	2023.01.24	2023.02.16	2023.03.02
Session name	Shoulder EMG	Paexo session 1	Paexo session 2	Paexo session 3

Annex II. Kinematics and kinetics report



Die approbierte gedruckte Originalversion dieser Diplomarbeit ist an der TU Wien Bibliothek verfügbar
The approved original version of this thesis is available in print at TU Wien Bibliothek.

List of Figures

1	Scapula and shoulder kinematics for right (red) and left (blue) limbs under elevation in the scapular plane. Subject 1, 2022.12.07. Shoulder EMG.	2
2	Scapula and shoulder kinetics for right (red) and left (blue) limbs under elevation in the scapular plane. Subject 1, 2022.12.07. Shoulder EMG.	3
3	Scapula and shoulder kinematics for right (red) and left (blue) limbs under elevation in the scapular plane. Subject 2, 2023.01.24. Paexo session 1.	4
4	Scapula and shoulder kinetics for right (red) and left (blue) limbs under elevation in the scapular plane. Subject 2, 2023.01.24. Paexo session 1.	5
5	Scapula and shoulder kinematics for right (red) and left (blue) limbs under elevation in the scapular plane with exoskeleton. Subject 2, 2023.01.24. Paexo session 1.	6
6	Scapula and shoulder kinematics for right (red) and left (blue) limbs under elevation in the scapular plane. Subject 3, 2023.02.16. Paexo session 2.	7
7	Scapula and shoulder kinetics for right (red) and left (blue) limbs under elevation in the scapular plane. Subject 3, 2023.02.16. Paexo session 2.	8
8	Scapula and shoulder kinematics for right (red) and left (blue) limbs under elevation in the scapular plane with weight. Subject 3, 2023.02.16. Paexo session 2.	9
9	Scapula and shoulder kinetics for right (red) and left (blue) limbs under elevation in the scapular plane with weight. Subject 3, 2023.02.16. Paexo session 2.	10
10	Scapula and shoulder kinematics for right (red) and left (blue) limbs under elevation in the scapular plane with exoskeleton. Subject 3, 2023.02.16. Paexo session 2.	11
11	Scapula and shoulder kinematics for right (red) and left (blue) limbs under elevation in the scapular plane with exoskeleton and weight. Subject 3, 2023.02.16. Paexo session 2.	12
12	Scapula and shoulder kinematics for right (red) and left (blue) limbs under elevation in the scapular plane. Subject 4, 2023.03.02. Paexo session 3.	13
13	Scapula and shoulder kinetics for right (red) and left (blue) limbs under elevation in the scapular plane. Subject 4, 2023.03.02. Paexo session 3.	14
14	Scapula and shoulder kinematics for right (red) and left (blue) limbs under elevation in the scapular plane with weight. Subject 4, 2023.03.02. Paexo session 3.	15
15	Scapula and shoulder kinetics for right (red) and left (blue) limbs under elevation in the scapular plane with weight. Subject 4, 2023.03.02. Paexo session 3.	16
16	Scapula and shoulder kinematics for right (red) and left (blue) limbs under elevation in the scapular plane with exoskeleton. Subject 4, 2023.03.02. Paexo session 3.	17
17	Scapula and shoulder kinematics for right (red) and left (blue) limbs under elevation in the scapular plane with exoskeleton and weight. Subject 4, 2023.03.02. Paexo session 3.	18

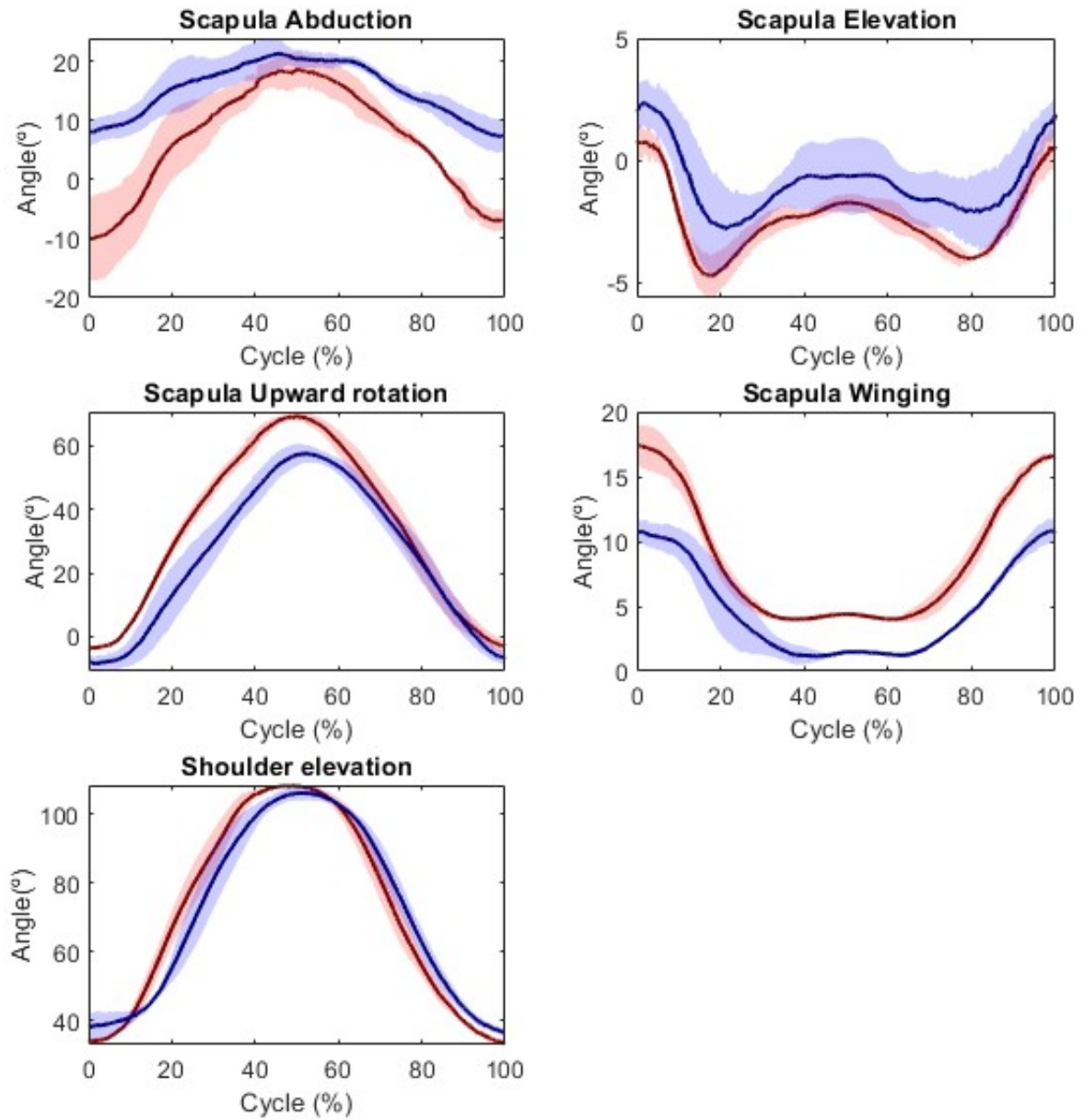


Figure 1: Scapula and shoulder kinematics for right (red) and left (blue) limbs under elevation in the scapular plane. Subject 1, 2022.12.07. Shoulder EMG.

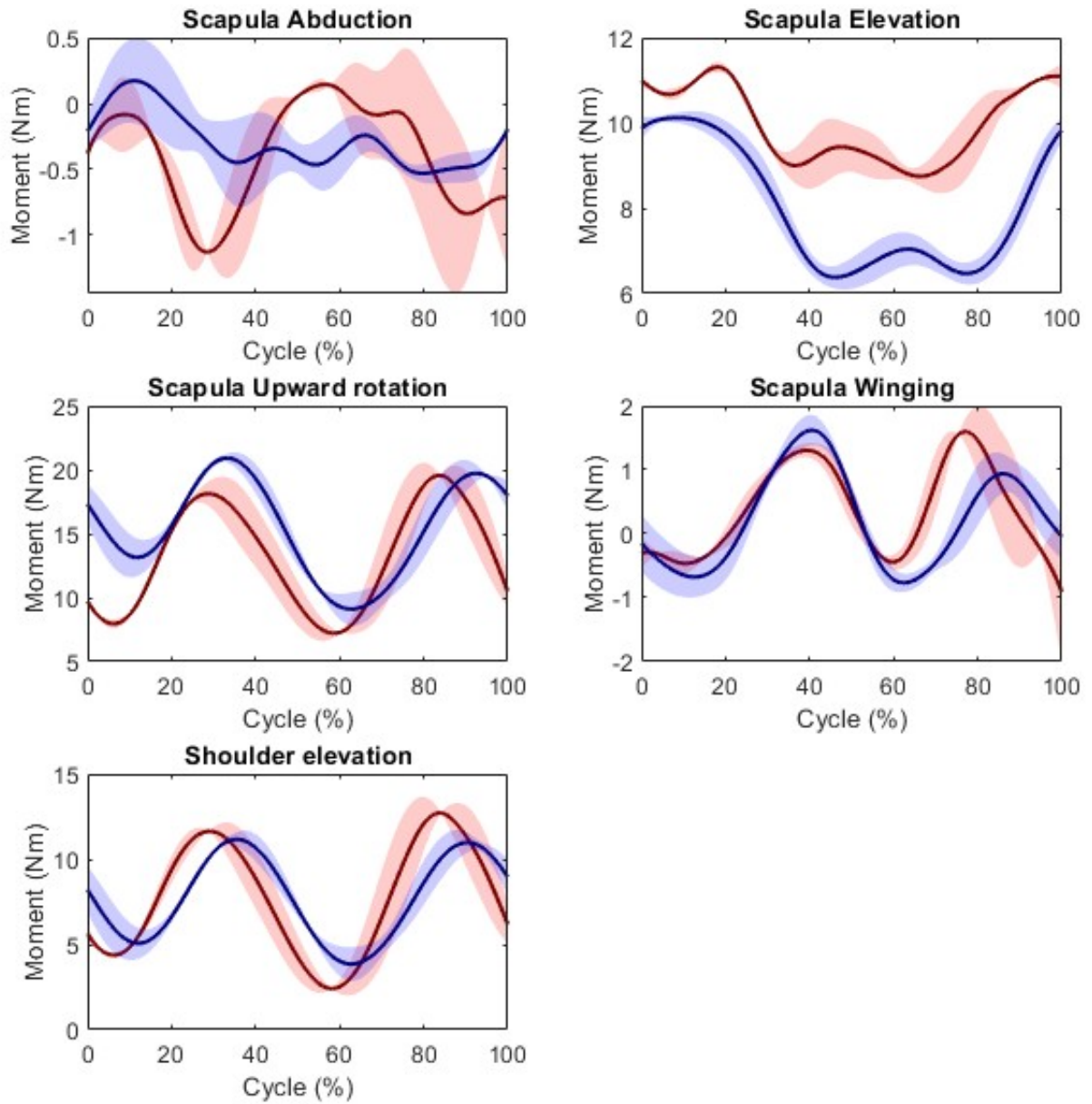


Figure 2: Scapula and shoulder kinetics for right (red) and left (blue) limbs under elevation in the scapular plane. Subject 1, 2022.12.07. Shoulder EMG.

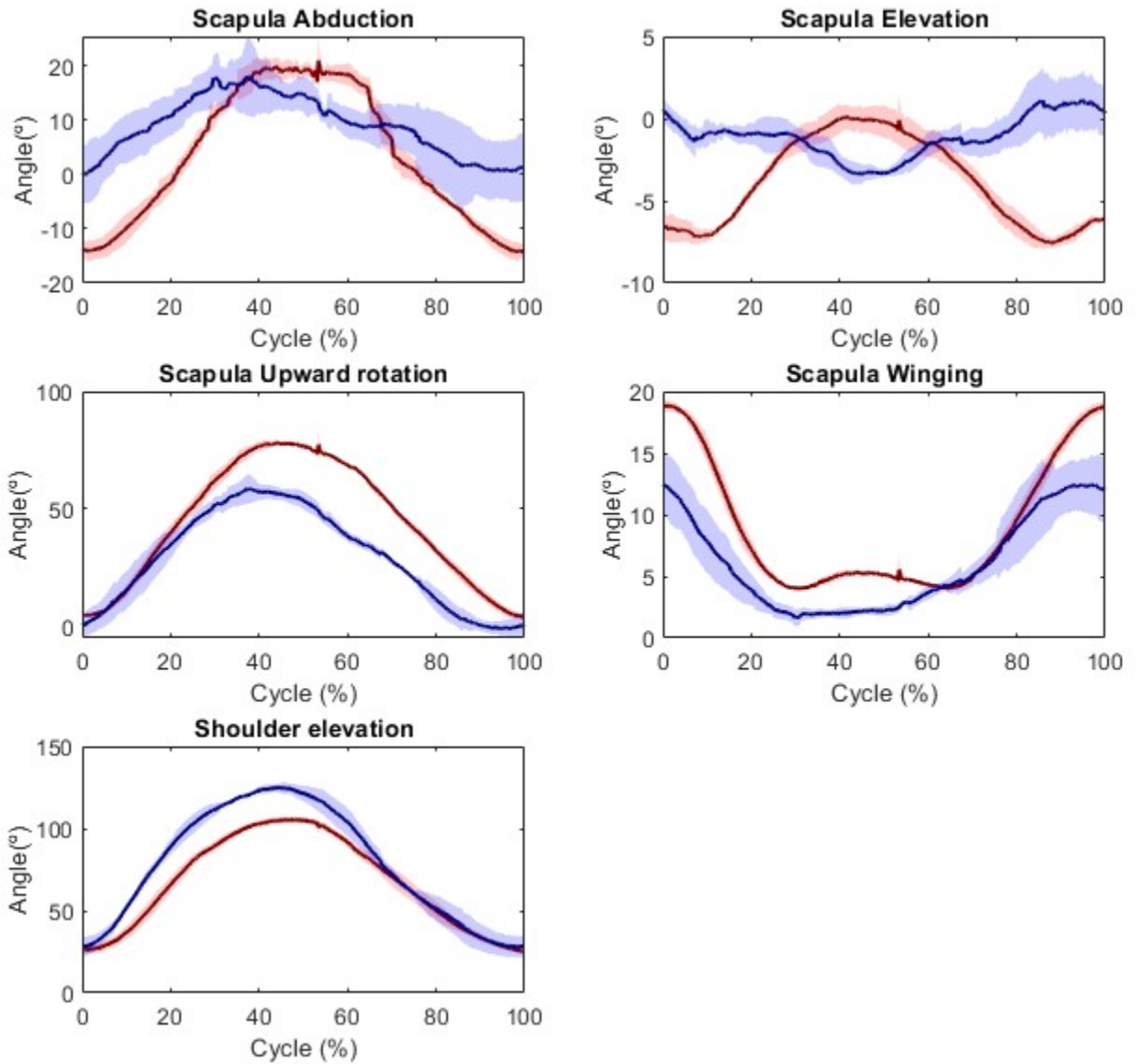


Figure 3: Scapula and shoulder kinematics for right (red) and left (blue) limbs under elevation in the scapular plane. Subject 2, 2023.01.24. Paexo session 1.

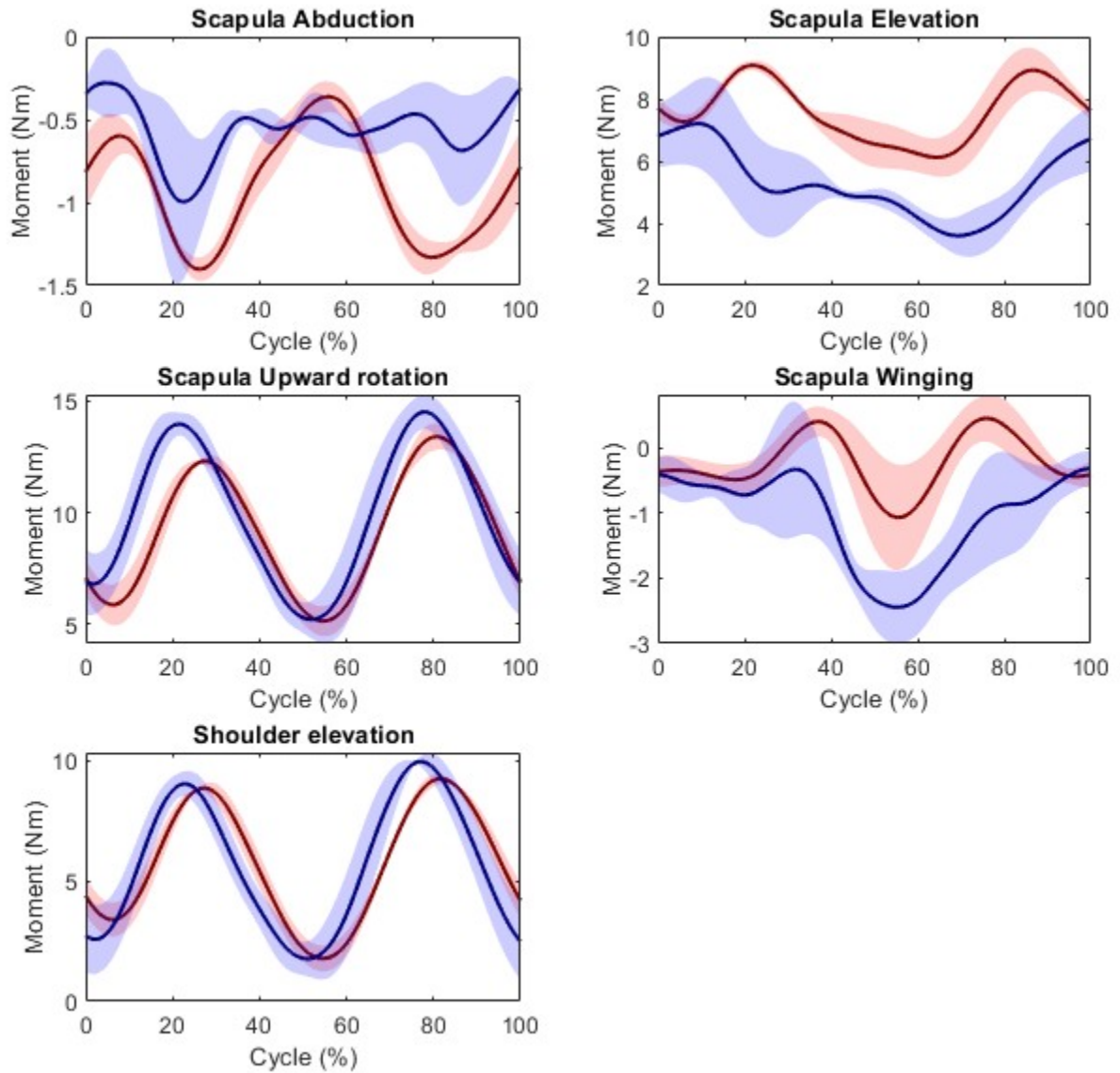


Figure 4: Scapula and shoulder kinetics for right (red) and left (blue) limbs under elevation in the scapular plane. Subject 2, 2023.01.24. Paexo session 1.

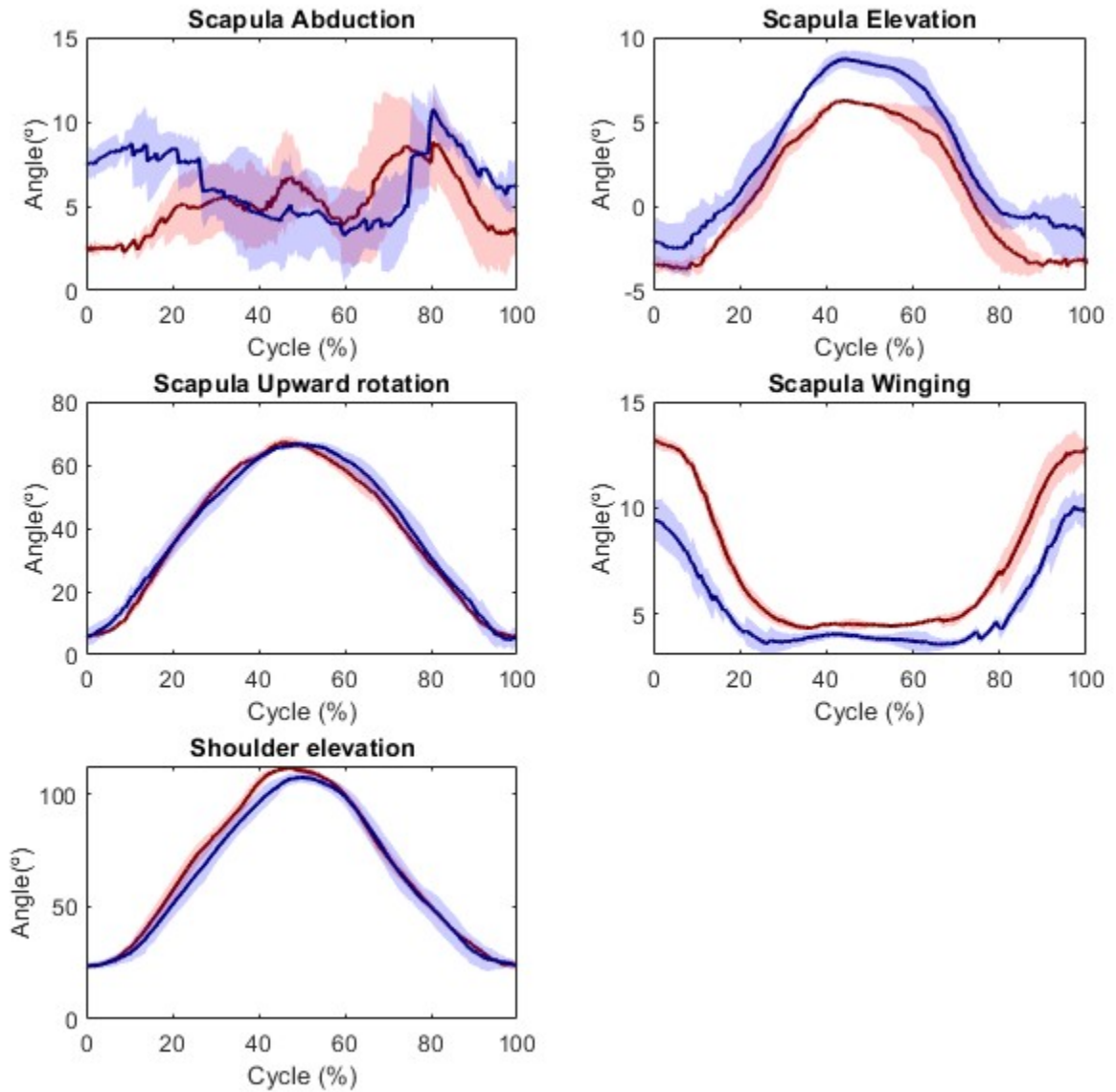


Figure 5: Scapula and shoulder kinematics for right (red) and left (blue) limbs under elevation in the scapular plane with exoskeleton. Subject 2, 2023.01.24. Paexo session 1.

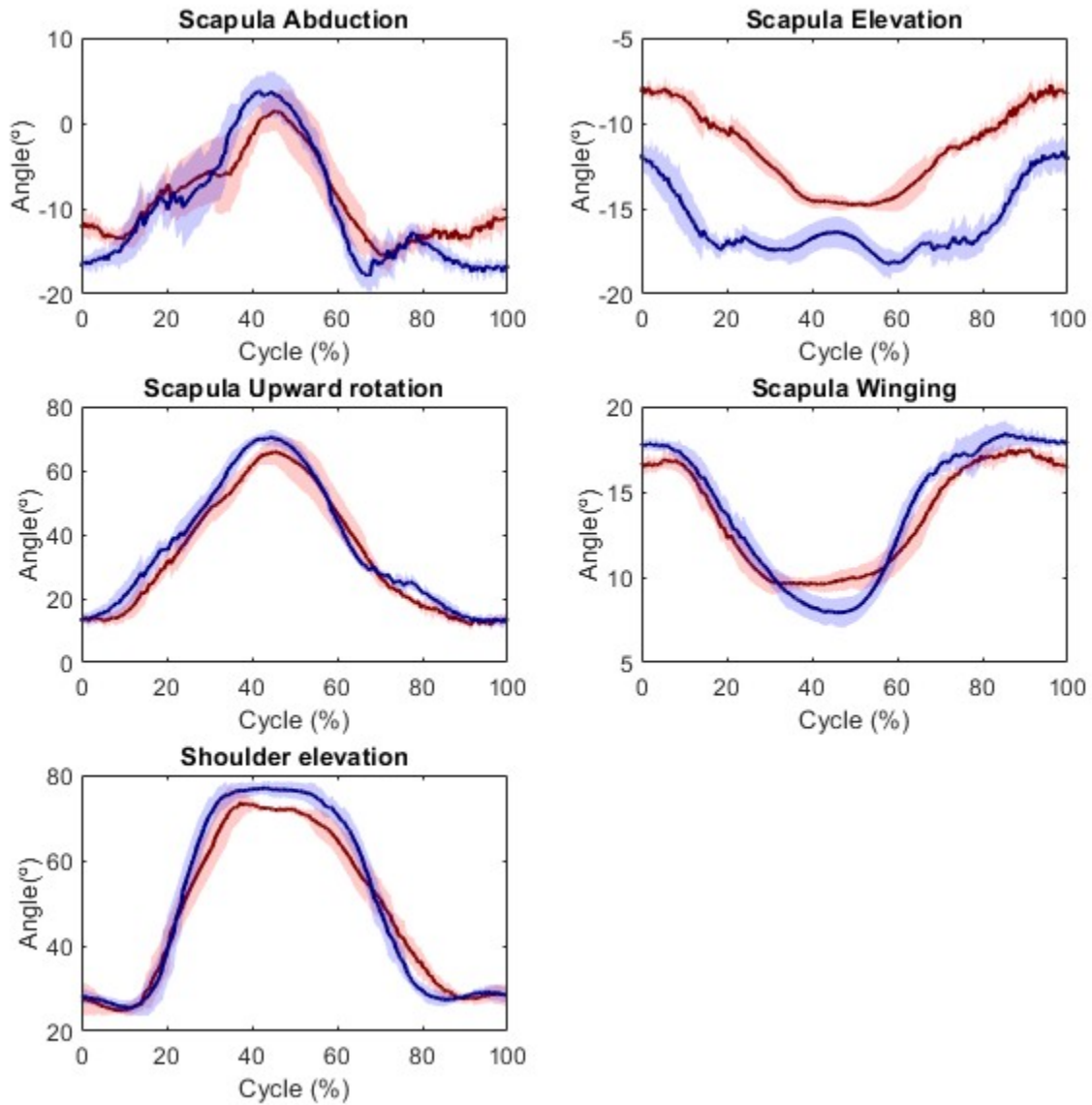


Figure 6: Scapula and shoulder kinematics for right (red) and left (blue) limbs under elevation in the scapular plane. Subject 3, 2023.02.16. Paexo session 2.

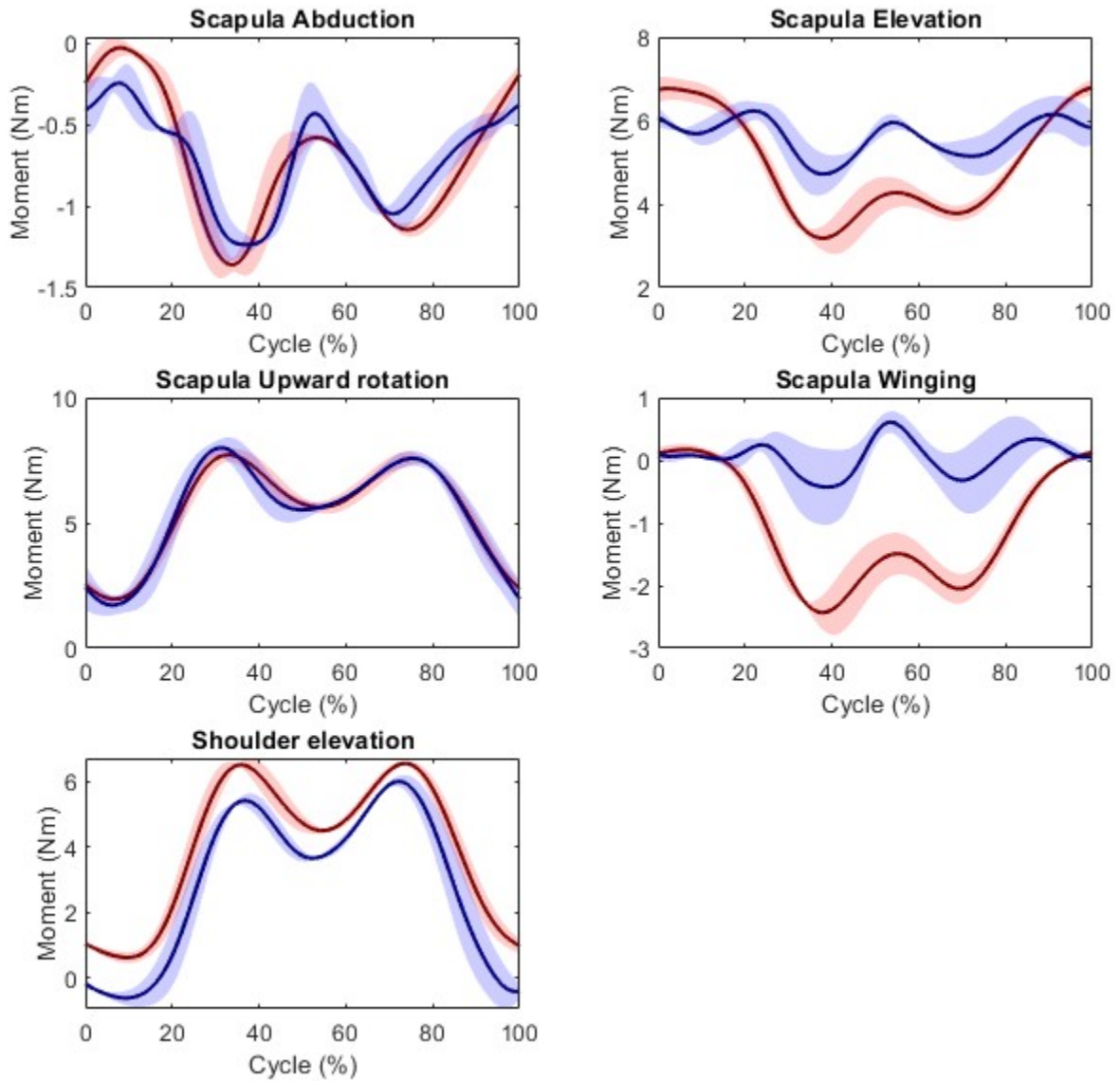


Figure 7: Scapula and shoulder kinetics for right (red) and left (blue) limbs under elevation in the scapular plane. Subject 3, 2023.02.16. Paexo session 2.

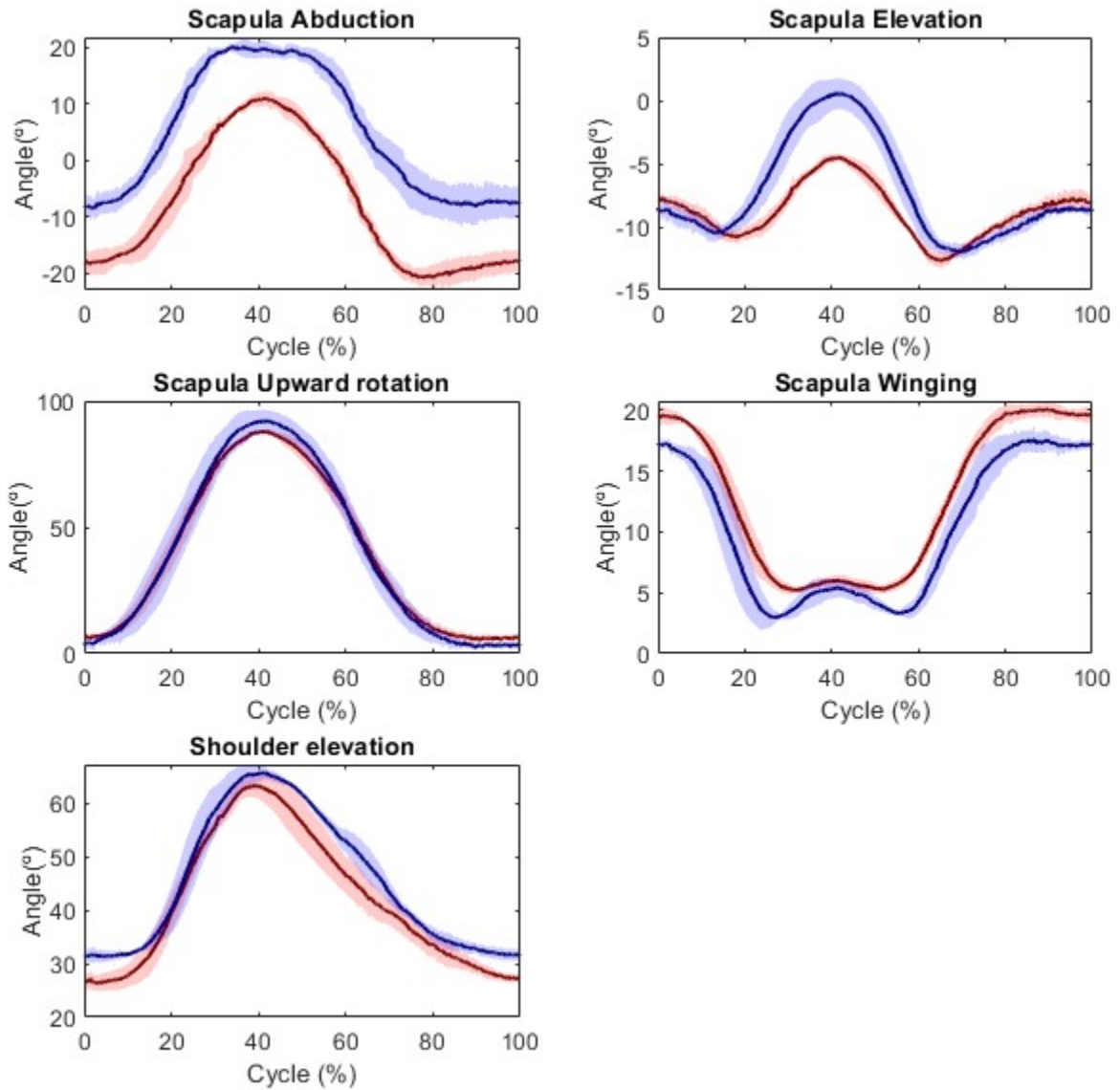


Figure 8: Scapula and shoulder kinematics for right (red) and left (blue) limbs under elevation in the scapular plane with weight. Subject 3, 2023.02.16. Paexo session 2.

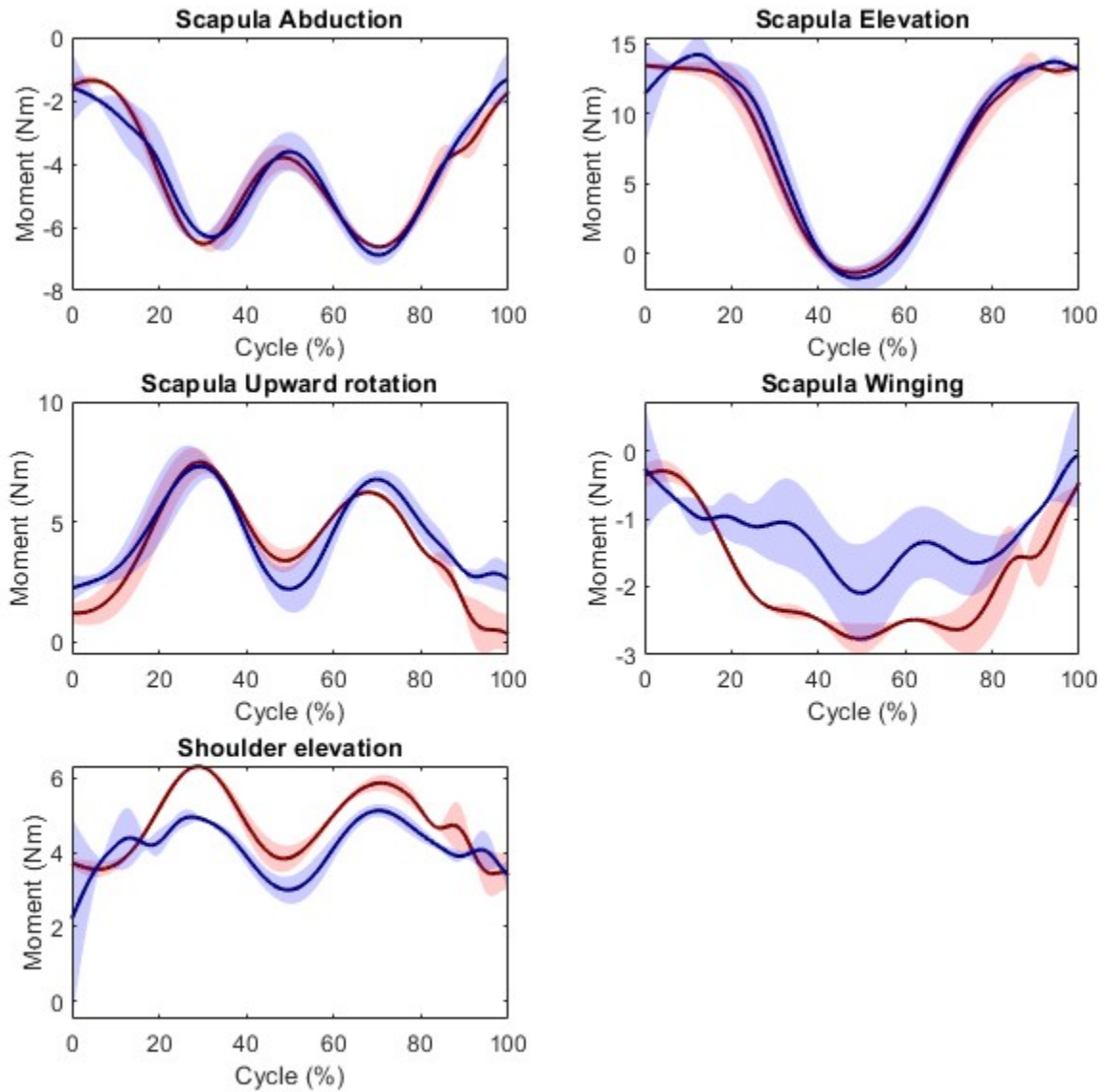


Figure 9: Scapula and shoulder kinetics for right (red) and left (blue) limbs under elevation in the scapular plane with weight. Subject 3, 2023.02.16. Paexo session 2.

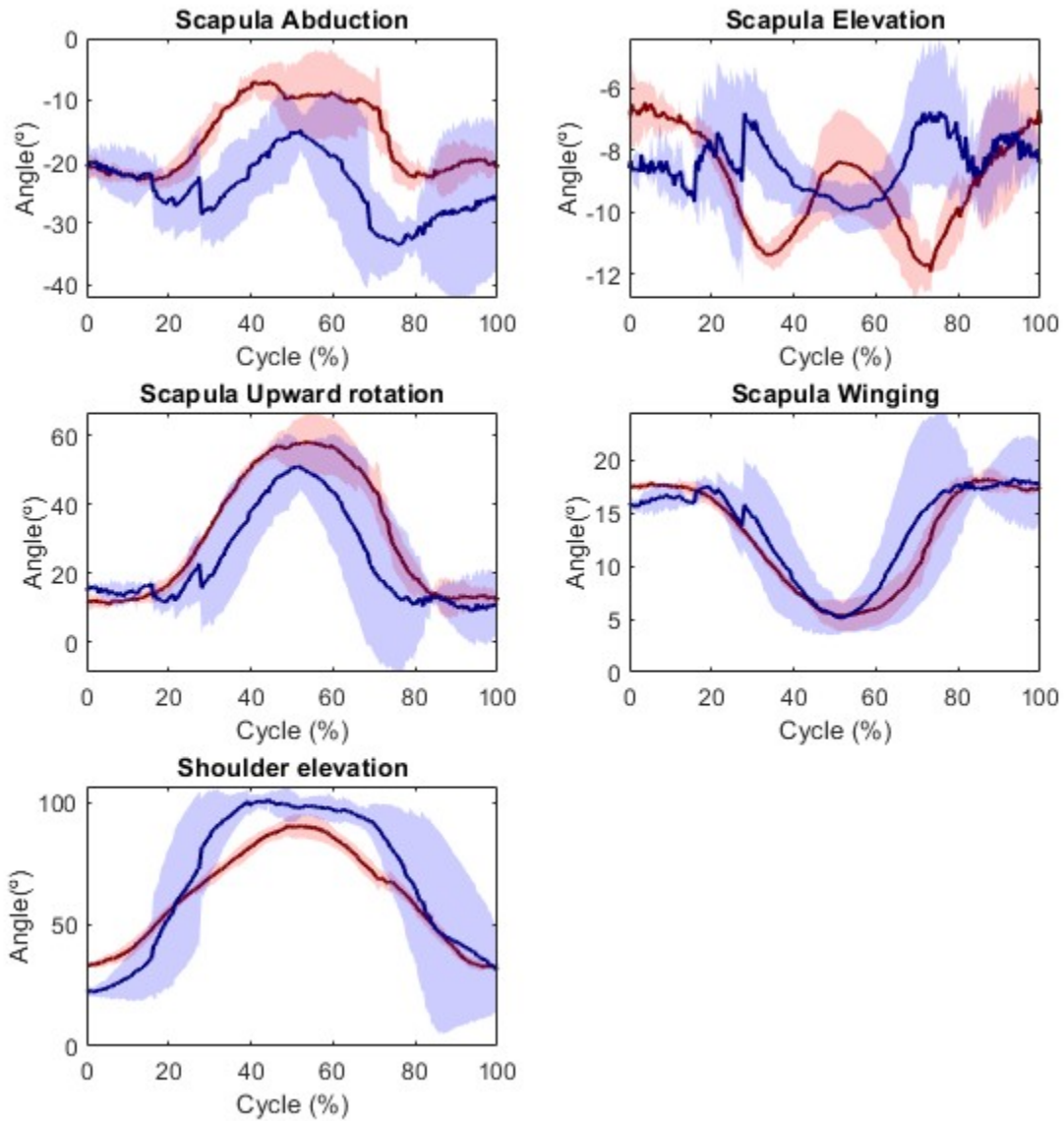


Figure 10: Scapula and shoulder kinematics for right (red) and left (blue) limbs under elevation in the scapular plane with exoskeleton. Subject 3, 2023.02.16. Paexo session 2.

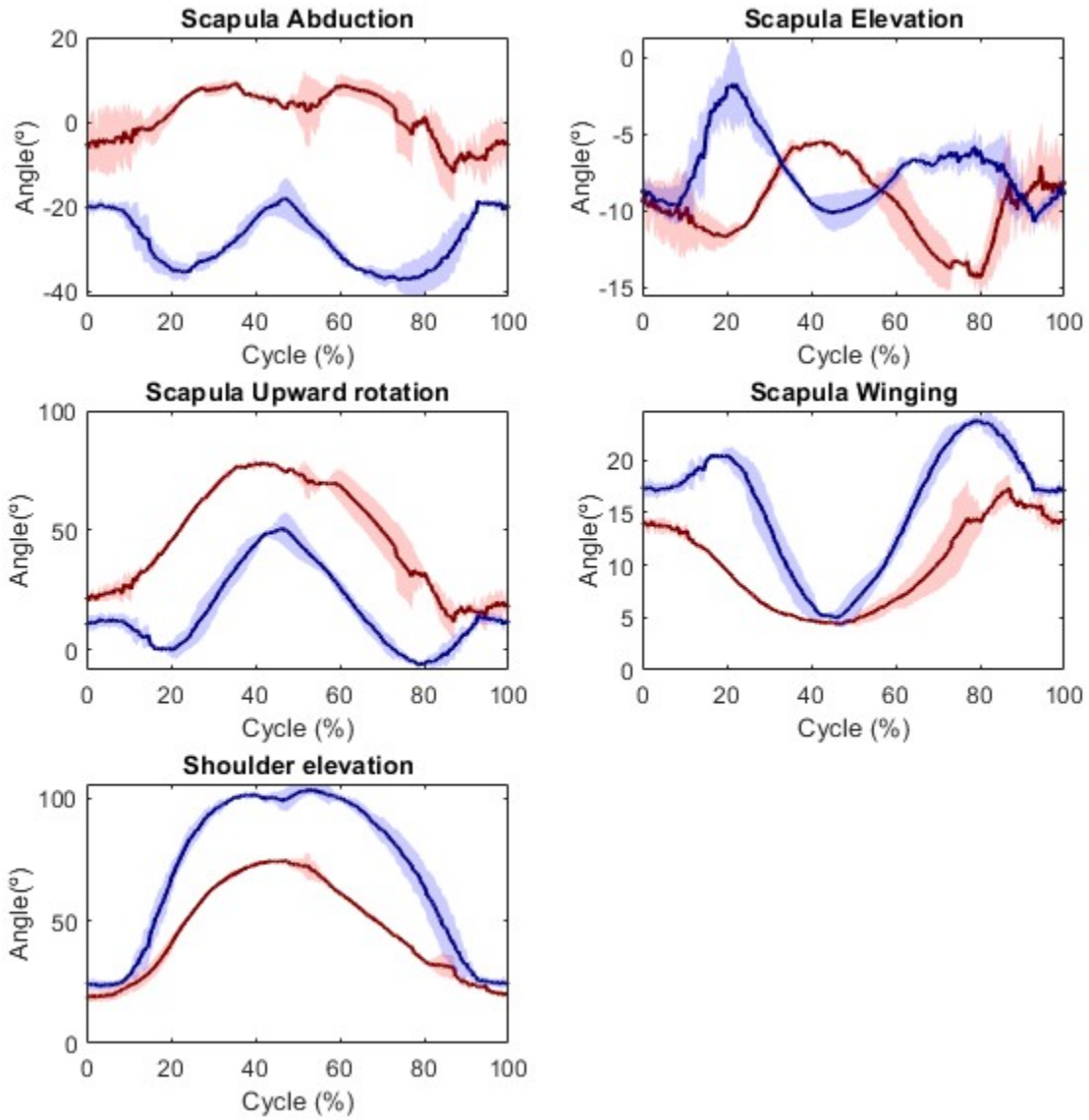


Figure 11: Scapula and shoulder kinematics for right (red) and left (blue) limbs under elevation in the scapular plane with exoskeleton and weight. Subject 3, 2023.02.16. Paexo session 2.

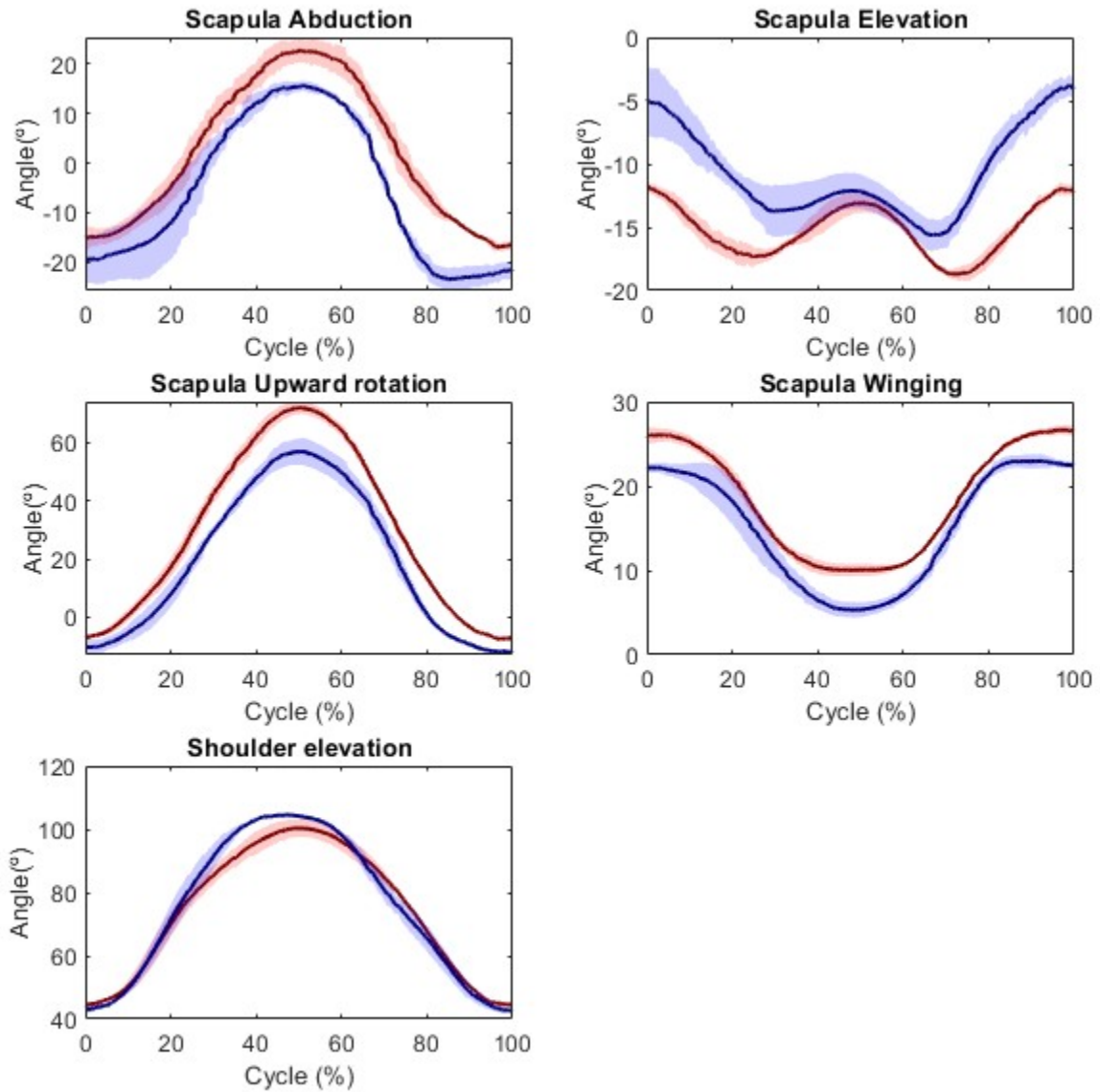


Figure 12: Scapula and shoulder kinematics for right (red) and left (blue) limbs under elevation in the scapular plane. Subject 4, 2023.03.02. Paexo session 3.

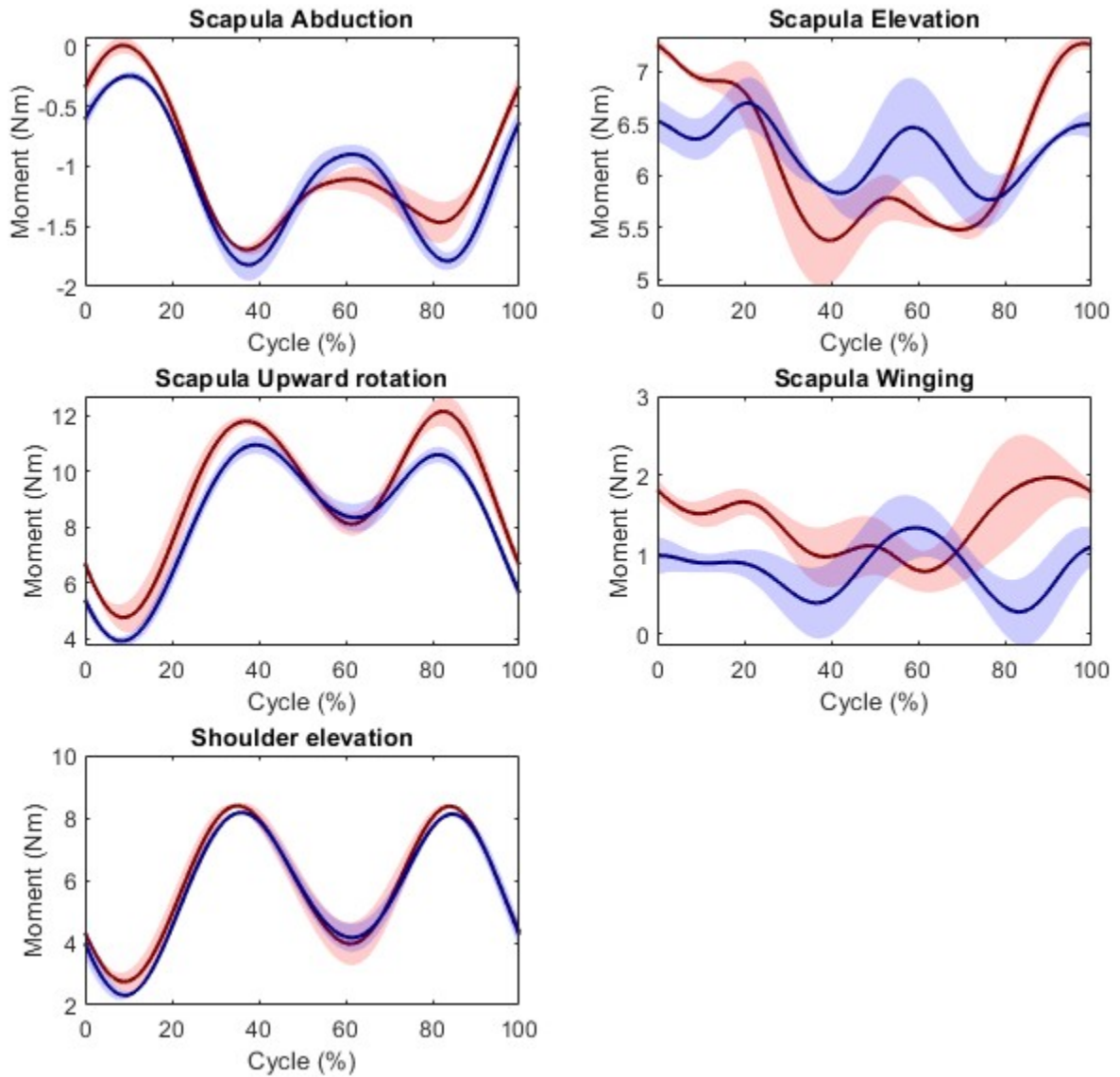


Figure 13: Scapula and shoulder kinetics for right (red) and left (blue) limbs under elevation in the scapular plane. Subject 4, 2023.03.02. Paexo session 3.

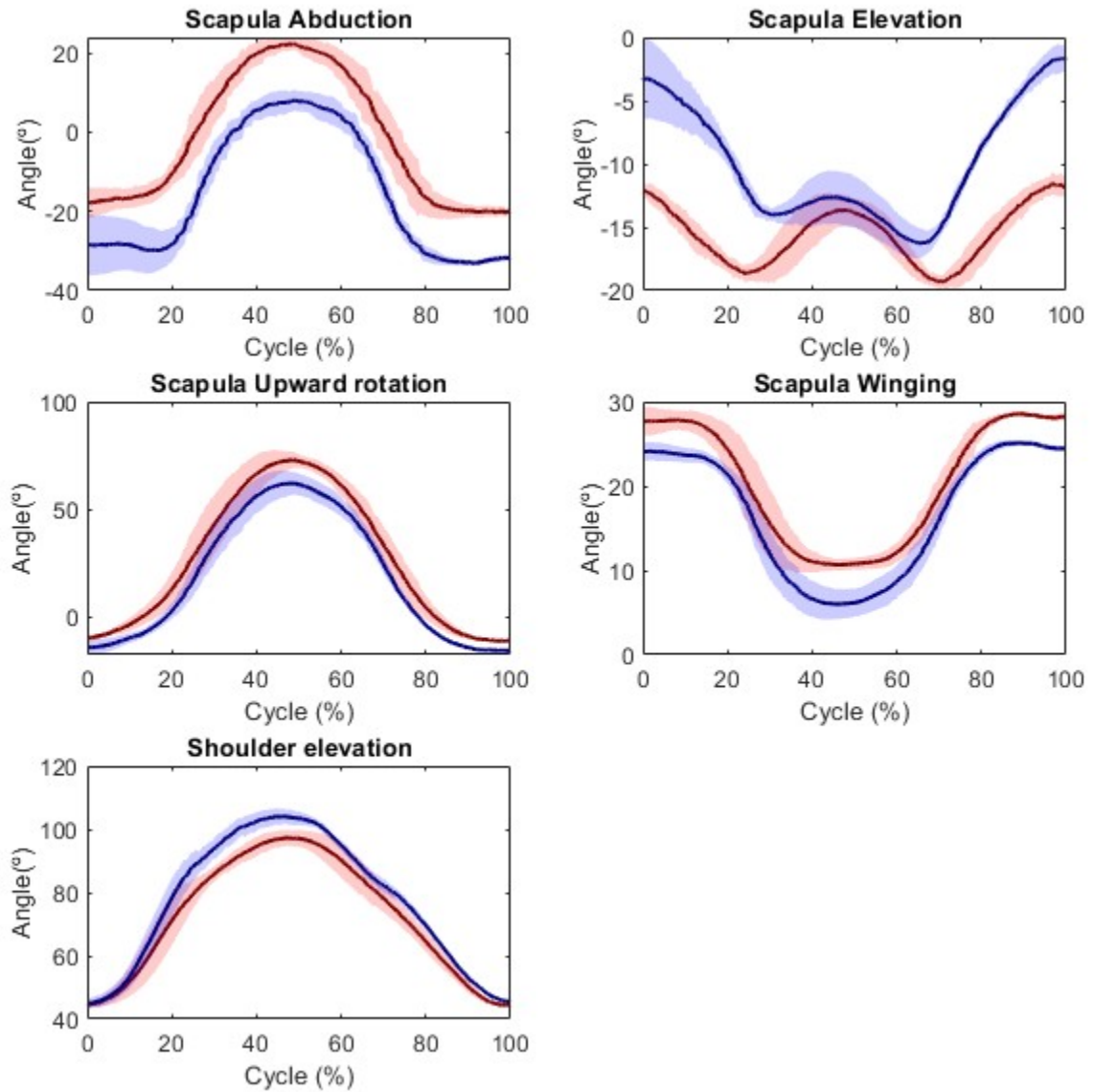


Figure 14: Scapula and shoulder kinematics for right (red) and left (blue) limbs under elevation in the scapular plane with weight. Subject 4, 2023.03.02. Paexo session 3.

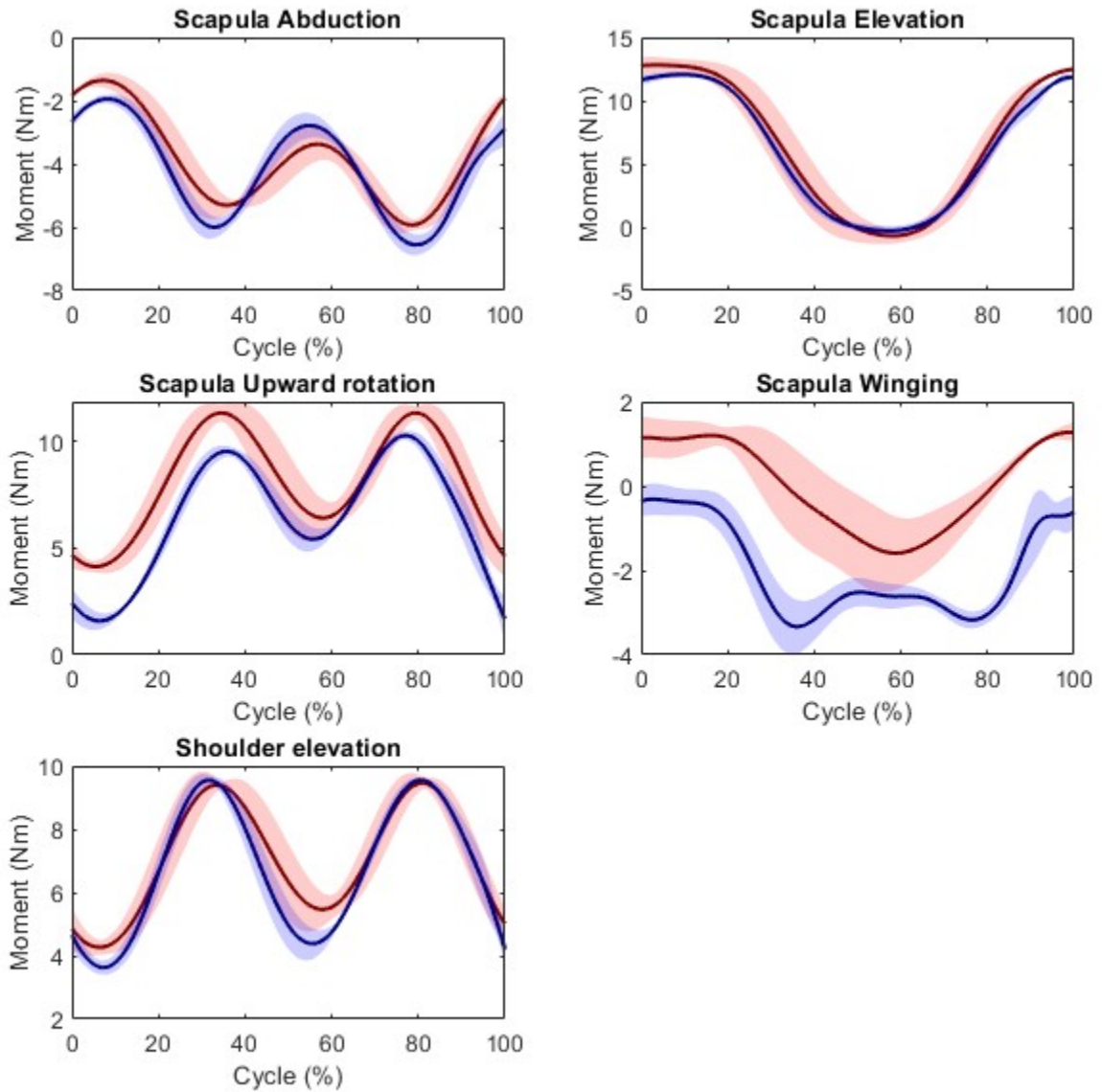


Figure 15: Scapula and shoulder kinetics for right (red) and left (blue) limbs under elevation in the scapular plane with weight. Subject 4, 2023.03.02. Paexo session 3.

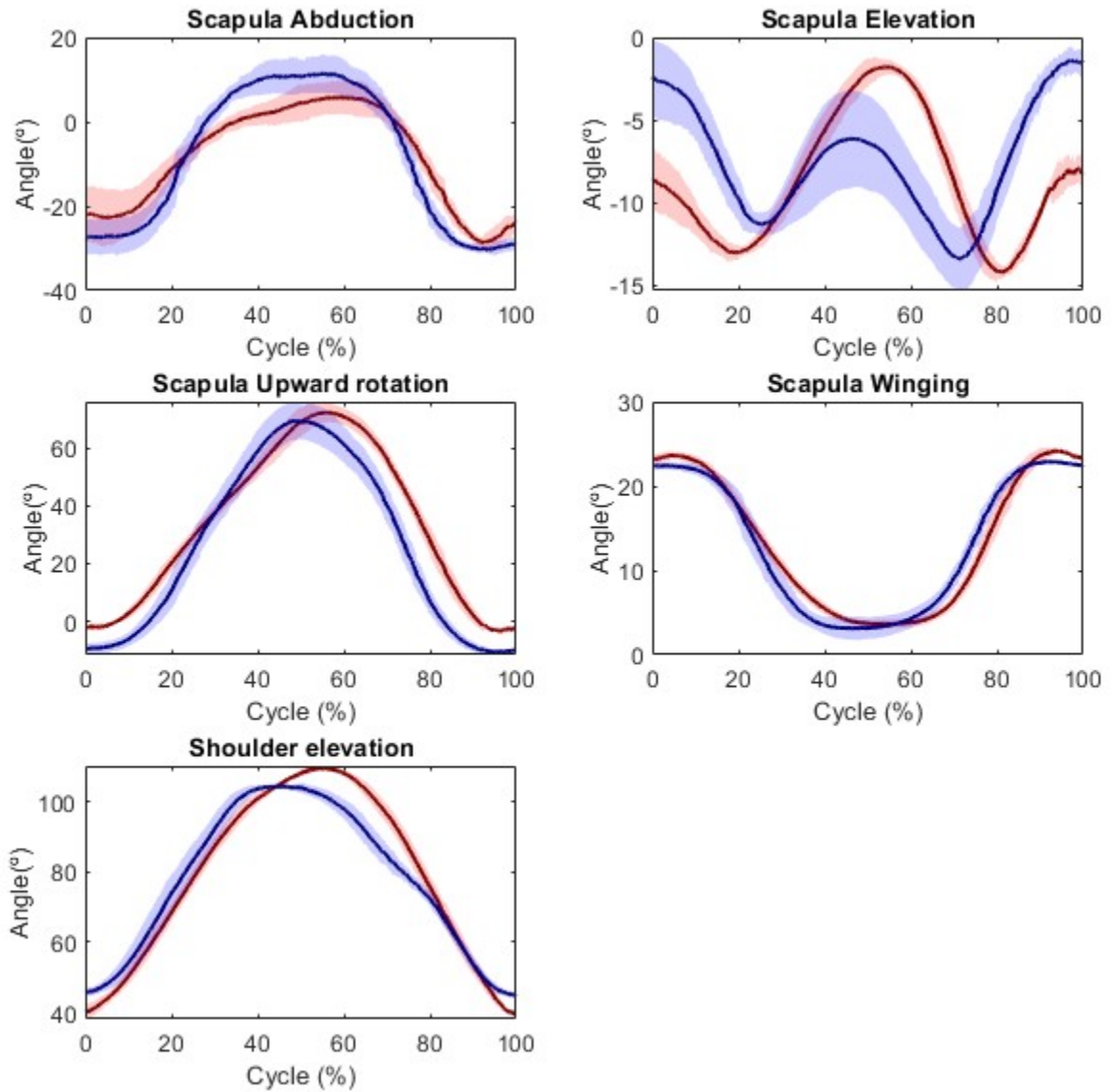


Figure 16: Scapula and shoulder kinematics for right (red) and left (blue) limbs under elevation in the scapular plane with exoskeleton. Subject 4, 2023.03.02. Paexo session 3.

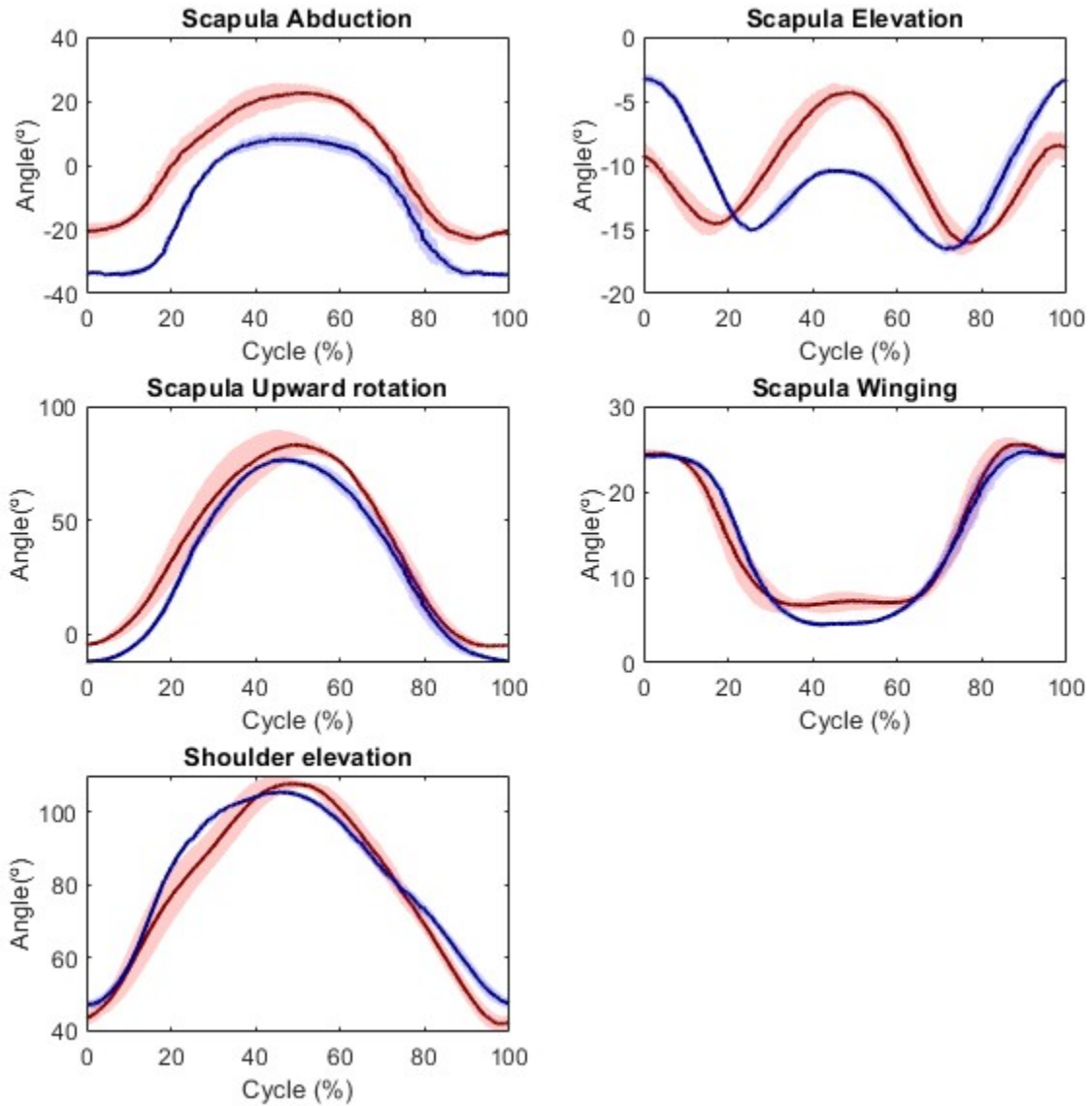


Figure 17: Scapula and shoulder kinematics for right (red) and left (blue) limbs under elevation in the scapular plane with exoskeleton and weight. Subject 4, 2023.03.02. Paexo session 3.

Annex III. EMG data

List of Figures

1	Raw EMG data for right abduction, subject 2, 2023.01.24. Paexo session 1.	2
2	Raw EMG data for left abduction, subject 2, 2023.01.24. Paexo session 1.	3
3	Raw EMG data for right abduction with exo, subject 2, 2023.01.24. Paexo session 1.	4
4	Raw EMG data for left abduction with exo, subject 2, 2023.01.24. Paexo session 1.	5
5	Raw EMG data for right abduction, subject 3, 2023.02.16. Paexo session 2.	6
6	Raw EMG data for left abduction, subject 3, 2023.02.16. Paexo session 2.	7
7	Raw EMG data for right abduction with exo, subject 3, 2023.02.16. Paexo session 2.	8
8	Raw EMG data for left abduction with exo, subject 3, 2023.02.16. Paexo session 2.	9
9	Raw EMG data for right abduction, subject 4, 2023.03.02. Paexo session 3.	10
10	Raw EMG data for left abduction, subject 4, 2023.03.02. Paexo session 3.	11
11	Raw EMG data for right abduction with exo, subject 4, 2023.03.02. Paexo session 3.	12
12	Raw EMG data for left abduction with exo, subject 4, 2023.03.02. Paexo session 3.	13

2023.01.24. Paexo session 1. Subject n.2

Raw EMG: Right abduction

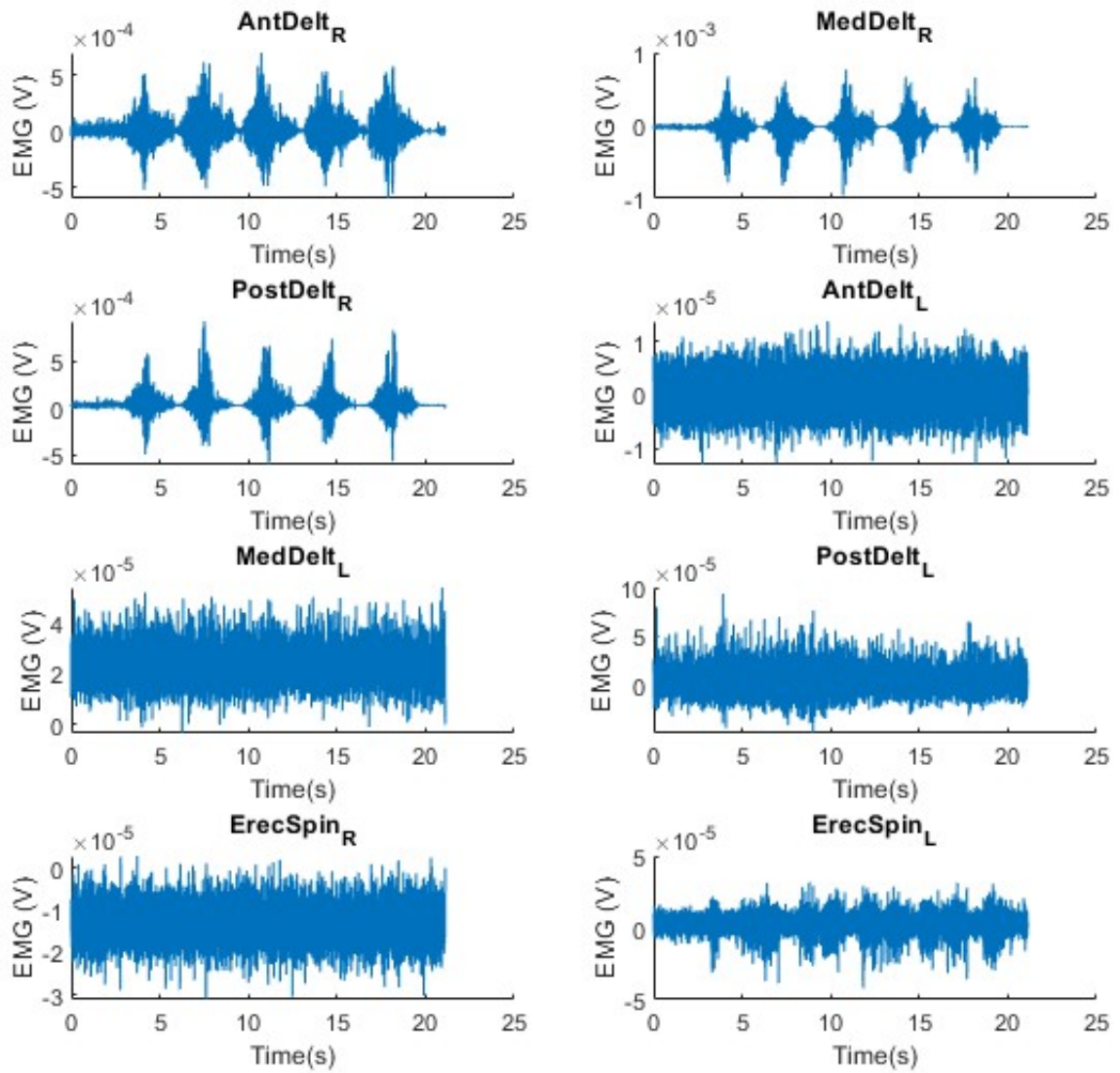


Figure 1: Raw EMG data for right abduction, subject 2, 2023.01.24. Paexo session 1.

2023.01.24. Paexo session 1. Subject n.2

Raw EMG: Left abduction

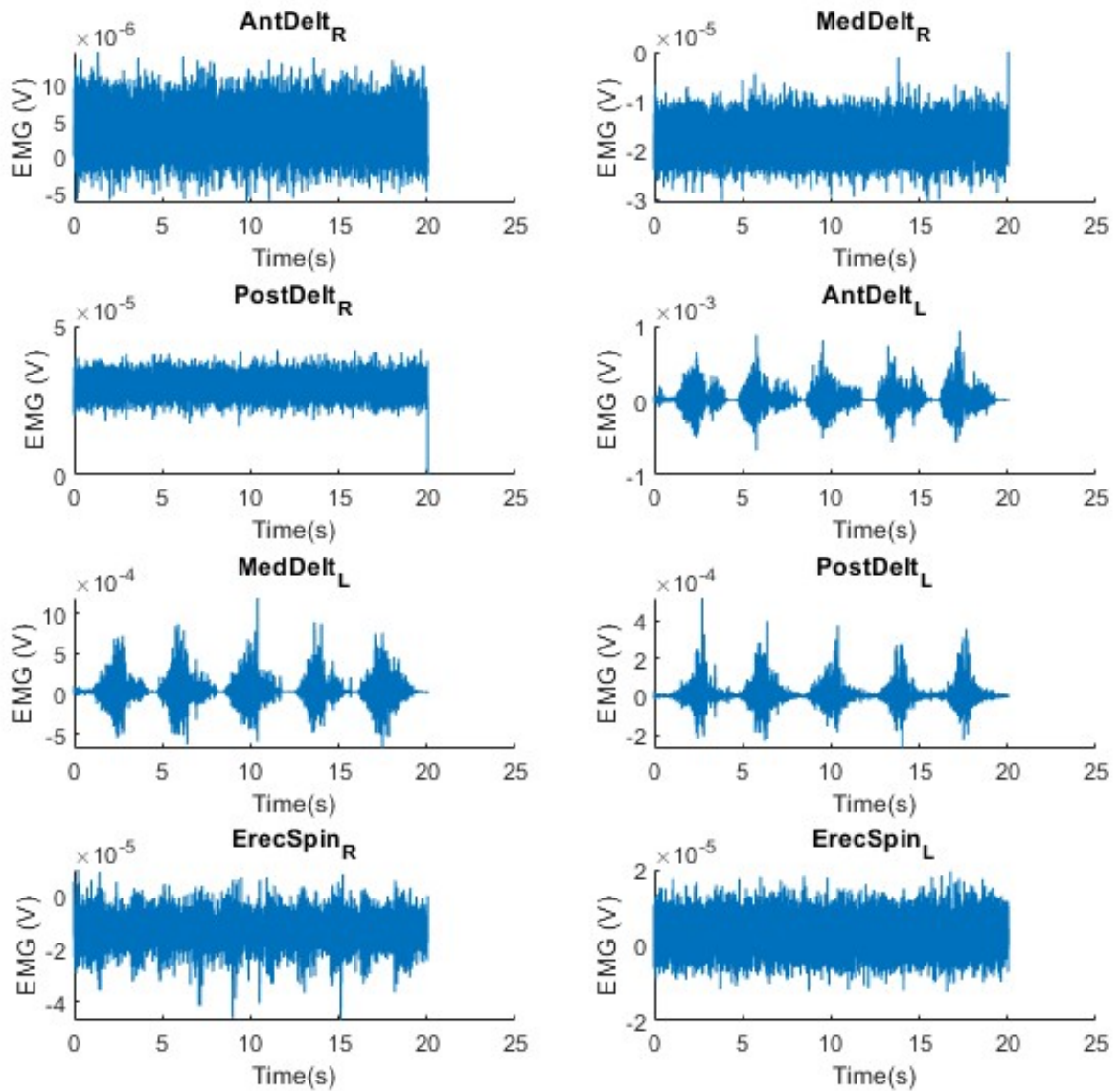


Figure 2: Raw EMG data for left abduction, subject 2, 2023.01.24. Paexo session 1.

2023.01.24. Paexo session 1. Subject n.2

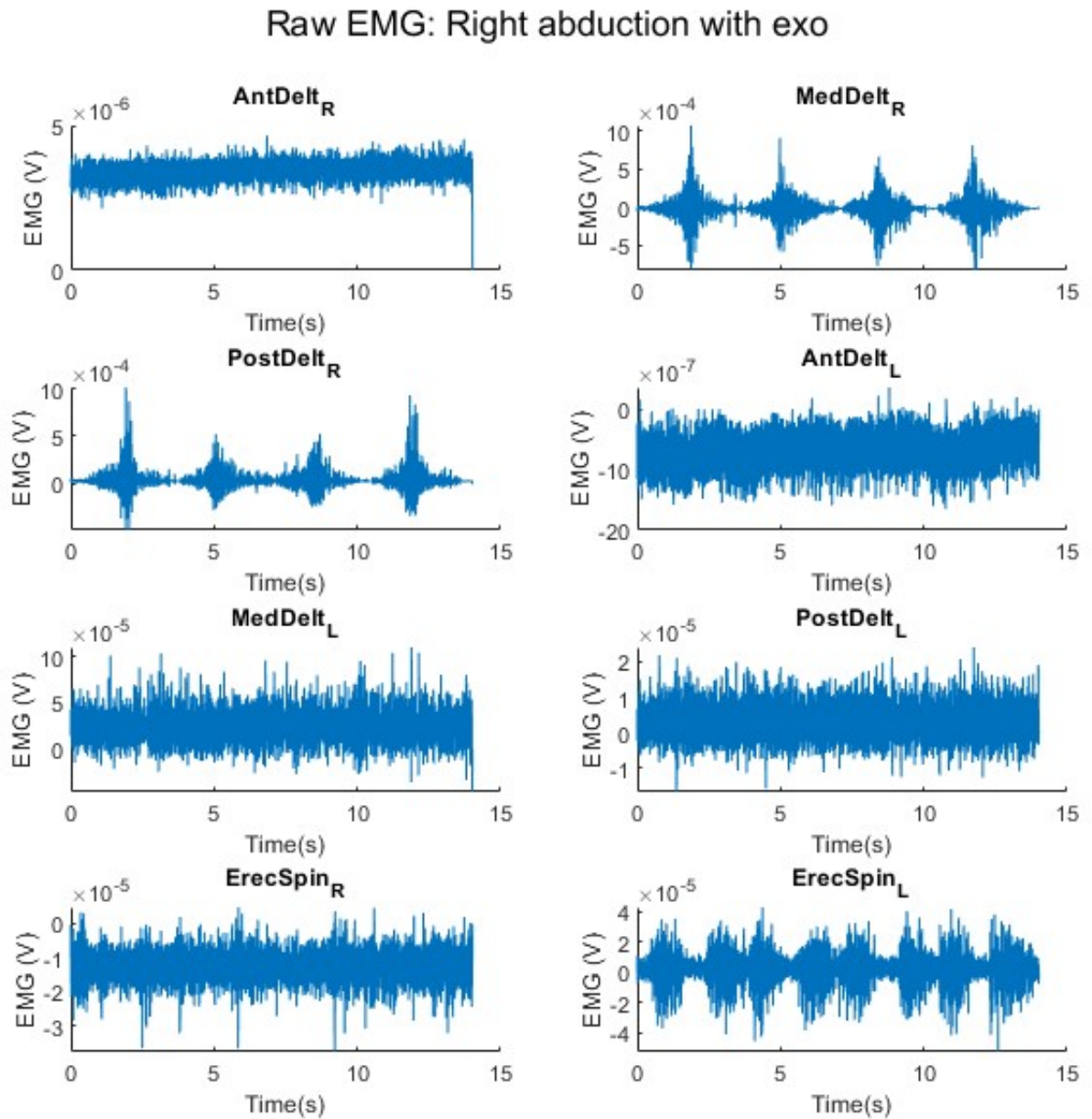


Figure 3: Raw EMG data for right abduction with exo, subject 2, 2023.01.24. Paexo session 1.

2023.01.24. Paexo session 1. Subject n.2

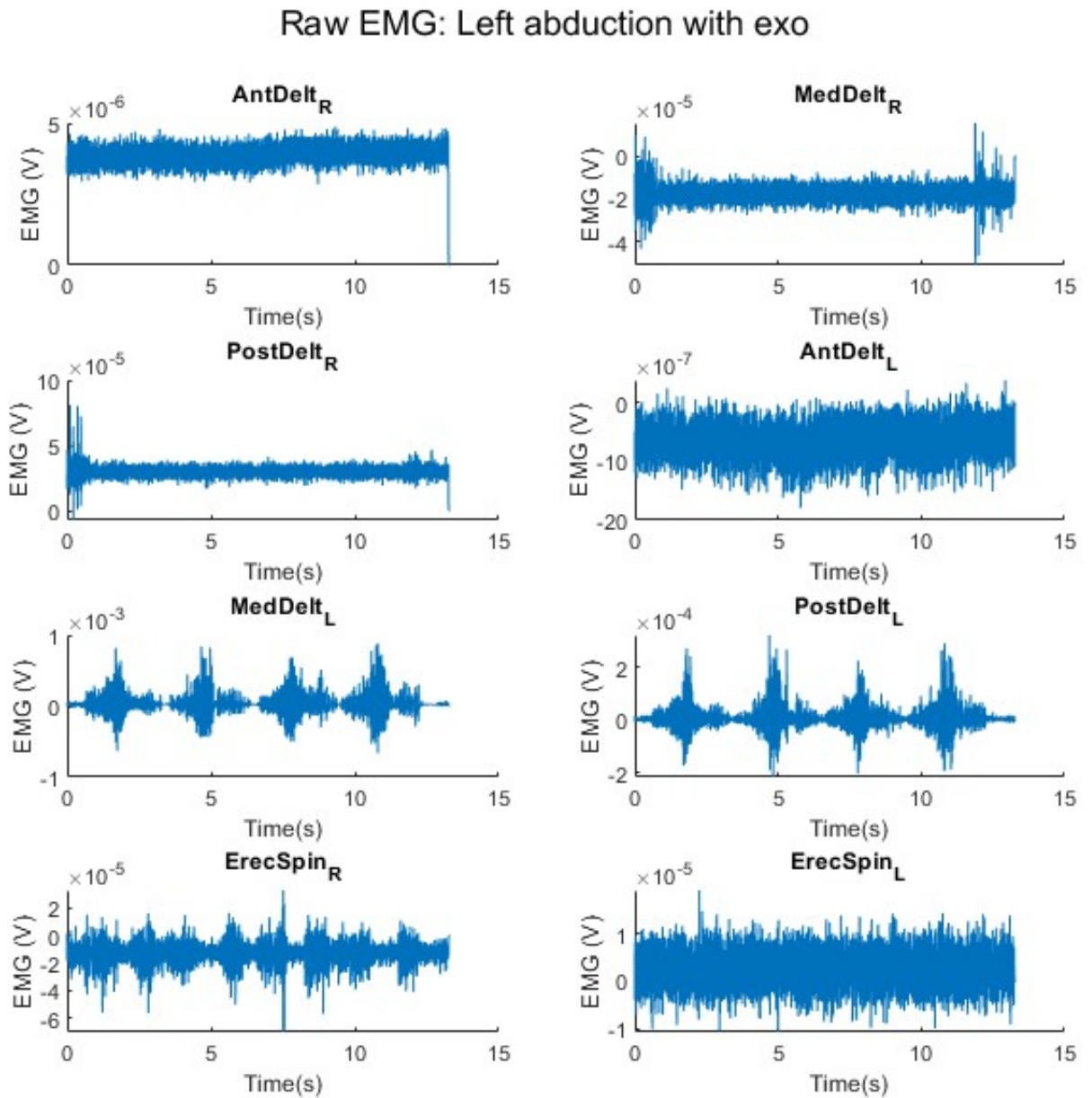


Figure 4: Raw EMG data for left abduction with exo, subject 2, 2023.01.24. Paexo session 1.

2023.02.16. Paexo session 2. Subject n.3

Raw EMG: Right abduction

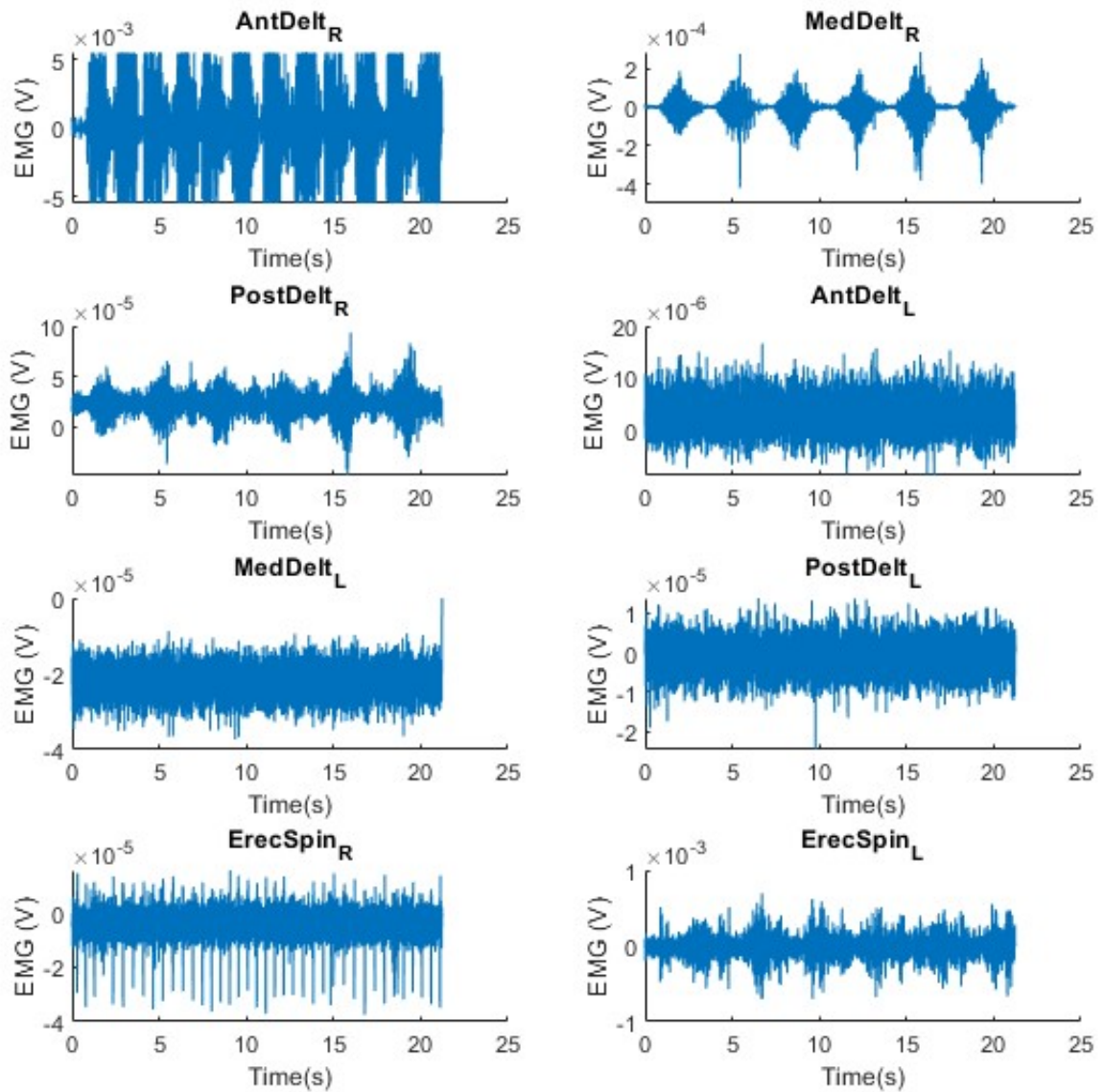


Figure 5: Raw EMG data for right abduction, subject 3, 2023.02.16. Paexo session 2.

2023.02.16. Paexo session 2. Subject n.3

Raw EMG: Left abduction

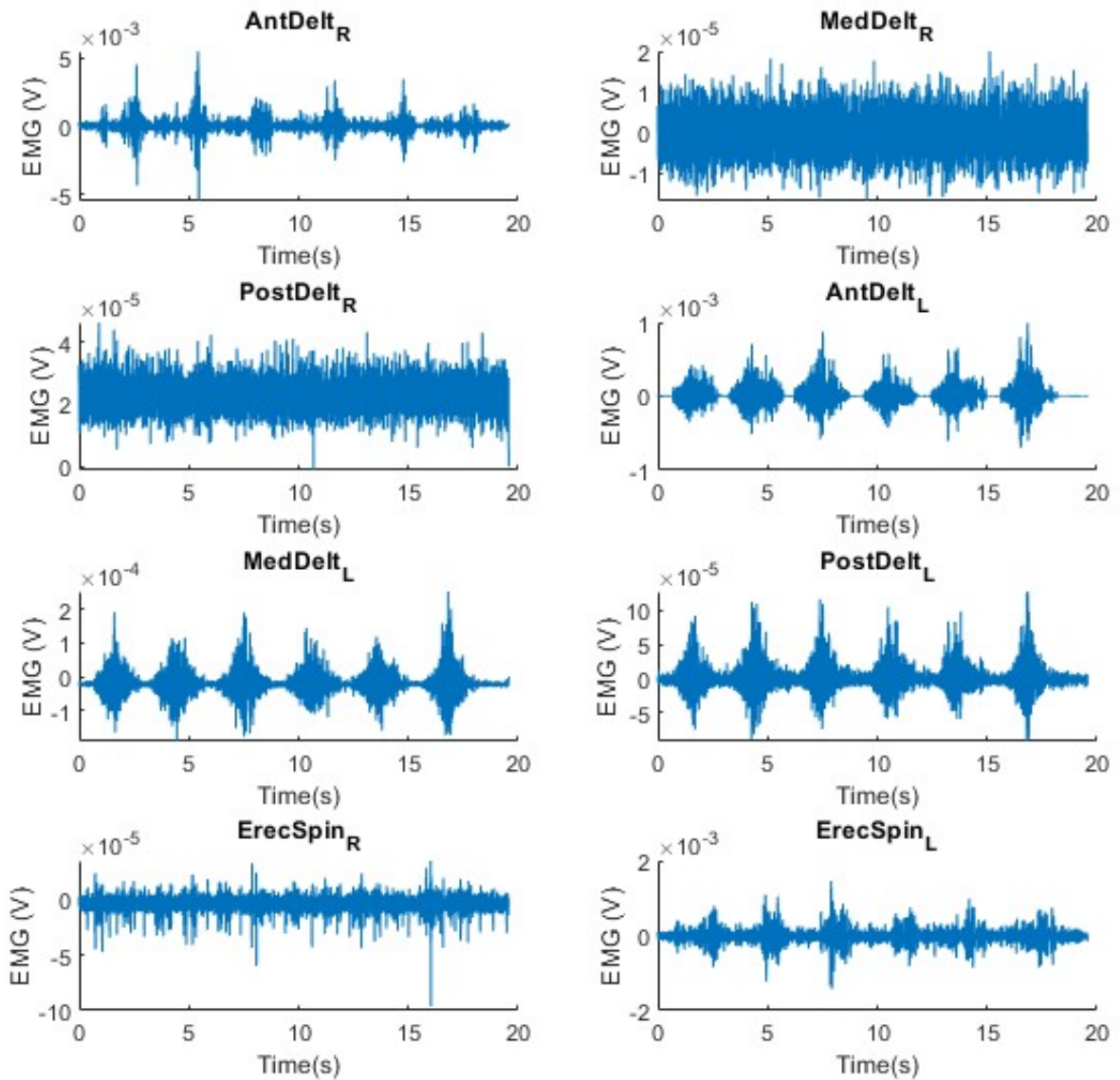


Figure 6: Raw EMG data for left abduction, subject 3, 2023.02.16. Paexo session 2.

2023.02.16. Paexo session 2. Subject n.3

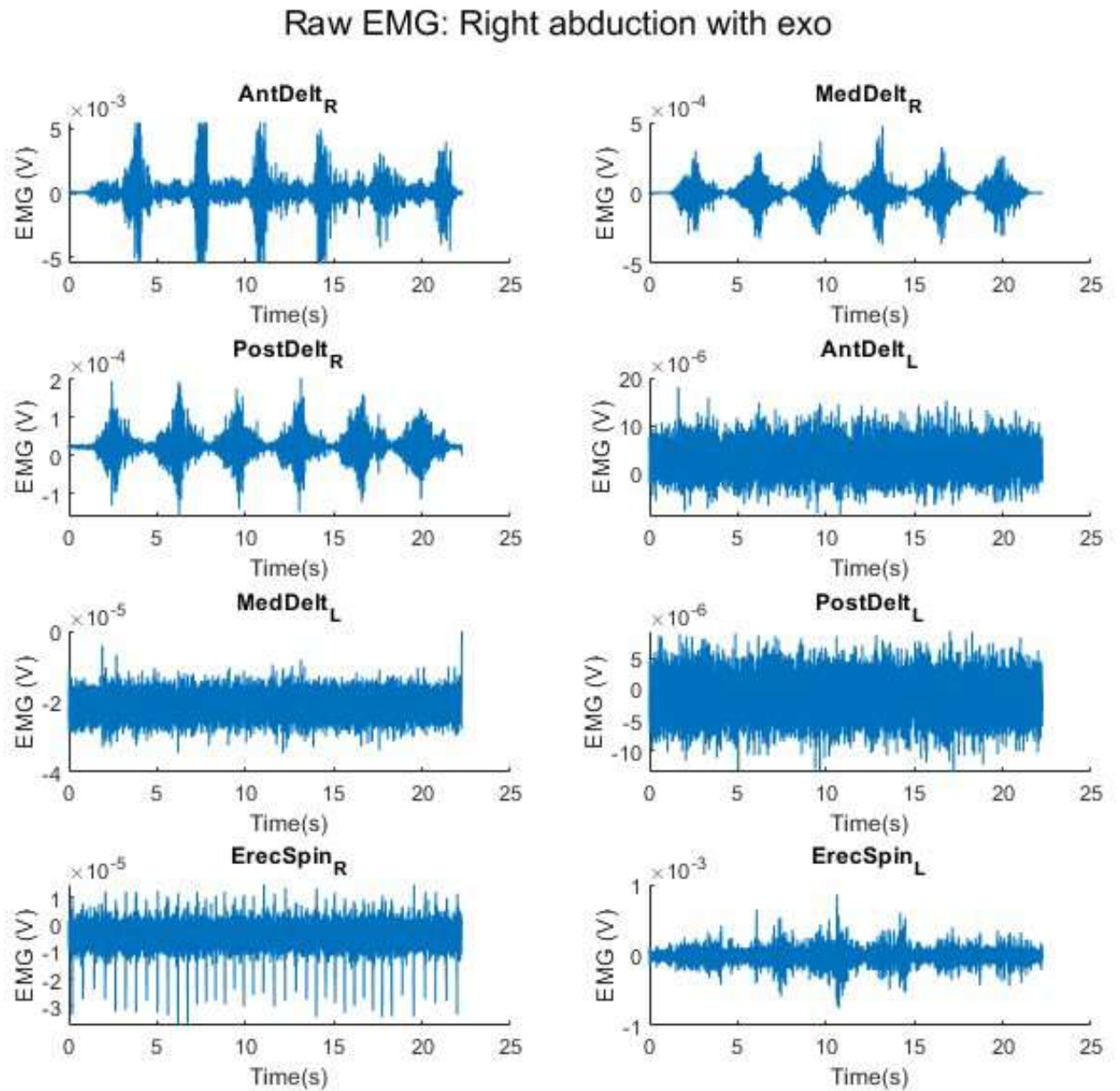


Figure 7: Raw EMG data for right abduction with exo, subject 3, 2023.02.16. Paexo session 2.

2023.02.16. Paexo session 2. Subject n.3

Raw EMG: Left abduction with exo

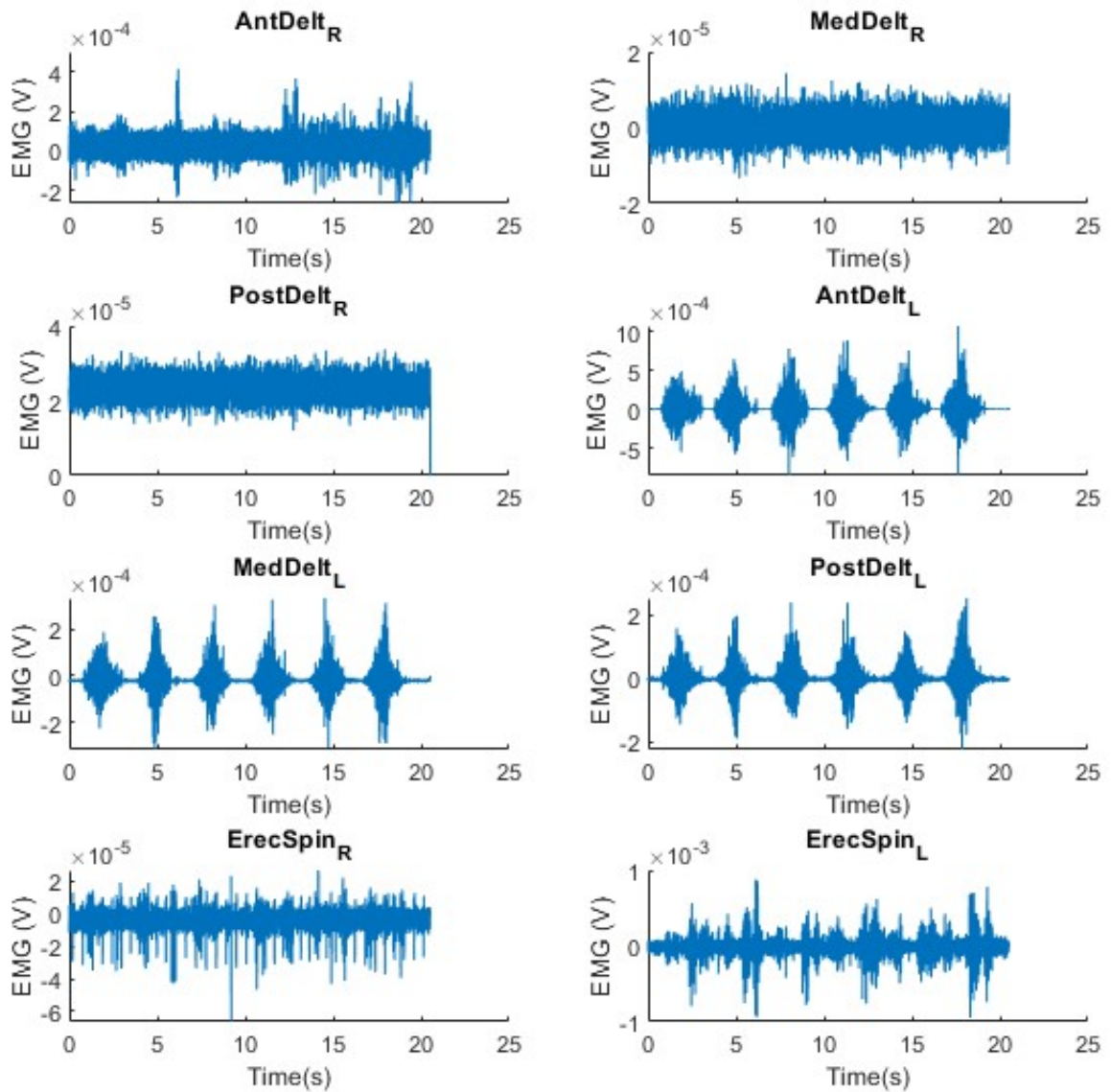


Figure 8: Raw EMG data for left abduction with exo, subject 3, 2023.02.16. Paexo session 2.

2023.03.02. Paexo session 3. Subject n.4

Raw EMG: Right abduction

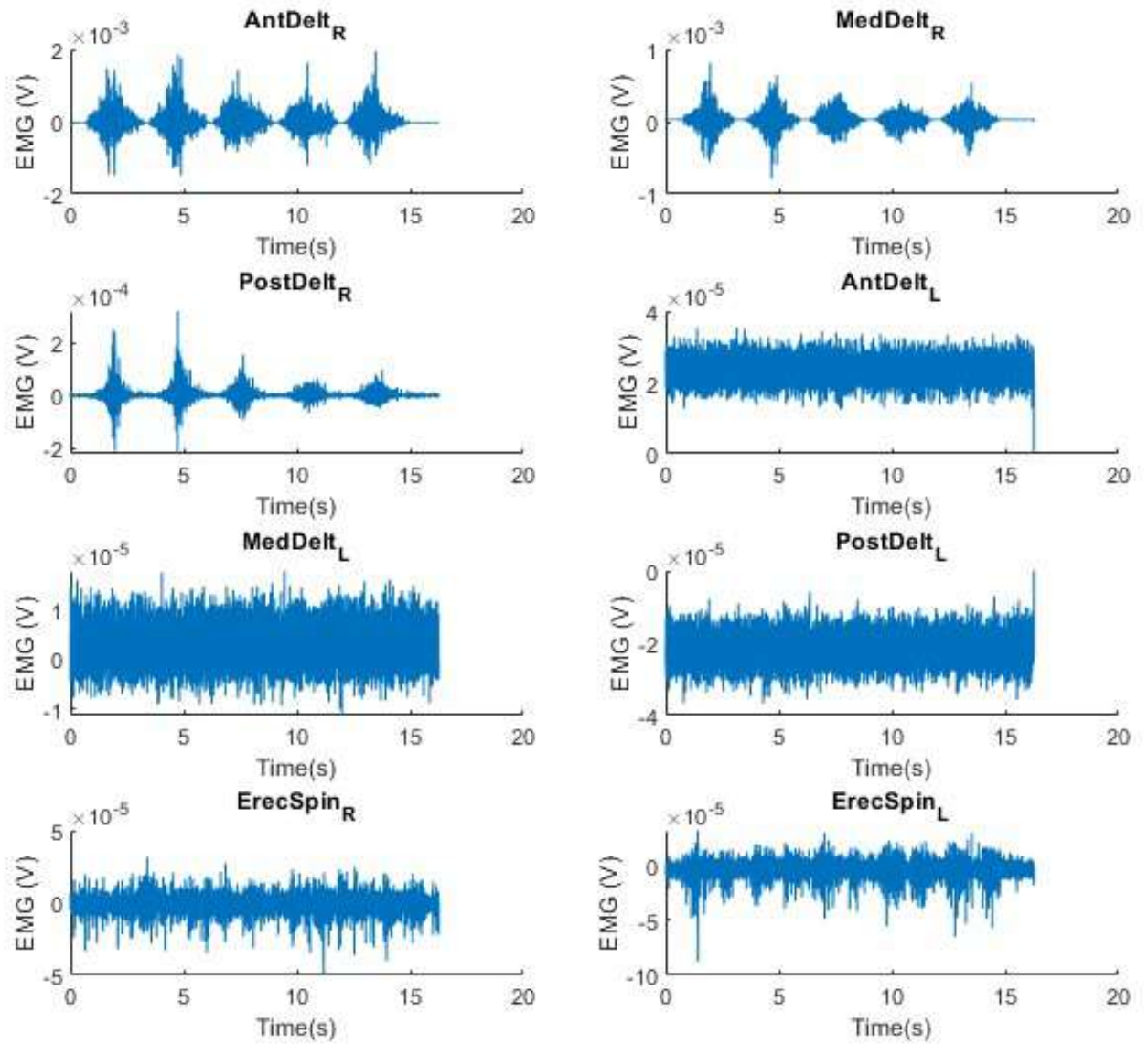


Figure 9: Raw EMG data for right abduction, subject 4, 2023.03.02. Paexo session 3.

2023.03.02. Paexo session 3. Subject n.4

Raw EMG: Left abduction

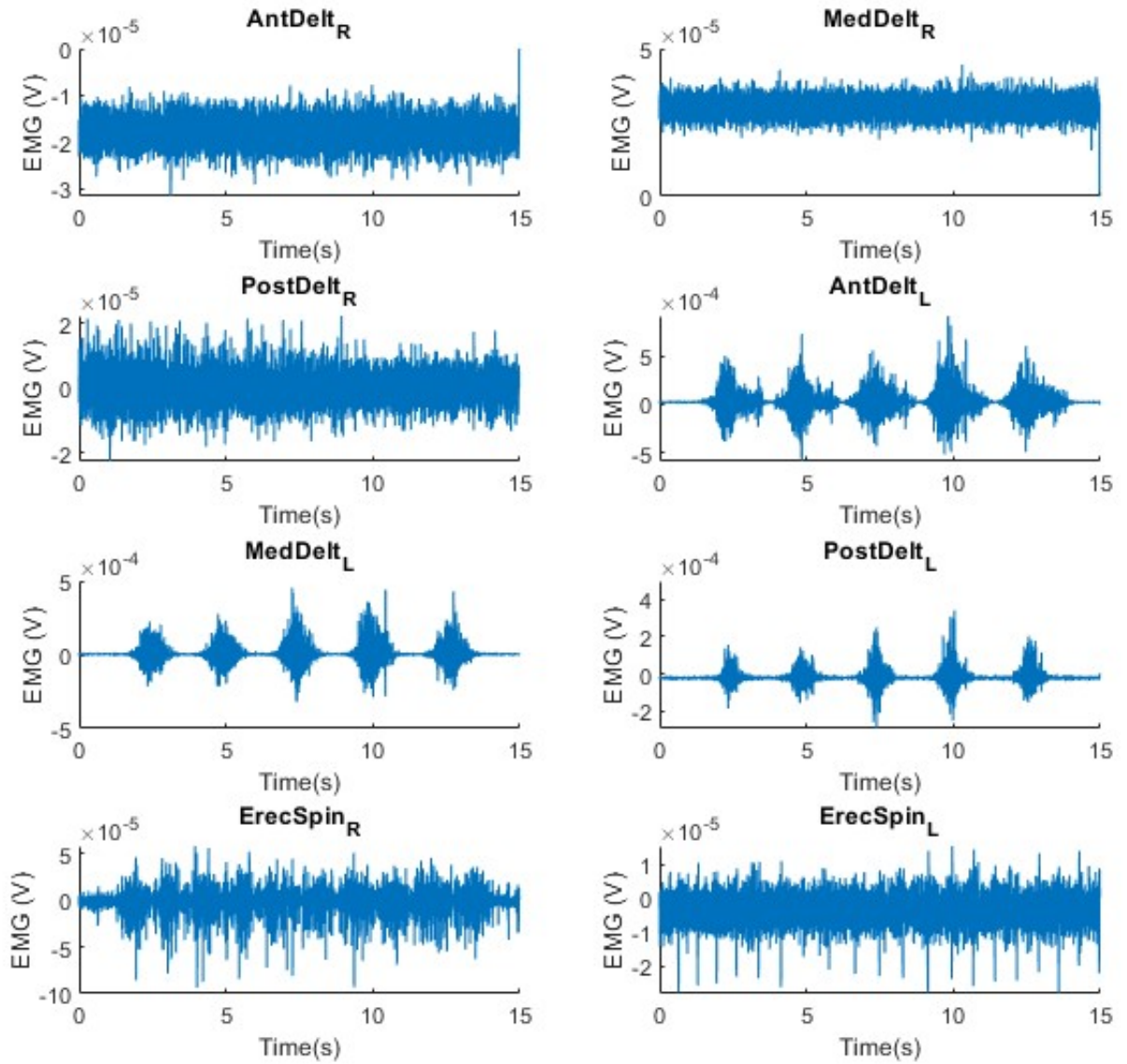


Figure 10: Raw EMG data for left abduction, subject 4, 2023.03.02. Paexo session 3.

2023.03.02. Paexo session 3. Subject n.4

Raw EMG: Right abduction with exo

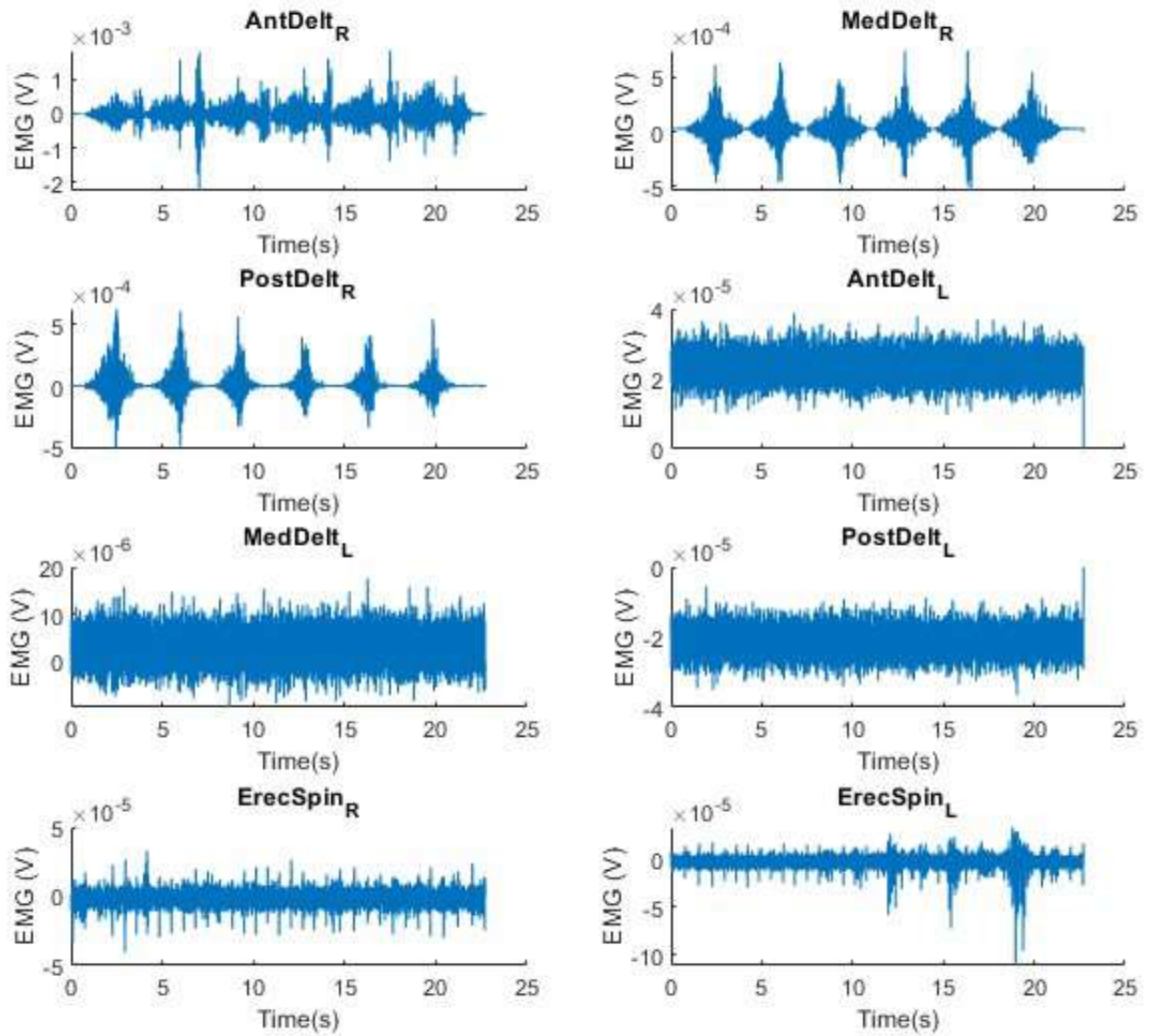


Figure 11: Raw EMG data for right abduction with exo, subject 4, 2023.03.02. Paexo session 3.

2023.03.02. Paexo session 3. Subject n.4

Raw EMG: Left abduction with exo

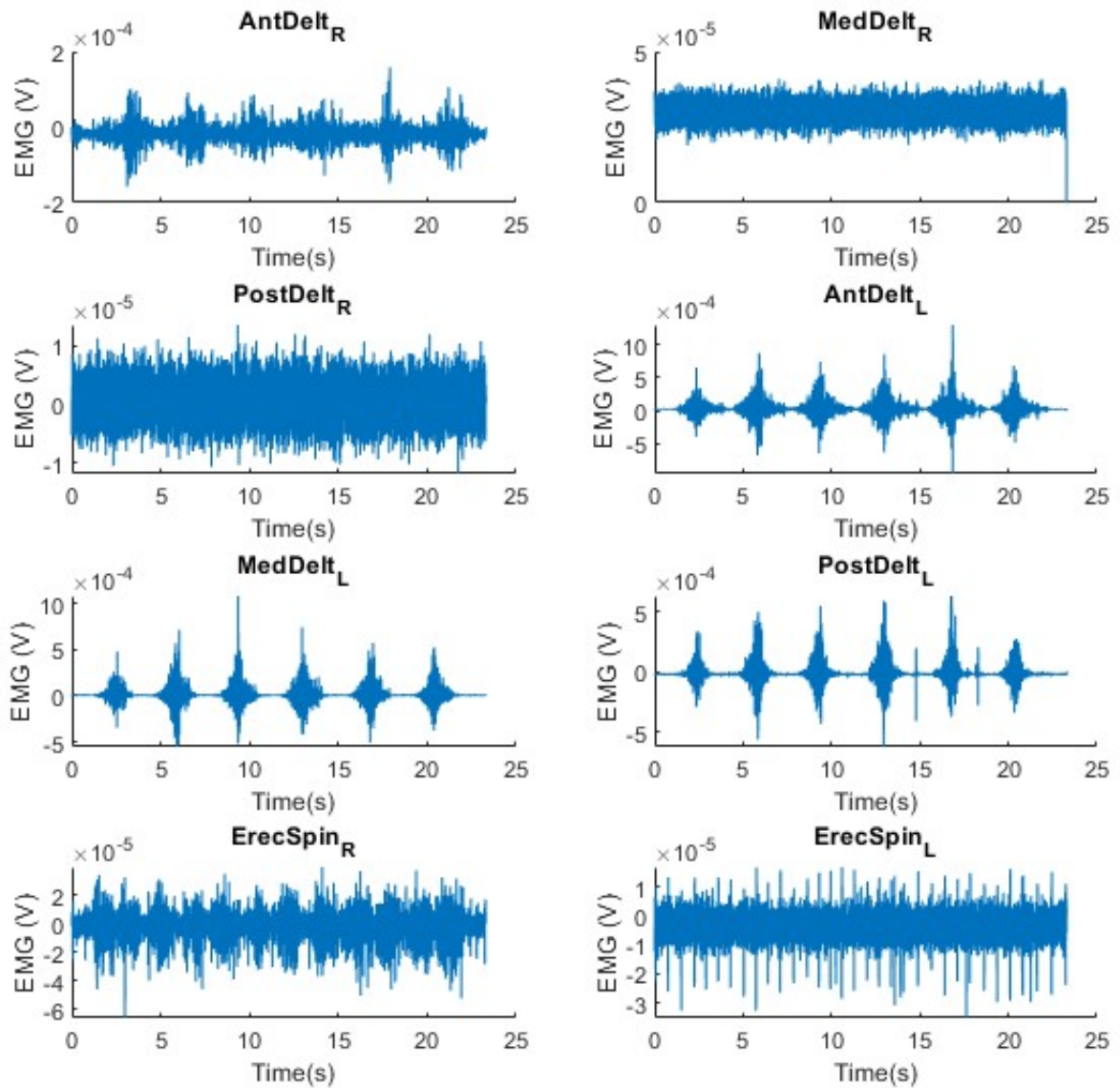


Figure 12: Raw EMG data for left abduction with exo, subject 4, 2023.03.02. Paexo session 3.